THE EFFECTS OF ATMOSPHERIC VARIABILITY ON ENERGY UTILIZATION AND CONSERVATION

by
Elmar R. Reiter, Principal Investigator
J.D. Sheaffer, H. Cochrane, J. Cook,
G.R. Johnson, H. Leong, and T. Nakagawa

Environmental Research Papers
COLORADO STATE UNIVERSITY
Fort Collins, Colorado

32

Research on the environment constitutes an important component of the graduate programs pursued by a number of Colorado State University departments. The more noteworthy results of these research efforts are normally published in the conventional professional journals or conference proceedings, but in very much abridged form. ENVIRONMENTAL RESEARCH PAPERS has been established to provide a formal means of disseminating such CSU accomplishments in all significant details, in order that individuals concerned with related interests at other institutions may review a more comprehensive treatment of the research reported than is customarily available.

Price $4.50 in USA

Subscriptions and correspondence to these papers should be addressed to: Secretary of Environmental Research Papers, Department of Atmospheric Science, Colorado State University, Solar Village, Ft. Collins, CO 80523.

DOE-EV01340-3

THE EFFECTS OF ATMOSPHERIC VARIABILITY ON ENERGY UTILIZATION AND CONSERVATION

Final Report of Research Conducted Between
1 January 1981 and 30 December 1981

Under Contract DE-AS02-76EV01340
The U.S. Department of Energy

by

Elmar R. Reiter, Principal Investigator
J.D. Sheaffer, H. Cochrane, J. Cook,
G.R. Johnson, H. Leong, and T. Nakagawa

Environmental Research Papers
Colorado State University
Fort Collins, Colorado

March 1982 No. 32

TABLE OF CONTENTS

ACKNOWLEDGMENTS

The authors greatfully acknowledge the following individuals for their timely cooperation and assistance in providing much of the information and data utilized in the preparation of this report: Mr. Ken Hooker, Mr. Glenn Monroe and Mr. Douglas Ryan of the Public Service Company of Colorado; Mr. Ross Zahler and Mr. Bruce Douglas of WYCO, Inc., Fort Collins, Colorado; Mr. Dennis Sanford of the Building Owners and Managers Association of Denver, Colorado; Ms. Jean Buchanan, Ms. Susan Piatt, Ms. Anne Ober, Mr. Don Vest, and Mr. Paul Rochette of the San Louis Valley, Rifle, Northwest Colorado, Pueblo, and Larimer-Weld County Regional Councils of Government, respectively. The economic studies presented in Section 4.1 were supported in part by National Oceanic and Atmospheric Administration Grant No. NA 80 RA-C-00183.

THE EFFECTS OF ATMOSPHERIC VARIABILITY ON ENERGY UTILIZATION AND CONSERVATION

by

Elmar R. Reiter, Principal Investigator
J.D. Sheaffer, H. Cochrane, J. Cook,
G.R. Johnson, H. Leong, and T. Nakagawa

ABSTRACT

Our weather dependent model of energy demand for space heating has been applied to estimate total daily demand for an entire region. Preliminary tests using a simplified version of the model have yielded results with accuracies comparable to those obtained previously for individual communities. Intraregional subareas exhibited considerable diversity in rates of demand, factors controlling demand and in overall accuracy of model predictions. Progress toward obtaining detailed building census and meteorological data for physical and physical-reference modelling of regional space heating energy requirements is also described.

A physical model of energy demand for air conditioning in large buildings has received preliminary testing. The Group Method of Data Handling (GMDH) algorithm that has consistently provided adequate parameterization for modular models of the space heating needs for an array of building types failed in its first application to air conditioning data. The reasons for this failure are complex and not completely resolved. Presently however, this failure is viewed as an opportunity to obtain additional basic insight into weather-energy demand relationships.

A model of local climate variability that considers both topography and urban "heat island" effects has been refined to an advanced state of development. This climate modelling capability will allow regional scale physical and physical-reference modelling of energy demand to proceed by reducing the requirements for mesoscale observational networks to obtain energy demand-weighted meteorological data for each city.

The potential value of improved weather forecast information to a large electric generation and transmission utility company has been studied. A simple weather-driven demand model for electricity uses weather forecasts to predict hour-by-hour loads, one day in advance. These load forecasts are in turn used by a system scheduling model to determine the most economical generating configuration to meet forecast demands. The results demonstrate significant potential value for improved accuracy of weather forecast services.

Lastly, we have examined the actual cost effectiveness of structural modifications and system retrofits for reducing energy consumption for space conditioning in large buildings. Data obtained for five rather diverse alterations suggest that considerable broad-based conservation potential is available through applications of improved energy utilization technology.

1.0 SCOPE OF WORK

The grant period 1 January 1981 to 31 December 1981 constituted the second year of a three-year research effort. As in previous years, our research was focussed on four major tasks:

(1) Planetary wave variability and climate fluctuations.

(2) Regional energy demand modelling.

(3) Energy demand modelling for air conditioning.

(4) Economic factors in energy use and conservation.

The aspects of planetary wave variability and climate fluctuations have been described in detail in our progress report (Reiter et al., 1981a) and have been published in the open literature (Reiter and Westhoff, 1981, 1982, and other papers listed on p. 3-4 in the progress report). The findings reported in these papers will not be repeated here. Instead, this report will focus on the energy modelling aspects, which were dealt with in a rather abbreviated fashion in our last progress report (Reiter et al., 1981a).

2.0 MODELLING OF WEATHER DEPENDENT ENERGY DEMAND FOR SPACE CONDITIONING.

During the past contract period we expanded the range of applications for the successful models of community energy demand described in our last report (Reiter et al., 1981b). Our studies, described below, include extension of the model to regional applications, streamlining and standardizing procedures for input data development, and the design and testing of a cooling model module applicable to an array of structures. Also, we are in the preliminary stages of assimilating the modelling procedures into "packaged" models with detailed instructions for their efficient application by potential users.

2.1 MODELLING OF REGIONAL ENERGY DEMAND FOR SPACE CONDITIONING.

The original objective in developing a regional model of weather dependent energy requirements for space conditioning was for the identification and analysis of potential emergency situations, such as the one which developed in the Eastern United States during the severe and prolonged winter of 1976-77. The likelihood that a similar emergency could occur at any time in other parts of the country, especially in areas of rapid or nonuniform growth, warranted the development of reliable methods for predicting future regional demands under extreme weather conditions. Apart from these "crisis" considerations, discussions with officials of energy distribution companies have also pointed to the less obvious, but equally important problem of projecting future fuel supply requirements in a rapidly changing market. Conservation, apparently in response to increased energy costs, has greatly complicated the task of projecting future supply needs by causing significant and unprecedented declines in observed, per-customer rates of demand. This problem is especially difficult on a regional basis wherein dissimilar climate regimes and economic circumstances create nonuniform levels of structural weatherization within the region and, consequently, nonuniform potentials for future conservation impacts on levels of demand. Our physical model of energy demand (described briefly below, and by Reiter et al., 1979, 1980, 1981b), applied on a regional scale, offers a reliable means for obtaining accurate assessments of these conservation effects.

A somewhat more manageable problem is the estimation of the energy demand impact of regional growth. The space conditioning energy needs for new buildings vary with the structural type and with their location and use. For example, because of both structural and meteorological factors, the energy demand for detached suburban dwellings often differs considerably from that for downtown condominiums of equivalent size. Superimposing the effects of diverse community growth on local energy demand is quite analogous to the demand problems posed by regional growth and development.

The community growth problem has been handled quite successfully and in a very cost effective manner by our hybrid physical-reference model of community energy demand (Reiter et al., 1981b). Application of the physical-reference model first requires the development of a successful statistical reference model (Reiter et al., 1979) for the community or region of interest. Note that this reference model avoids any consideration of the structural characteristics of existing buildings. A physical model of energy demand can then be constructed for any hypothetical configuration of new or modified buildings and used to adjust the predictions of the current statistical reference model. This procedure was tested to simulate the demand impact of more than 1500 new buildings in Greeley, Colorado. Even though this test was complicated by the impact of conservation (a 20 percent drop over five years in the rate of demand for existing buildings), the hybrid model predicted total daily demand to within four percent (RMSE) for the test period. The construction and testing of a hybrid physical-reference model for regional energy demand is presently in progress.

We have begun an analysis of the weather dependent demand for natural gas for the entire service region of the Public Service Company of Colorado (PSCC). This utility company distributes natural gas to nearly all the major municipalities within the state of Colorado and, by virtue of the mountainous terrain, serves a variety of climatological regimes typically found only in a much larger region. Figure 1 shows the ten major service areas supplied by PSCC. The north-south orientation of the Rocky Mountains, illustrated in Fig. 1, frequently causes contrasting weather conditions to occur simultaneously in the eastern and weatern portions of the region. Also, much of the mountain service area is at much higher elevations than the other service areas and, consequently, requires larger average per capita fuel supplies.

Public Service Company of Colorado has provided daily demand data for January and February, 1981 for each of the ten service areas. Detailed data on the spatial distribution of customers within each area have also been provided. A breakdown of the total demand, number of customers, and average fuel consumption (industrial fuel usage removed) per customer during this period is shown in Table 1. Rates of fuel consumption, crudely adjusted for weather (i.e. heating degree days), vary from 14324 Btu/customer/degree day in the Rifle service area to 28748 Btu/customer/degree day in the relatively nearby mountain service area. Because the variations in Table 1 are only partially explained by weather differences, we are

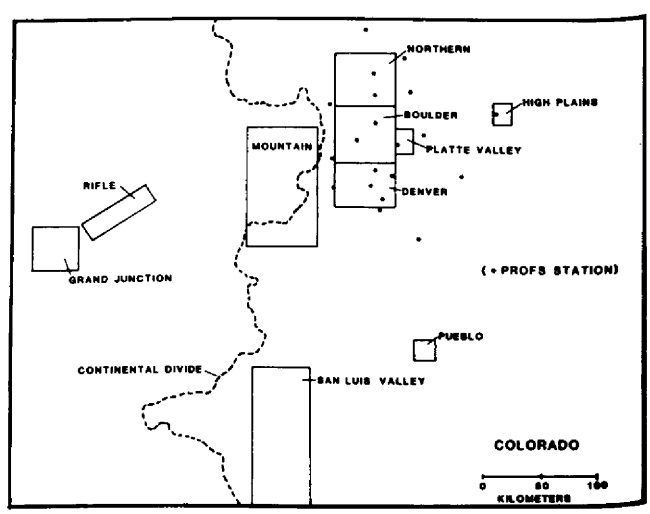

Fig. 1 Approximate locations of the ten service areas to which the Public Service Company of Colorado supplies natural gas. The PROFS weather network (asterisks) and the orientation of the Rocky Mountains (Continental Divide; dashed line) are also shown.

Table 1 Natural gas consumption statistics for the ten PSCC service areas.

Service Area	Customers	Demand/Day (MCF/Customer)	Btu/Customer/ Deg. Day
Denver	452952	0.82	25814
Boulder	60844	0.74	22745
Platte Valley	47271	0.89	25739
Pueblo	40621	0.65	18742
San Luis Valley	6469	0.68	14857
Mountain	8597	1.35	28748
Rifle	3100	0.55	14324
Grand Junction	28934	0.71	22624
High Plains	2246	0.85	23201
Northern	47271	0.65	19033

acquiring local demographic data for each area to determine if other factors can be identified. We have determined, for example, that in the Rifle service area a disproportionately large portion of the current population consists of single men working in the construction of new synthetic fuel processing facilities. Most of these individuals apparently live alone in mobile homes or similar small detached housing units and account for the comparatively small per-customer demand rates [Rifle Regional Council of Government (oral communication)]. More detailed population and building census data for each service area will allow broader interpretation of other factors influencing demand, such as weatherization and life styles.

Although detailed input data for demand modelling in each service area are not finalized, we have performed a preliminary statistical simulation for each area using PSCC's demand data and meteorological data obtained from the National Oceanic and Atmospheric Administration and from the Colorado State Climatologist's office. The modelling procedure used for these simulations, termed the "Phase I Statistical Reference Model", uses the Group Method of Data Handling (GMDH) algorithm (Reiter et al., 1978, 1979, 1980, 1981b) to generate a response function for estimating weather dependent energy demand for each service area. Comparative modelling results for each service area are summarized in Table 2. Graphical displays of daily observed and predicted demands, along with daily averaged meteorological parameters, are shown for each area in Figs. 2A through J.

Interpretation of the preliminary results in Table 2 must be prefaced by several comments regarding procedural shortcuts in their development. Because only a brief period of demand data (59 days) are available at this time it was necessary to construct and test the model with the same data. To make some distinction between the data used to construct the models and those used for testing, the 59 daily demand values for each area were partitioned into 19 groups or states[1] ranging from the highest to lowest values. Each of the 19 state groups consists of five values wherein two values are common to each pair of adjoining states. The mean value for each of the 19 states was used for model identification purposes (see Reiter et al., 1978). A separate "testing" data set was then generated using the median value for each of the 19 states. The limited number of data points resulted in some significant differences between mean and median values, especially for the extremely high and low response states, and hence produced an artificial but unavoidable source of error.

[1] The partitioning of response variables into overlapping "state" groupings is part of the standard procedure in the Group Method of Data Handling (GMDH) model identification technique, (Reiter et al., 1978).

Table 2 Summary of Phase I statistical reference model results for each of the ten PSCC service areas.

Service Area	Model Error* (%) RMSE	ABSE	GMDH Met. Parameter Selection**
Denver	7.7	6.0	$\bar{T}$, STEP
Boulder	12.0	8.9	$\bar{T}$, T_{min}
Platte Valley	11.4	8.3	$\bar{T}$, $\log(WS)^2$
Northern	11.0	8.4	$\bar{T}$, $\log(WS)^2$
Pueblo	9.0	7.7	$\bar{T}$, T_{max}
San Luis Valley	7.0	5.0	T_{min}, T_{max}
Mountain	6.4	4.5	$\bar{T}$, STEP
Rifle	3.8	2.9	$\bar{T}$, WS x SOL
Grand Junction	7.2	5.7	T_{max}, DEGD x SOL
High Plains	13.8	12.2	T_{min}, SOL

* For comparison, typical error of refined, Phase III model is less than 5 percent RMSE and less than 1 percent seasonal error, defined as total predicted consumption minus total observed consumption for the season. (RMSE = root mean squared error; ABSE = absolute error.)

**Abbreviations are as follows: $\bar{T}$, T_{max}, T_{min}: daily mean, maximum and minimum temperatures, respectively; WS: daily mean wind speed; SOL: total solar radiation; DEGD: heating degree days; STEP: stepped adjustment to accommodate weekend demand rates.

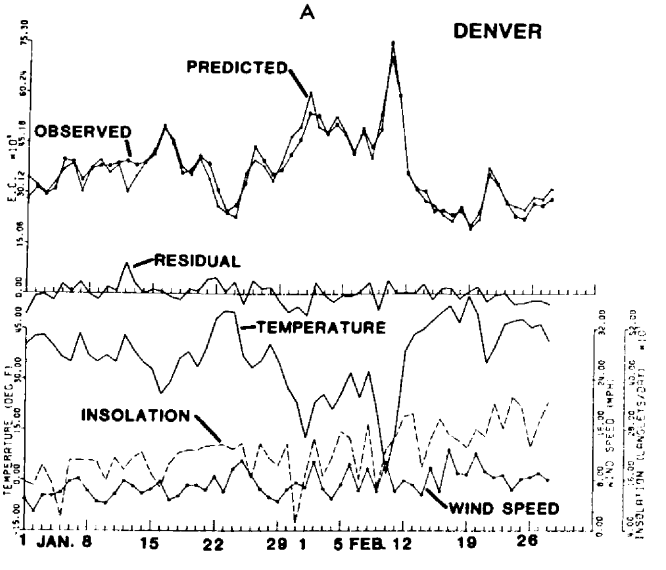

Fig. 2(A-J) Daily mean values of weather parameters plus observed versus predicted energy demand (MCF/DAY) for the ten PSCC service areas. The residual is the observed minus the predicted demand.

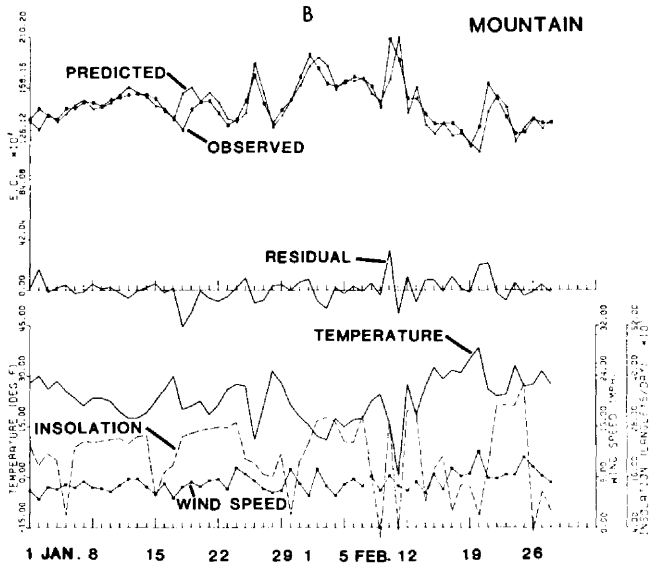

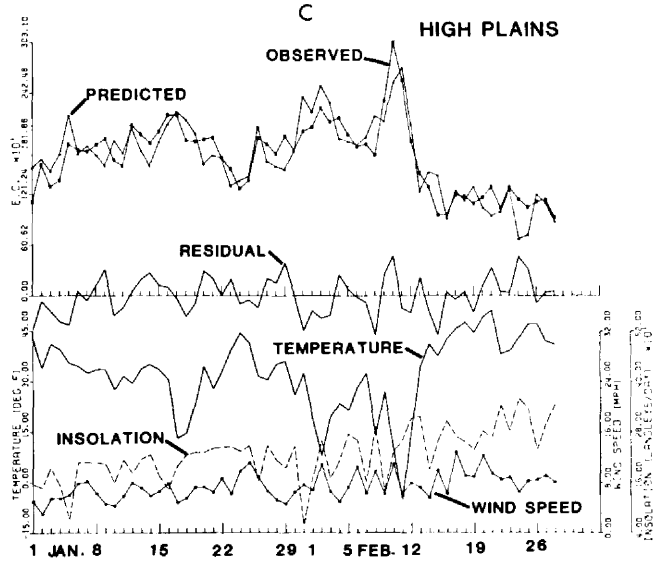

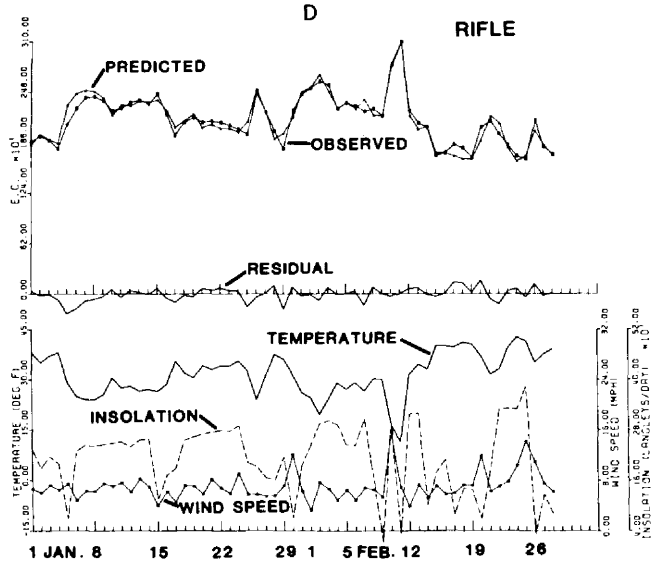

Fig. 2 (Continued)

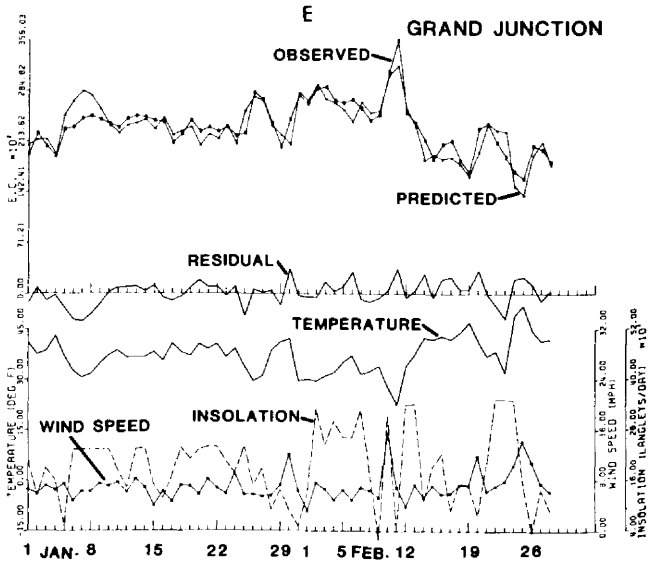

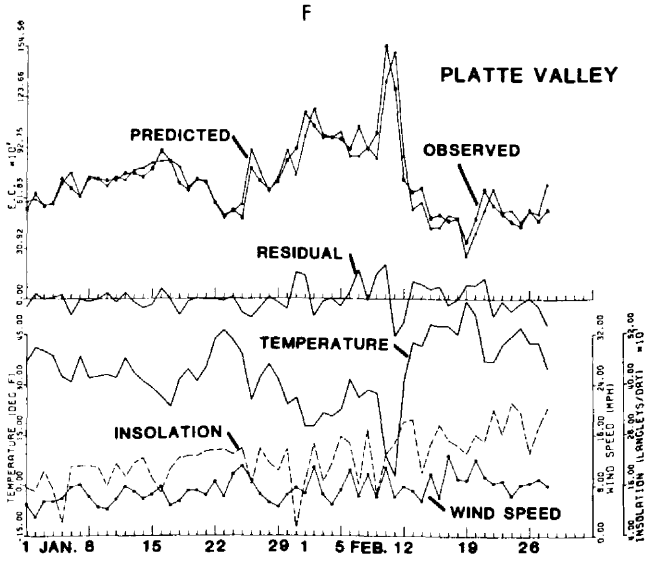

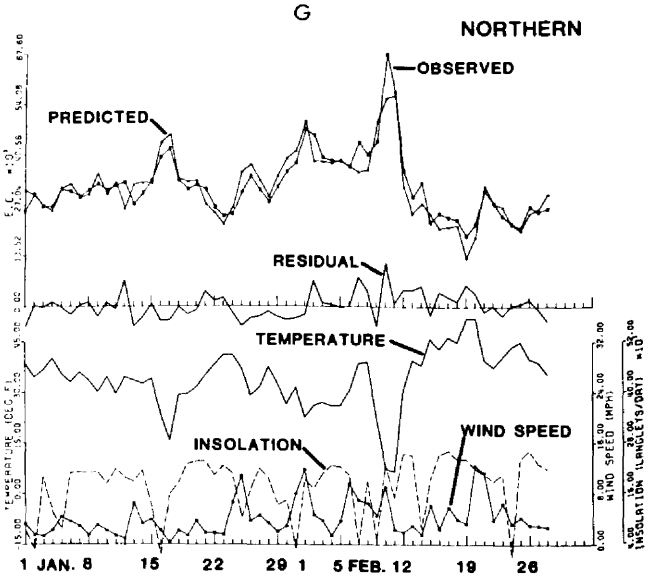

Fig. 2 (Continued)

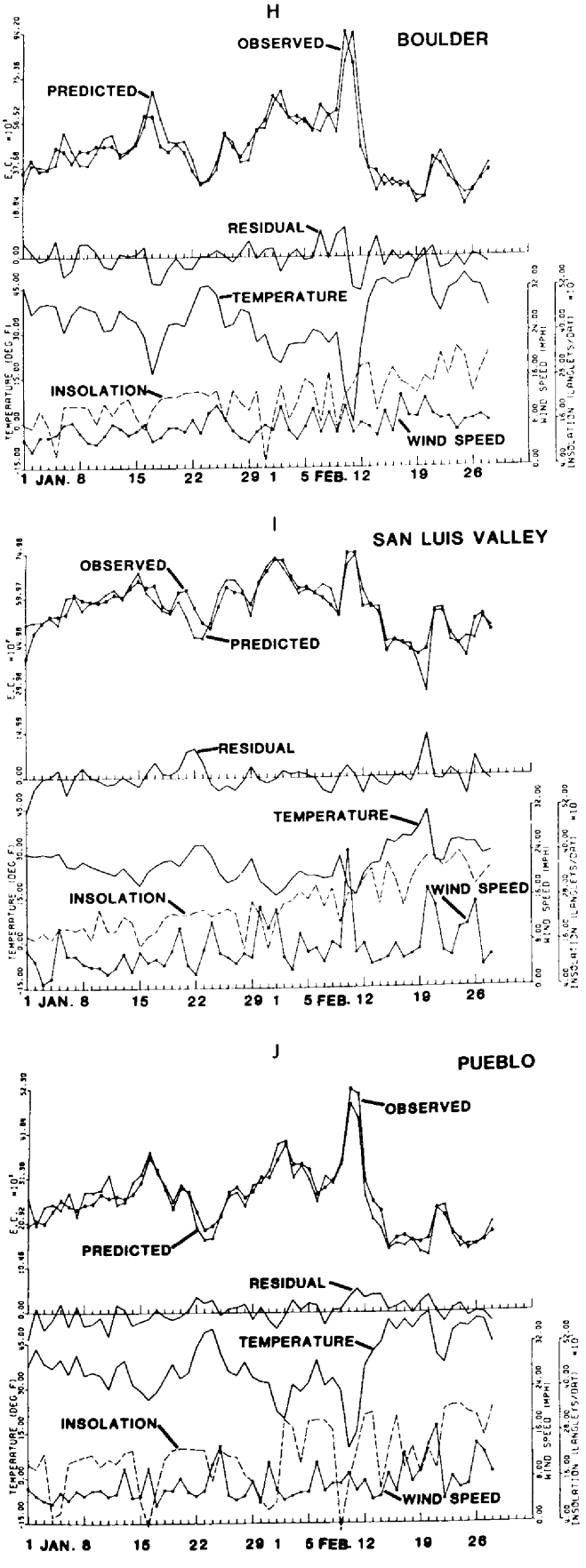

Fig. 2 (Continued)

The daily mean temperature data used for these preliminary tests were determined as the average of reported maximum and minimum values rather than from 12 bihourly values, as is our normal procedure for statistical models. Although bihourly temperature data have already been prepared for several of the service areas, it was decided to initially model all areas with temperature data of equal, but inferior, quality. Because of this procedure the mean daily temperature values used were occasionally rather misrepresentative of the actual daily average temperatures that occurred. Nevertheless, as shown in Table 2, the mean daily temperature was selected by the GMDH model identification algorithm as the most important demand-related variable in 7 of the 10 service areas. As a consequence we anticipate that the accuracy of the model predictions will improve when more detailed temperature data sets are completed.

It must be emphasized that the results shown in Table 2 and Fig. 2 are for the Phase I reference model only. Phase II and Phase III model identification procedures, the time series adjustment for stochastic residuals and sequential updating of the time series adjustment, respectively, (Reiter et al., 1981b) in our past studies have substantially improved model performance. Moreover, demand predictions by the physical models (based on actual heat loss calculations for all structures in a community) are in general more accurate than those made by the statistical reference models. Application of these more sophisticated models will be made as more energy demand data become available and when the building census (detailed structural data) and meteorological data sets are finalized.

We are encouraged by the overall accuracy of these rather crude preliminary regional tests. The best results in Table 2, in terms of the average root mean square error of prediction, are for the Rifle area which consists of four small mining communities scattered along the Colorado River, above Grand Junction, Colorado. We previously noted that this area also had the lowest per customer rate of demand among the ten service areas studied. We will not attempt to speculate on the implications of this or other results shown here until more model runs and analyses have been completed. With the incorporation of more refined models and data (including consideration of local urban climate effects as described in the next section), we anticipate that all areas can be modelled with accuracies comparable to our best prior efforts (i.e. less than 5 percent RMSE).

Another effort being undertaken is the development of a gridded model of regional energy demand. This study uses the Phase III, sequentially updated model to simulate demand in each sector of a region and to provide a visual display of current or forecast energy demand. Much of the meteorological data base for this model is being obtained from the Prototype Regional Observing and Forecasting Service (PROFS), an experimental program operated jointly by Colorado State University, NOAA, and the University of Wisconsin. Shown in Fig. 1 are the locations of 20 PROFS weather stations that provide 15-minute average data in real time for an array of meteorological parameters. This network reports to CSU via satellite and also contains additional experimental sounding systems. Utilizing PROFS forecasting expertise, the energy model will be capable of making hourly energy demand forecasts 24 hours in advance. Comparing the predicted demand in each grid sector to the existing utility supply capability will allow more timely

notification of interruptable customers, avoid many unnecessary interruptions and, when necessary, permit the timely rerouting of additional fuel from adjacent areas.

We had originally planned to use PROFS data in the regional simulation for the past 1980-81 winter. However, a series of technical problems resulted in incomplete or unreliable data prior to February 18, 1981. We are now studying the existing PROFS data as part of the planning phase for our regional gridded model.

2.2 DEVELOPMENT OF METEOROLOGICAL DATA FOR ENERGY DEMAND MODELS.

We have acquired essentially all of the meteorological data that are available for the ten service areas in our regional studies. These data, mostly from airports or local weather service stations, are not in general representative of the mean (energy demand weighted) conditions in the respective PSCC service areas and certainly do not indicate the range of conditions that occur within each area. In addition to natural variations of temperature, wind, and insolation likely to occur due to local topography, each city generates its own microclimate, most notably the urban heat island.

In our past reports we have described efforts to deal with local climate variability in the development of representative meteorological data for input to our community demand models. During the developmental phase of our modelling studies mesoscale meteorological monitoring programs, though expensive and time-consuming, were necessary for holding computational uncertainties to a tractable level. Networks of temperature and wind recorders were operated in several cities to document carefully both the local urban heat island effects and the frictional slowing of surface winds by large and small buildings. Comparable monitoring efforts, on a regional scale, would require the operation and processing of data from literally hundreds of meteorological instruments. It is unlikely that many potential users of our demand models will have either the resources or motivation to undertake such monitoring programs. Consequently, we have developed procedures for simulating local variations of urban temperatures and wind speeds using a single set of local weather observations. In the past contract period a modest effort directed toward this end has produced very encouraging results which are described in detail in Section 3.0.

2.3 BUILDING CENSUS FOR REGIONAL DEMAND MODELLING.

Our physical model of community energy demand uses representative structural data for buildings in each community to calculate actual heat losses and hence the energy requirements to maintain internal temperatures at a comfortable level. This is achieved by computing the weather dependent demand response for each of 43 "typical building" modules (Reiter et al., 1980). The computed response for each module is weighted according to the average size and frequency of occurrence of each building type in each portion of the community. The estimated demands for all modules in all portions of the city are then summed to determine total community energy requirements. To use this model, a detailed building census must first be developed to account for the size, use, and type of construction for all buildings in the community. Moreover, since weather parameters often vary throughout each city (especially in communities with more than 10,000 inhabitants) the spatial distribution of these buildings within the community must also be considered.

In the past we have obtained building census information using "brute force" methods. These methods included an actual house-by-house survey of Greeley, Colorado, and detailed analysis of the assessor's files for more than 100,000 buildings in Minneapolis, Minnesota. The procedures for developing building census data, in direct analogy to the meteorological data programs described previously, needed to be simplified and standardized for regional applications of our physical model of energy demand.

In a prior report (Reiter et al., 1979) we described results of a preliminary attempt to use readily available indicators (e.g. U.S. census data) to estimate the square footage of detached, single family dwellings in a community. This effort was quite successful for relating mean assessed valuation to the mean square footage of residences in Greeley, Colorado and Cheyenne, Wyoming. However, the same procedure failed when applied to building data from Minneapolis. Multivariate regression that included the percent of residential structures with substandard plumbing (as an index of urban blight) and the number of occupants per residence improved the size estimates for Minneapolis structures, but the degree of accuracy was still not adequate. During the past contract period we extended these previous studies to create a more efficient procedure for obtaining suitable building data through indirect means. This study involves identifying and testing alternative regression variables including the mean (census tract) number of rooms and number of bathrooms to improve our model of average residence size.

Meanwhile we have gone ahead with the development of a regional building census based largely on data from our earlier studies. This work is proceeding as follows: We assume that the statistical descriptions of building types, developed from our Greeley data, are applicable to most of the municipalities in the region served by the Public Service Company of Colorado. Our justification for this assumption is that in our previous studies (Reiter et al., 1978) we encountered a remarkable degree of homogeneity of construction materials and floor plans after structural data for each city had been stratified by building age and use. Spot checks of the validity of this assumption are being developed from assessor's data for several cities in the Colorado front range area. We anticipate that many buildings in the city of Denver and in some mountain communities may differ significantly from the Greeley pattern and more in-depth analyses of assessor's data will be needed for these communities. We have obtained a copy of the Denver, Colorado, assessor's file which contains detailed physical data for more than 270,000 buildings. A preliminary review of these data indicates that fairly complete information on the location, age, size, construction and, most importantly, the use of each building are available.

In applying our Greeley building data distribution to other areas of the state it is necessary to allow for differing concentrations of building ages and use patterns. Detailed data for the age of buildings are available on a tract basis from the 1970 census and the preliminary 1980 U.S. census. In addition, PSCC has provided us with detailed counts of residential, commercial, and industrial customers for all communities and incorporated districts for each of its ten service areas. The level of detail of these data is such that customer counts, by type, are delineated for 53 subareas in the Denver metropolitan area

alone, with several hundred additional customer listings for the remaining nine service areas. By combining these census and customer count data, we are constructing a building distribution census for each of the ten PSCC service areas. Even though compromises such as interpolations and simple estimates are necessary in some areas, we anticipate that significant improvements toward a satisfactory description of regional energy demand will be achieved in this way.

2.4 DEVELOPMENT OF A QUASI-PHYSICAL MODEL FOR AIR CONDITIONING.

The construction of a physical model for air conditioning loads in buildings is a much more difficult task than the corresponding heat loss modelling during the heating season. Typically the air conditioning process is called a "heat gain" calculation and is usually considered as the inverse of the heat loss calculation. However, in the heat gain calculation internal heat loads from lights, electrical systems and occupant behavior become an additive rather than a conservative factor as in space heating. Moreover, the internal heat load in the heat gain problem is large in comparison with the influence of external weather factors.

In our current modelling efforts we have decided not to pursue the construction of a detailed physical heat gain model for air conditioning because of the vast complexity of the sophisticated and diverse mechanical systems and operating strategies and because of the diverse use patterns within the buildings to be modelled. There are already a number of complex physical models such as BSLD and DOE-2 that are suitable for simulating energy demand in the detail required in order to physically size air conditioning equipment and to determine its effectiveness. However, these models require extensive input data which are beyond what can be either collected or used in aggregated model approaches used in community heating-energy models. Consequently, a different approach was tried for the development of a cooling model that closely parallels the earlier development of the heat loss model (Reiter et al., 1978). In this approach, simple heat gain equations were used and an attempt was made to refine the model through the use of the GMDH algorithm (described in Section 2.1 of this report) for coefficient identification.

The scheme used is basically as follows: As in our heat loss modelling approach, a simple computer program was built incorporating the heat gain equations from the ASHRAE standards using coefficients based upon the thermal characteristics of the building. These coefficients, taken directly from ASHRAE information, are primarily thermal resistances. In addition, a typical behavior usage and a ventilation strategy of air changes per hour as well as the electrical internal heat loads were introduced into the model. The model was then subjected to an input stream of meteorological data and the heat gain calculated from these equations. This scheme was then run through the identification process of the GMDH algorithm in order to determine whether or not the resulting coefficients would reach a constant and physically believable value. The algorithm was constrained so that the major terms of the equations had to be retained; that is, the GMDH algorithm was not permitted to throw out any of the meteorological terms contained in the initial heat gain model. Lagged values of particular ambient conditions and radiation were also left in the equations so that some of the effects of thermal inertia would be retained.

The building studied was an older office building in Denver, Colorado. For this building we had the necessary thermal characteristics information and approximately 60 days of summer meteorological data. The computational algorithm divided the data into two sets. The first set was the training set for determination of the coefficients and the second set was used as a testing set to determine the overall accuracy of the resulting model. Typically, after several iterations, the model coefficients derived by the GMDH began to converge to nearly constant values and, when no significant improvement of the model occurred, the process was terminated (Reiter et al., 1978, 1981b). For all cooling model simulations attempted, no matter how the data were divided, a consistent set of coefficients could not be obtained. The primary reason for this failure may be the inadequacy of the assumptions concerning the user behavioral patterns, ventilation modes and, perhaps more importantly, the operating strategy of the ventilation and air conditioning equipment contained within the building. Also, additional meteorological factors including indirect effects of neighboring buildings need further consideration. Since the coefficients did not become stable and could not be adequately correlated with any ambient meteorological conditions, the approach was abandoned. Much more work was necessary than could be accomplished in the time available.

An identified heat gain model may be beyond the ability of a simple approach. In general, it would appear that our effort was overly simplistic for large complex office buildings. Previous results using this modelling approach for the space heating demands for simple residential structures met with success because the coefficients identified and retained consistently represented physical reality. Perhaps we should have anticipated failure in modelling air conditioning for large office buildings because, when the statistical reference model was used to identify the cooling demands of large office buildings, each building seemed to retain different sets of driving terms (Reiter et al., 1981b). That is, for each particular building and corresponding use pattern, the ventilation and mechanical systems and operating strategy, in some sense, responded to different meteorological conditions and, in effect, responded differently to different sets of input conditions. This should have warned us that no simple physical model of air conditioning would meet all of our needs.

There appears to be two possible future directions for this work. The first approach is to attempt to isolate a set of identified models with combinations of use, internal loading, mechanical systems and operating strategies so that a number of models are used. However, this would be an extremely large task. Consequently, it would perhaps be better to attempt to average out these effects rather than model individual buildings. In this way a larger aggregate of buildings would be modelled in the hope that the differences among buildings and their responses to weather variations could be kept within a single identified model over the aggregate. Unfortunately, resources have not permitted an examination in either direction. It ultimately may be necessary to abandon the hybrid physical reference model approach which has worked so well in the heating loss calculation and to find an alternative approach for heat gain calculations. To pursue these options we have developed a voluminous meteorological and air conditioning energy demand data base for 14 large buildings in the Denver, Colorado, area. These data include an extended record of 15-minute average electricity demands for each building

and 15-minute mean values for temperature, wind speed and direction, insolation and humidity for five metropolitan area weather stations. The energy demand data have been obtained with the assistance of the Building Owners and Managers Association of Denver. The buildings selected represent a diversity in ages and designs while retaining a common commercial office use pattern. The weather data have been obtained from the "PROFS" network which is described in Section 2.1 of this report.

3.0 URBAN CLIMATE MODELLING

3.1 INTRODUCTION

We previously called attention to the importance of local climate variability for modelling of weather dependent community energy demand. Efforts to accommodate local weather variability, including both monitoring and modelling studies, have been described in several prior reports (Reiter et al., 1976, 1978, 1979, 1980, 1981b). In this section we describe our most recent efforts to improve the level of detail of our meteorological data through the application of urban climate models.

Our prior studies show that the effect of solar radiation on energy requirements for heating is generally quite small for the cities we have modelled. In fact, for temperatures below 0°C, we have detected no significant effect of variable insolation (Reiter et al., 1978). Consequently, solar radiation is considered spatially invarient in our energy demand models and a single set of local observations is adequate. The influence of wind speed is also very secondary to temperature in determining energy needs for space heating. Our approach to estimating local variations of wind speed in urban areas involves either multiple monitoring stations or the application of a simple power law to adjust airport wind speed observations for varying degrees of urban surface roughness (Spera and Richards, 1978; Reiter et al., 1981b). Because of the major importance of air temperature in determining energy demand, considerable attention has been given to modelling urban temperature fields and the so-called "urban heat island".

We begin by briefly describing our urban temperature model. Details for several case studies of the Minneapolis heat island are then presented. Later we describe several innovations and modifications that improve the general performance of the model for a variety of weather conditions.

3.2 MODEL DESCRIPTION.

Additional details of our urban temperature model, adapted from origional work by Summers (1965), are summarized by Reiter et al. (1981b). This model simulates the cumulative modification of air temperatures at the base of a stable layer of rural air as it is advected across warmer urban surfaces. The computed thickness of a surface-based neutrally buoyant sublayer, assumed to be formed by the urban heating, is then used to estimate urban-rural temperature differences for any location in a city. These concepts are illustrated in Fig. 3.

The computational form of the urban temperature model is given by Eqs. 1 and 2,

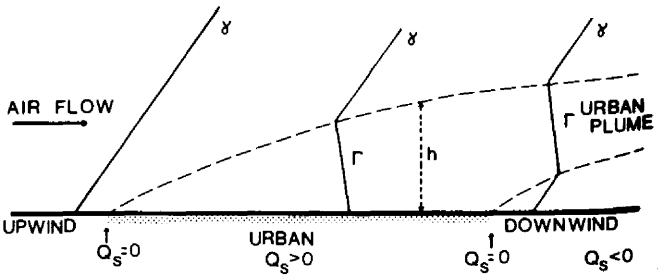

Fig. 3 Conceptual representation of the formation of a neutrally buoyant sublayer ($\frac{\partial T}{\partial Z} = \Gamma$) of thickness h as stably stratified rural air moves across an urban area.

$$h(x)^2 = \frac{2}{C_p \rho \alpha U} \int_{x_o}^{x} Q_s \, dx \qquad (1)$$

$$\Delta T_{u-r} = h\alpha \qquad (2)$$

where h is the thickness of the neutral urban sublayer. Urban-rural temperature differences, ΔT_{u-r}, are related to h by Eq. 2. This form of the model was derived by Leahey and Friend (1971) and Henderson-Sellers (1980).

The independent variables in Eq. 1 are the specific heat of air at constant pressure, C_p; air density, ρ; wind speed, U; the change of potential temperature in the modified air layer, α (i.e. $\alpha = \gamma - \Gamma$, where Γ is the dry adiabatic lapse rate and γ is the ambient lapse rate in the stable rural air); the excess urban heat flux, Q_s; and x, the linear distance following the mean wind direction. Important simplifications in the derivation of Eq. 1 include the assumption of constant wind speed and direction and heating at the bottom of the advected air layer only.

Equation 3 summarizes the quantities used to calculate Q_s for nighttime conditions.

$$Q_s = Q_h(T) + Q_t(t) + Q_e(t) + Q_{sc}(\gamma, u) + Q_i(\Delta T) \qquad (3)$$

The right-hand side of Eq. 3 includes three heat source terms. These are: Q_h, the temperature dependent energy use for space heating; Q_t and Q_e, the time dependent values of heat input from transportation and electrical power consumption, respectively. Equation 3 also includes two sink terms: Q_{sc}, the turbulent transport of sensible heat to the surface and Q_i, the increased radiative heat loss from the city due to warmer urban temperatures. Equation 3 is used to compute bihourly values of Q_s for each of the 224 grid areas represented in Figs. 11, 12 and 13. Values for the source terms in Eq. 3 were derived from energy demand data developed for our energy demand modelling of Minneapolis (Reiter et al., 1981b). The function of the sink terms in Eq. 3 is illustrated in Fig. 3 where, at point (0), the sum of Q_{sc} and Q_i exceeds the urban heat sources and a new surface inversion begins to form downwind of the city. Values for Q_{sc} are computed using Eq. 4,

$$Q_{sc} = \frac{C_p \rho Z_i \Delta T_r}{2 \Delta t} \quad (4)$$

where Z_i and ΔT_r are the depth of rural forced turbulence and the recent (Δt = 2 hours) change in rural temperatures, respectively. The net increase of outgoing surface radiative flux within the heat island, Q_i, is given by Eq. 5.

$$Q_i = \sigma(T_u^4 - T_r^4)(1 - C^2) \quad (5)$$

In Eq. 5, surface emissivity is assumed to be unity, surface temperatures are equal to air temperatures, and σ and C are the Stefan-Boltzman constant and opaque cloud cover (tenths), respectively. During windy and clear conditions Q_{sc} becomes fairly large and tends to restrict the spatial extent of the heat island. For relatively calm and clear conditions, Q_{sc} tends to be relatively small because of reduced turbulent mixing. In this case the heat island intensifies, especially in suburban areas. For windy and cloudly cases, significant advective warming effects may occur in the city when Q_s becomes large through the combined influence of comparatively small ΔT_r values and/or large C values.

The use of Eq. 4 to estimate Q_{sc} departs from previous applications of Summers' model wherein simple gradient equations were used for this calculation (see Leahey and Friend, 1971). The important variable in Eq. 4 is Z_i, which is also used to estimate values for γ, the rural vertical temperature profile (described later). Equation 4 thus adds consistency to our estimates of urban and rural surface energy budgets and improves the overall precision of the modelling procedure.

Mean surface elevations and empirical roughness lengths have also been determined for each of the grid areas in Fig. 11-13. The elevation data are used for adiabatic adjustments of air temperatures and also, under calm conditions with strong stability, to allow for pooling of cold air in low-lying areas. The roughness length values are used for adjusting observed (airport) wind speeds to urban conditions. Estimates of the roughness length (Plate, 1971) range from 0.1 meter at the airport to 3.5 meters in downtown Minneapolis.

3.3 HEAT ISLAND OBSERVATIONS.

Most heat island studies focus on extreme effects under ideal conditions with clear skies and light winds. For our work however, it was necessary to consider the spatial detail of urban temperature fields for all weather conditions and for all times of the day. Before considering additional details and recent modifications of the heat island model, it is useful to examine the urban effects that we have observed and attempted to reproduce. In this section we also examine the extent to which the underlying physical assumption of our model, the formation of a surface-based neutral layer over the city, is born out by our observations.

We have used data collected in Minneapolis for the following analyses, primarily because of the size of the city but also because of the availability of temperature and wind data from a centrally located 150-meter television broadcast tower. The meteorological monitoring network, shown in Fig. 4, was operated

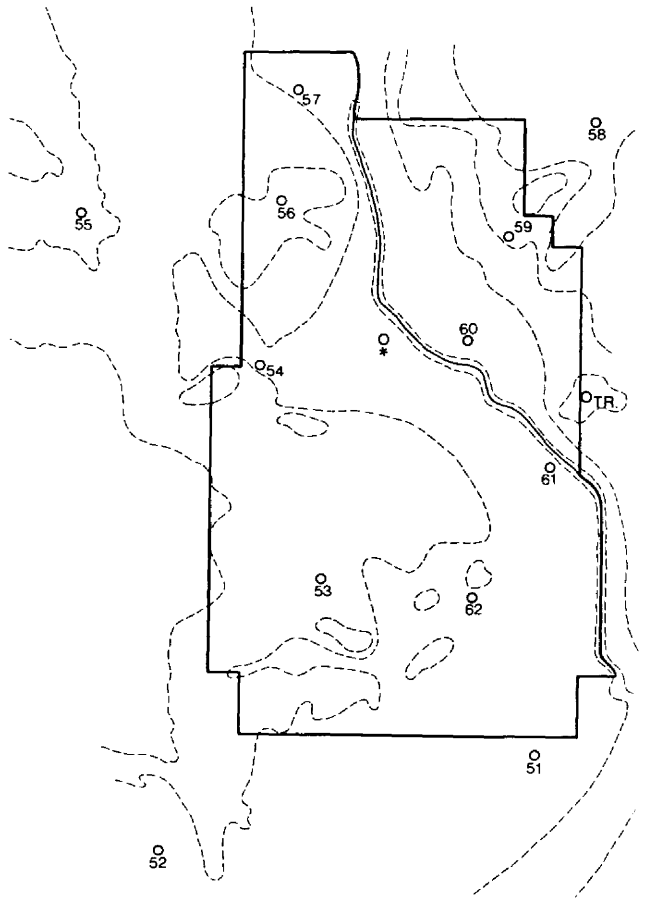

Fig. 4 Locations of meteorological observation stations in Minneapolis (Reiter et al., 1980). Station 51 is the National Weather Service and the 150-meter tower is designated TR. The location designated by "*" was operated during the 1977-78 winter only and is used for a special analysis shown in Fig. 10.

in the Minneapolis-St. Paul area during January, February and March, 1979. Data from this network were used to model space heating energy demands in Minneapolis and are described in detail in Reiter et al., 1980. Temperature data were collected at 11 stations in addition to the National Weather Service station and at three levels (20, 50 and 150 meters above the surface) on the television tower. Wind speed and direction were monitored at six stations and at two levels (20 and 150 meters) on the tower. In addition, sky cover and precipitation data were obtained from the National Weather Service. Solar radiation data for one central location were provided by the University of Minnesota. Exceptionally heavy snow cover and relatively low temperatures occurred throughout the study area for all but the last two weeks of the monitoring period. A series of analyses of these data verified the existence of a heat island in Minneapolis for virtually all weather conditions (Reiter et al., 1980).

Because urban temperature model calculates warming as a cumulative advective effect, we were especially interested in seeing to what extent heat island intensity increased with fetch across the city and

where and how local surface factors appear to outweigh sensible heat advection. In a simple test for advective effects we computed the mean temperature difference between the most rural station, No. 55, in Fig. 4 (actually, a suburban location) and other stations as a function of wind direction and speed (Reiter et al., 1980). These differences for several stations in peripheral urban locations are shown in Fig. 5. It is apparent in this figure that winds from the city at these stations were warm relative to air flowing in from rural areas. We also observed cases wherein air flowing out of the gorge of the Mississippi River (running northwest to southeast across the city) was occasionally associated with comparatively low temperatures at either Station 60 or 61 (Fig. 4), depending upon wind direction. These findings provide at least qualitative evidence for both the occurrence of net advective warming in the city and of the potential (cooling) impacts of fairly large local terrain features.

In a series of case studies, some evidence of a surface-based neutral layer over the city was noted for most conditions. Temperature values and elevation differences for various stations and the tower were used to evaluate the modification of air temperatures along a trajectory following the mean wind direction across the city. Figure 6 shows the approximate relative elevations of several surface stations and the tower sensors. Results for several case studies are illustrated in Figs. 6, 7, 8 and 9.

Figure 6 also shows a set of observed temperature differences for three surface stations relative to the top of the tower. These observations were made at 0200 to 0400 local standard time (LST) with clear skies and airport (NWS) wind speeds of 4.8 meters per second. At both the upwind and downwind locations (Stations 55 and 51, respectively) the surface temperatures are stable relative to higher level temperatures observed at the tower. However, the vertical temperature gradient over the urban stations appear to be neutrally buoyant all the way to the surface (consistent with model assumptions) when the tower temperature profile is extended to nearby Stations 60 and 61. Similar profile relationships are observed when skies are clear and wind speeds exceed about five meters per second. For clear conditions with wind speeds less than about five meters per second, the

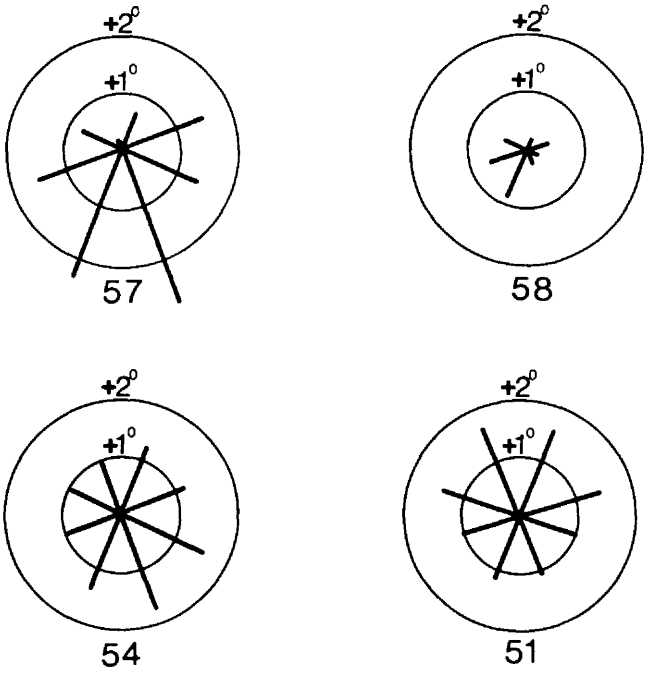

Fig. 5 Mean temperature differences between four peripheral urban stations (see Fig. 3) and Station 55, stratified by wind direction to show apparent directional dependence of advective urban warming.

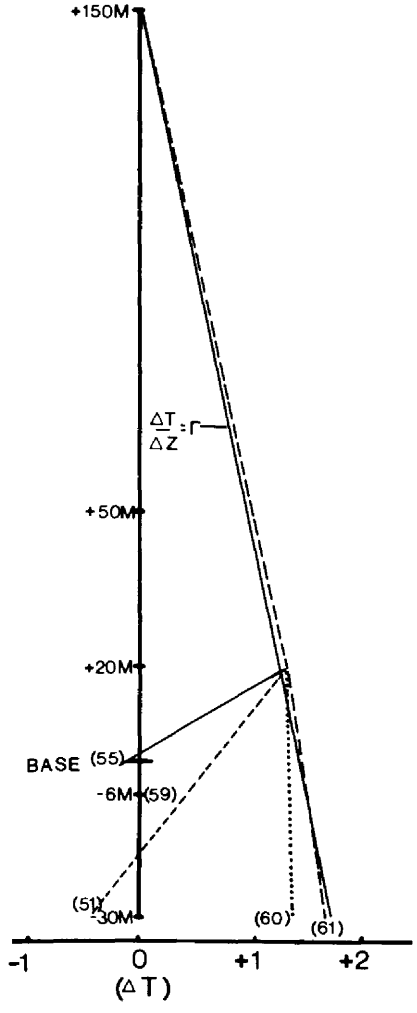

Fig. 6 Observed vertical temperature differences over Minneapolis for 0200 to 0400 LST, January 14, 1979. Neutral stability ($\frac{\partial t}{\partial z} = \Gamma$) is represented by the solid line on the right extending from the top of the tower to the bottom of the figure. The elevation of Stations 51, 55, 59, 60 and 61 and the tower sensors (20, 50 and 150 m) are shown relative to the tower base. The extension of the tower profile (dashed) to Stations 60 and 61 is probably reasonable, whereas the lines drawn from 20 m to the upwind (#55) and downwind (#51) stations are for the purpose of comparison only. Local meteorological conditions for this time period are: winds at 5.8 m/s from 310°, clear skies, and temperature is -25.2°C.

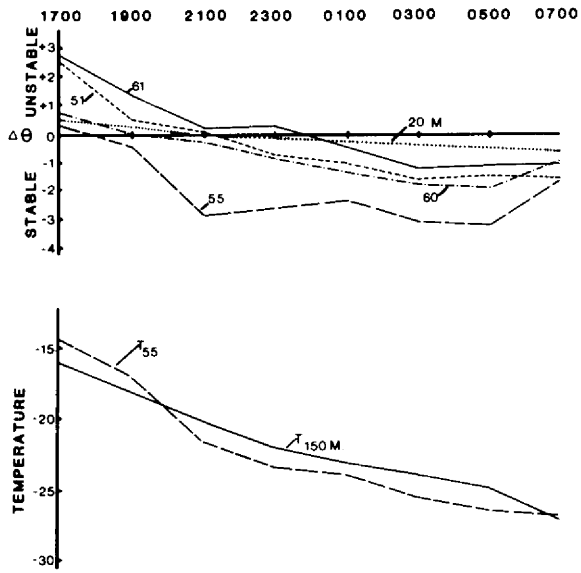

Fig. 7 Analysis of low level atmospheric stability between 1700, February 6 and 0700, February 7, 1979, in Minneapolis for strong winds accompanying a frontal (cold) passage. Top: Vertical differences in potential temperature (relative to the top of the 150-meter tower) for Stations 55 (upwind), 51 (downwind), 60 and 61 (urban) and the 20-meter level on the tower. Bottom: Ambient temperatures observed at Station 55 and at the top of the tower. Wind and cloud cover data for each bihourly period are given in Table 3.

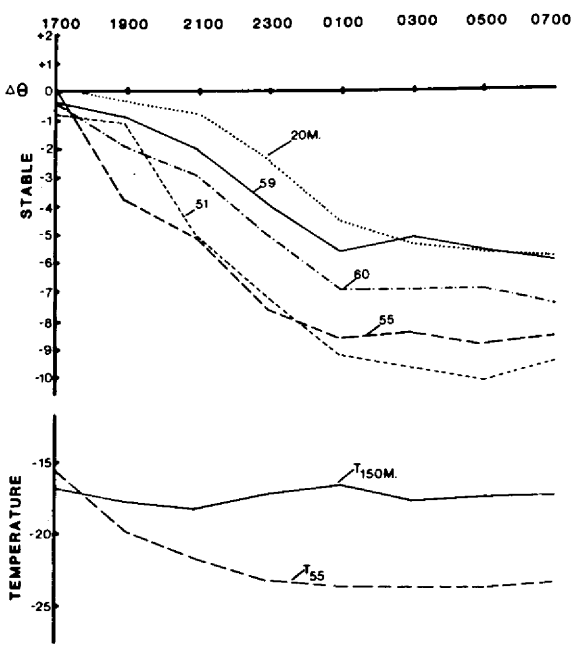

Fig. 8 Similar to Fig. 7, but for clear and nearly calm conditions. Also Station 59 (urban) replaces Station 61 in this analysis.

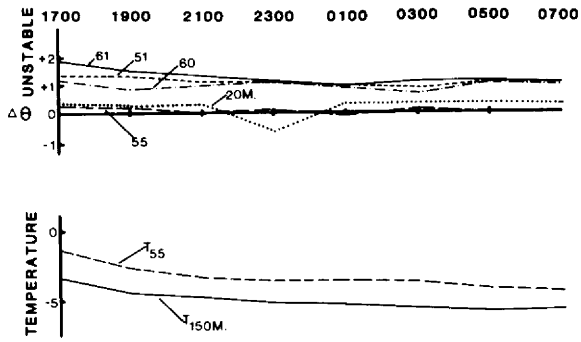

Fig. 9 Similar to Fig. 7, but for very strong winds and heavy snowfall.

strength of the surface cooling appears to suppress the thickness of the surface-based neutral layer so that it frequently does not extend to the height of the lowest tower sensor. Consequently, for these conditions surface temperatures throughout much of the city are generally stable.

Figures 7, 8 and 9 show time sequences of nighttime potential temperatures (computed relative to the top of the tower) for selected stations situated along the trajectory of the observed mean wind. These time sequences show the development of a nocturnal heat island for three contrasting weather conditions. Mean wind speed, direction and cloud cover data for each bihourly period in Figs. 7, 8 and 9 are given in Table 3. In Fig. 7, slightly superadiabatic profiles are initially observed for the stations in, and just downwind of, the city during strong cold advection; that is, for strong winds and rapidly falling temperatures associated with a frontal passage. These superadiabatic profiles generally persists until falling temperatures begin to stabilize at about 2000 LST, after which suburban temperatures and eventually, urban temperatures, (initially neutral) become stable relative to the tower top values. Although these conditions occurred relatively infrequently, the synoptic scale cold advection case is of interest because estimation of Q_{sc} depends upon distinguishing the effects of local radiative cooling from larger scale effects. The "crossover" of the temperature time series for the upwind station and the tower top, shown at the bottom of Fig. 7, is interpreted as the approximate time when local cooling overtakes that due to large-scale advection.

Temperature relationships in Minneapolis under ideal heat island conditions are shown in Fig. 8. All surface temperatures in this case are strongly stable relative to the top of the tower. However, the temperature difference between Station 59 and the lower level of the tower follows a nearly neutral profile after about 0300 LST as required by the heat island model. Because Station 59 is situated on relatively high ground within the city, the data in Fig. 7 suggest that an elevated neutral layer may form above the city during calm conditions with cold air collecting in the lower lying areas.

The temperature differences for the case shown in Fig. 9 occur during heavy snow and strong winds. Upwind of the city surface temperatures are nearly neutral relative to the tower, whereas within, and downwind of, the city the values are clearly superadiabatic. This effect appeared rather consistently during heavy snowfall or with low heavy cloud cover.

Table 3 Summary of mean bihourly weather conditions at the Minneapolis-St. Paul airport for the vertical temperature differences shown in Figs 5, 6 and 7: Wind speed (m/s) and direction (azimuth) were measured at 10 meters and cloud cover is in percent.

Hr.	1700	1900	2100	2300	0100	0300	0500	0700
(Fig. 5, February 6-7, 1979)								
WS	7.5	6.1	6.9	7.6	6.2	5.8	4.7	4.3
WD	820	310	320	320	320	320	320	310
C	10	0	0	0	0	0	0	20
(Fig. 6, January 24-25, 1979)								
WS	2.6	1.6	1.3	0.9	0.7	0.7	0.7	0.7
WD	330	290	310	---	---	---	---	---
C	0	0	0	0	0	0	0	0
(Fig. 7, March 3-4, 1979)								
WS	10.0	11.2	10.4	11.0	10.0	9.5	10.3	10.3
WD	20	10	20	10	10	360	10	10
C	100	100	100	100	100	100	100	100

Apparently, under these conditions, suppression of radiative heat loss allows sensible heat released with in the city to accumulate in a relatively shallow layer near the surface. The result is a surprisingly intense advective heat island effect.

The bulk effects of wind speed and cloud cover on the heat island are summarized in Fig. 10. This figure shows observed heat island intensities for Vancouver, B.C. as a function of wind speed (Oke, 1976), and for variable wind speed and cloud cover conditions in Minneapolis. Whereas Oke's values are for three hours after sunset, the Minneapolis data are for all nighttime observations. Notable in Fig. 10 is the persistence of significant and rather constant urban warming for wind speeds greater than about 4 m/s (this study; 8 m/s for Oke's data).

3.4 MODEL REFINEMENTS AND RESULTS.

Oke (1976) has pointed out that there are probably two distinct urban heat island effects that occur simultaneously: a boundary layer heat island responding to atmospheric dynamics above the city and a canopy heat island below rooftop level that is strongly influenced by very localized urban factors. It is difficult to parameterize a gridded physical model of the boundary layer in sufficient detail to reproduce precisely the maximum heat island intensities likely to be observed deep within the urban canopy where most heat island observations are made. Consequently, Oke found that for predicting maximum (clear sky) heat island intensity, Eqs. 1 and 2 were consistently outperformed by a simple empirical model based on wind speed and population.

Part of this problem is due to the requirement of Summers' (1965) model that wind speeds be constant throughout the area. We have modified Summers' model to allow for vertical (two-level) wind speed variation by introducing a separate calculation for temperature in the surface canopy layer. In the modified procedure an advective heat island is first computed for the grid area with Eq. 1 using observed (airport) wind speeds. A second heat island computation is then made wherein wind speeds for each grid area are adjusted for local surface roughness. This wind speed adjustment, using the power law referenced previously, systematically reduces the speed for each area and, in

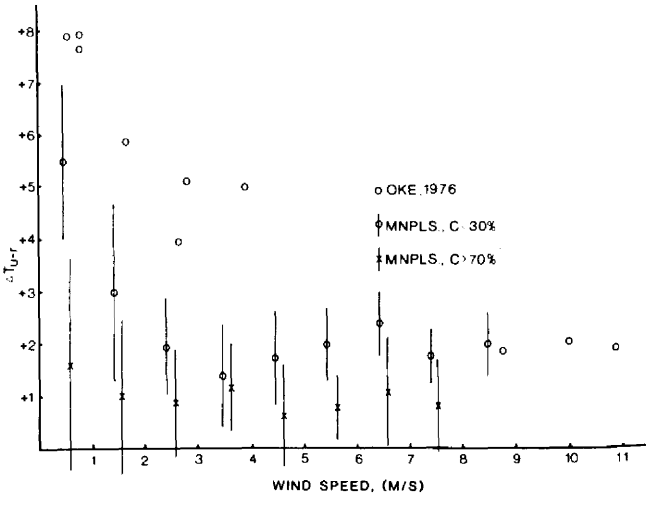

Fig. 10 Summary of nocturnal urban-rural temperature differences (ΔT_{u-r}) as a function of wind speed in Minneapolis during the winter of 1977-78 (November-March). The rural station for this analysis is #55 and the urban station location is represented by "*" (see Fig. 3). The vertical bars represent one standard deviation of the mean Minneapolis values for all nighttime data. The open circles without bars represent individual wintertime observations by Oke, 1976 for Vancouver, B.C. at three hours after sunset during clear conditions.

heavily urbanized areas, allows for significantly increased local temperature values. Exaggerated advective effects are avoided by using temperature values predicted by the initial (constant wind) computation for the initial upwind temperature of air entering each grid area. A more rigorous procedure using exchange coefficients to simulate mixing between the upper "boundary layer" and lower "canopy" heat islands is being studied.

Figure 11 shows typical model output for the entire grid area with the city limits (Minneapolis and western St. Paul) superimposed. In Fig. 12 comparative model runs show effects of the canopy adjustment. Also shown in Figs. 11 and 12b are observed urban-rural temperature differences (ΔT_{u-r}) for the same time periods. Relatively low observed values are indicated by (*). In each case, this monitoring station was situated several hundred meters downwind from the Mississippi River. The river gorge, although 300 to 400 meters wide, is a subgrid feature in the present model. Consequently, although its presence is grossly compensated for in the local area heat source distribution, its apparent local influence is not explicitly predicted.

The impact of the heat sink terms, Q_{sc} and Q_i, in Eq. 3 is illustrated in Fig. 13. The physical significance of the Q_{sc} term is to adjust Q_s for sensible heat loss from the air that is assumed to occur continuously throughout the area. Consequently, this rate of heat loss, plus Q_i, must be at least equaled by the source terms before the neutral urban sublayer (and hence the heat island) can begin to form. If Q_{sc} is simply removed from Q_s, frequently little or no heat

island effect will be predicted for large suburban portions of the study area. Moreover, Q_{sc} may occasionally surpass the maximum source values for the entire area causing no heat island to be predicted. We have adjusted the model for this unrealistic effect by assuming that in areas where the heat sink terms exceed the source terms (i.e. $Q_h + Q_t + Q_e - Q_{sc} - Q_i < 0.0$), the heat island intensity is estimated by Eq. 6.

$$\Delta T_{u-r} = \left(\frac{Q_h+Q_t+Q_e-Q_i}{Q_{sc}}\right) \Delta T_r \qquad (6)$$

In Eq. 6 the current rate of rural nocturnal cooling (ΔT_r) is partly offset by urban heating in each area, even though a neutral layer may not be predicted to develop in all grid areas. This adjustment also requires that air exiting a portion of the grid where heat sinks exceed sources has an initial h value (Eq. 1) of

$$h = \frac{\Delta T_{u-r}}{\alpha_o}$$

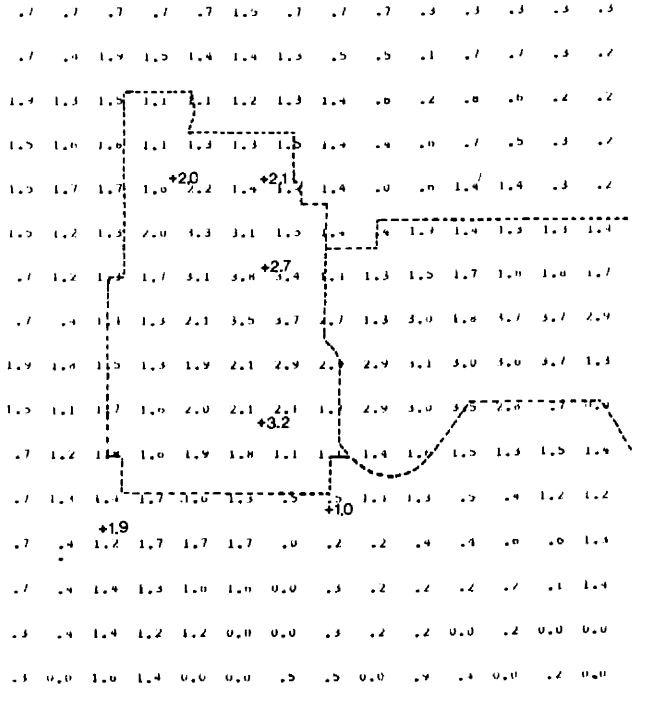

Fig. 11 Typical heat island model output showing ΔT_{u-r} for the Minneapolis-St. Paul area. Dashed lines represent the city limits of Minneapolis and St. Paul. Grid spacing in this figure is 2.0 km. Comparative observed values of ΔT_{u-r} are shown for stations that were operating during this time period (1800-2000, February 8, 1979). Meteorological conditions are clear skies, calm winds (.7 m/s) and temperature of -23.4°C.

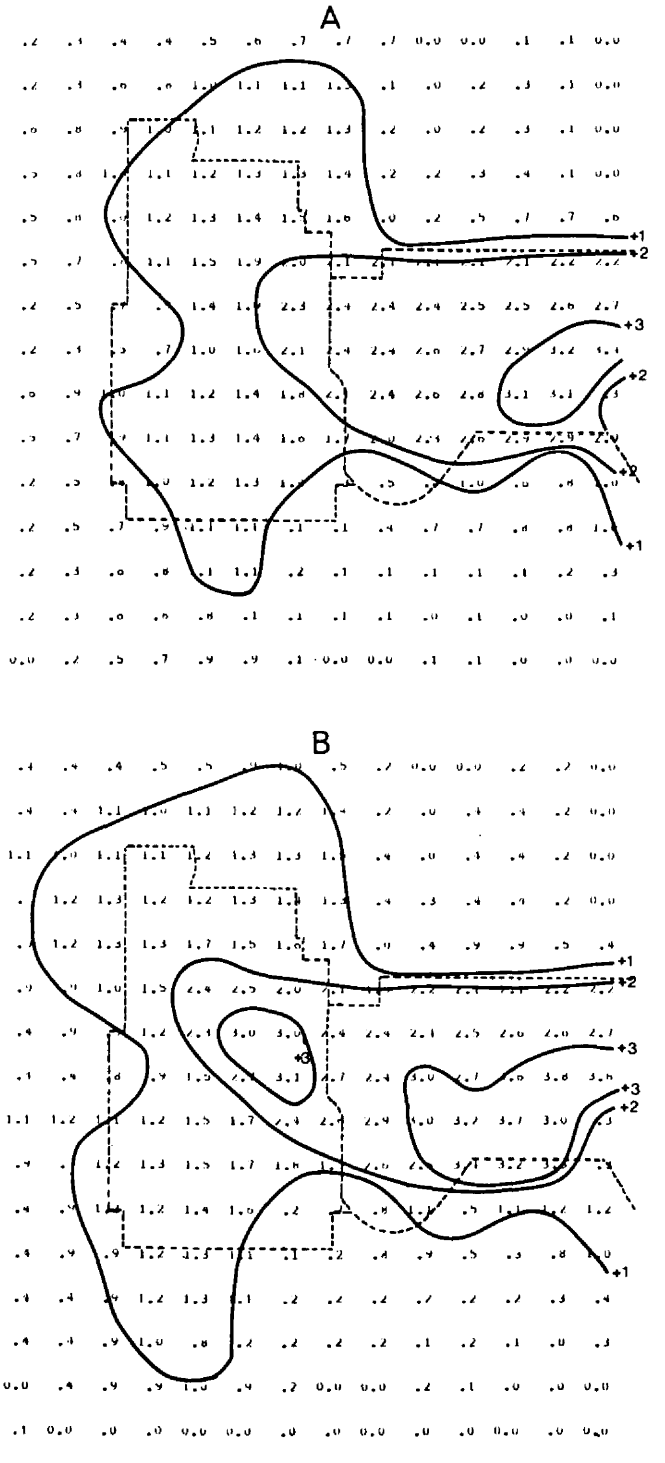

Fig. 12 A) Model output showing the mean estimated boundary layer heat island (ΔT_{u-r}) in the Minneapolis-St. Paul area for 1900 LST, January 21, 1979. During this time period skies were clear, winds were 3.5 m/s from 300° and temperature was -8.1°C. B). Estimated canopy layer heat island for the same time period.

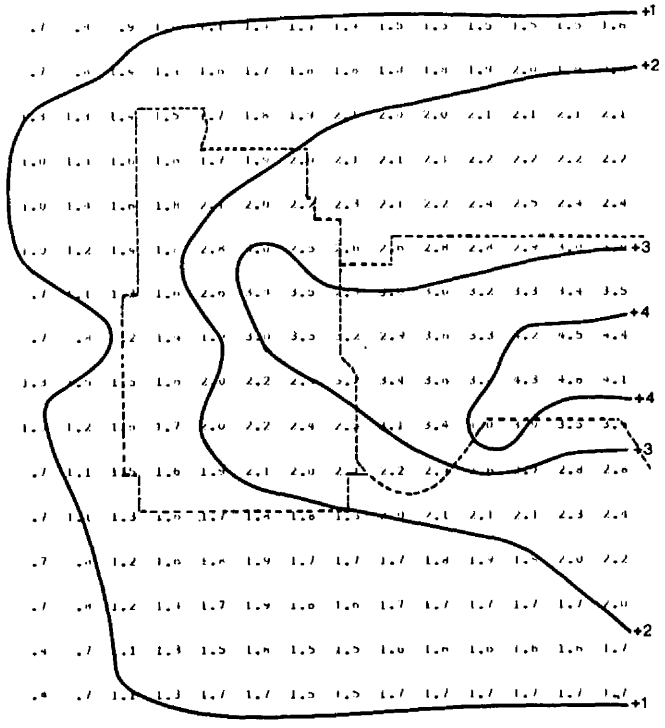

Fig. 13 Similar to Fig. 12B but with Q_i and Q_{sc} set equal to zero. Here gross overestimates of ΔT_{u-r} for purely advective warming but neglecting heat sinks are especially evident in downwind suburban areas.

where $\alpha_o = \Delta\gamma_r - \Gamma$, and $\Delta\gamma_r$ refers to the change in rural lapse rate during the current bihourly interval.

Other investigators have relied on various means to obtain values of γ including special radiosonde launches, aircraft soundings and simple estimates. Our computations require bihourly values of γ for entire seasons. Because bihourly rural sounding data are not available, vertical temperature profiles must be estimated from simple observations of local temperature, wind speed and cloud cover. However, the reliability of such procedures is limited. In attempting to develop a more reliable means for predicting γ, considerable effort was spent analyzing the mean temperature profile required to reproduce (using Eqs. 1 and 2) observed heat islands for various wind and cloud cover conditions. For wind speeds of less than 4 m/s, the required stability values were generally simple inverse functions of wind speed and cloud cover. However, for wind speeds greater than 4 to 5 m/s, increasingly strong and obviously unrealistic stabilities were required to obtain the persistent heat island effects illustrated in Fig. 10.

Restricting our attention to nighttime heat islands, we have derived a system of simple empirical equations (Eqs. 7, 8 and 9) that provide useful approximating of γ for most conditions. These equations, which have not been rigorously optimized, use available atmospheric observations to estimate the effects of radiative and turbulent processes controlling stability in the lower boundary layer.

Our approach to estimating γ for variable weather and times of day is to first restrict γ to stable values for all weather conditions. A limiting, slightly stable value applies for all daytime and very windy or cloudy cases. For other conditions, beginning at sunset, we assume that air temperature remains constant at some level, Z_i (Eq. 7). M_1 is an empirical constant, the present value of which is 100. Below this level sensible heat is assumed to be lost radiatively at the surface and cold surface air is mixed by forced convection. The depth of turbulent mixing, or Z_i, for each time step increases with wind speed and is decreased with increased rates of surface cooling where cooling is indexed by the current (last 2 hours) change in rural air temperature, ΔT_{ri}. A linear profile is then computed as the ratio of ΔT_{ri} and the estimated mixing depth, Z_i (Eq. 8).

$$Z_i = M_1 \frac{U_i}{\Delta T_{ri}} \tag{7}$$

$$\gamma = \frac{\sum_{t=0}^{t} \Delta T_{ri}}{Z_i} \tag{8}$$

$$\alpha = (\gamma - \Gamma)\left(\frac{M_2}{U_i}\right)(1 - C_i^2) \tag{9}$$

Formulations for estimating Z_i have been advanced by several authors (see Deardorff, 1972; Delage, 1974; and Blakadar, 1976). Yu (1978) tested some of these formulas against actual observations. A simple relation of the form,

$$Z_i = \frac{k u_*}{f},$$

which simplifies to

$$Z_i \simeq 125\ U,$$

has been shown to provide fairly good hourly estimates of Z_i when repeatedly initialized with the closest available sounding data (Benkley and Schulman, 1979). Here k, u_* and f are the Von Karman constant, friction velocity and the coriolis parameter, respectively. This formula and several others including Eq. 5 were tested, following Yu (1978), against the stability requirements of Eqs. 1 and 2 for observed Minneapolis heat island data. Sets of profiles were predicted with Eq. 8 using the Z_i values from each mixing height formula. Correlation coefficients for several sets of predicted versus required γ values are shown in Table 4. On the basis of these results Eq. 7 has been adopted for our model.

As noted in the previous section, Eqs. 7 and 8 also allow us to compute a consistent value of Q_{sc} rather than relying on gradient relationships and estimates of thermal diffusivity. The second and third factors on the right-hand side of Eq. 9 further adjust the vertical temperature profile for specific observed effects of strong winds and clouds. The present value of the empirical constant M_2 is 4.5.

Bowling and Benson (1978) has illustrated the importance of γ by showing that the shape of the vertical lapse rate profile near the surface, in addition to the mean intensity of the lapse rate, is crucial to heat island predictions using Summers' (1965) model. For example, if the rural profile is

Table 4 Comparative correlation coefficients for predicted linear temperature profiles versus profiles required to satisfy Eqs. 1 and 2 for observed Minneapolis heat island values. Conditions for this test were restricted to relatively clear skies (C < 50%) and winds from the northwest. Predictor No. 3 is Eq. 7 where M = 100.

Z_i Predictor	Wind Speed Less than 4 m/s (n=22)	Wind Speed Greater than 4 m/s (n=27)
	r	r
1. $125U$	0.54	0.44
2. $\frac{50U^2}{\Delta T_r}$	0.65	0.79
3. $\frac{100U}{\Delta T_r}$	0.75	0.84

strongly stable in a shallow layer at the surface and less stable above, strong temperature gradients will develop at the urban periphery with much weaker gradients through much of the city. Conversely, strong stability in an elevated layer may result in small peripheral gradients and more intense gradients closer to the center of the city. For changing wind and temperature conditions that might create variable or layered profiles (i.e. $Z_2 < Z_1$), the present model can retain and apply lapse and thickness values for as many as four distinct overlying layers.

We have noted that under very stable conditions cold air pooling following the topography occurs within cities (Reiter et al., 1980, 1981b). For light and variable winds (speeds less than 1.5 m/s) the model algorithm is modified to limit the upwind fetch. In this case, a minimum wind speed of 0.15 to 0.3 m/s is assumed and advection restricted to the immediate grid area. Also, under these conditions, urban-rural temperature differences are calculated for a single reference elevation (the level of the highest source area) and surface values are then computed for lower-lying areas assuming that the lapse rate in the surface layer follows the estimated rural value.

Several additional adjustments are made to γ for specific weather conditions. If nighttime temperatures begin to rise sharply, the model defaults to the limiting, slightly stable value. If heavy cloud cover appears, but observed temperatures do not rise, established stable profiles are retained and effected by winds only; that is, the cloud cover adjustment in Eq. 9 is deleted. Moreover, if heavy cloud cover develops in the morning before sunrise, established stability is retained until increased temperatures or clearing skies warrant the default stability value. This rather complex sequence of adjustments has yielded values of γ that allow us to reproduce the bulk features of our observed urban temperature fields for most cases. However, significant departures have been observed and the current procedures require additional refinement. Our ultimate goal is to reproduce a seasonal urban temperature "climatology" at each of the urban observation stations and, when sufficient accuracy is obtained, to run off our energy demand models using exclusively modelled meteorological data.

4.0 ECONOMIC FACTORS IN WEATHER DEPENDENT DEMAND FOR ENERGY.

4.1 THE IMPACT OF WEATHER FORECAST ON THE COST OF GENERATING ELECTRICITY.

4.1.1 Background

It is commonly known that the demand for electric power is sensitive to weather factors. Because of this linkage it is generally believed that accurate load forecasts based on improved weather forecast information could enable operators to utilize more efficient schemes for scheduling generating plants and thereby reduce fuel and operating costs. In this section we describe a three-part study to assess the potential value of improved weather forecasts to generation and transmission utilities. The three parts of this study are: 1) estimate the effects of weather variables on electricity demand, 2) construct a model to schedule generating plants in light of forecast loads, and 3) estimate the economic value of improved weather forecasts by determining how they alter forecast loads and subsequent generation schedules.

The study centers on the area supplied by the Public Service Company of Colorado (PSCC), the regional energy utility serving most of the State of Colorado (see Fig. 1 in Section 2.1). Seventy percent of PSCC's power customers are located in the immediate Denver metropolitan area, and hence it was presumed that most of the company's load variability was closely linked to conditions in this one relatively concentrated geographical location.

The demand forecasting model, displayed schematically in Fig. 14, reflects this assumption. The weather-related load was predicted using the variables shown in the lower block. The proportion of the load which is sensitive to the patterns of industry and commerce are displayed in the upper block. Weekends were treated differently than weekdays, and Mondays and Fridays were distinguished within the work week. A set of 24-regression equations was utilized to capture the hour by hour variation in load stemming from the normal behavioral patterns anticipated throughout the day. The end product is a model which forecasts the PSCC 24-hour load profile. These forecasts can be made sensitive to either anticipated temperature variations or they can be obtained by

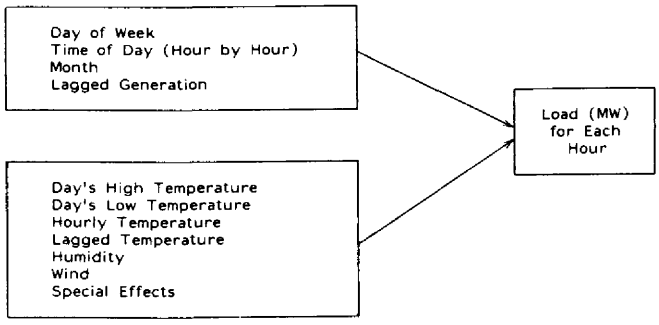

Fig. 14 Conceptual illustration of the demand forecasting model showing both the meteorological and nonmeteorological factors used to estimate hourly power demand.

assuming some form of persistence in the weather or load pattern.

One would expect a direct relationship between weather and load forecast accuracy. However, the worth of improving PSCC's ability to predict the hourly profile hinges on the cost of generating electricity to meet the anticipated demand. Such costs in turn are shaped by the marginal expense of individual generating units, start-up and shutdown costs, spinning reserve requirements, and the amount paid other producers for supplemental power. The benefits of improving the PSCC's ability to predict its load profile are derived from: 1) a reduction in the number of instances when excess capacity is unnecessarily maintained, 2) a reduction in the number of times expensive power is unnecessarily purchased from outside sources, and 3) an improvement in overall scheduling efficiency.

As shown in Fig. 15 a variety of weather forecasts were fed to the load forecasting model. The resultant hourly demands were used to drive an economic model which was designed to minimize the daily cost of meeting these loads. The resultant costs were then compared, as is illustrated in Fig. 16, to determine the value of refining weather forecasts. The conclusions were sharpened through a series of experiments performed to determine both the accuracy and timing needed before a utility such as PSCC would routinely utilize weather forecast data in its day-to-day scheduling operations.

4.1.2 Estimating the Effects of Weather on the Demand for Electricity.

The record of PSCC's power demands displays a sinosoidal pattern which in part can be explained by weather but also reflects the pattern of daily and weekly activity observed throughout the service region. One can isolate the "normal" daily pattern of household and business power demands by treating weekends and holidays separately. Also, as will be demonstrated below, Monday and Friday exhibit patterns of use that are quite different from those recorded for midweek days.

In examining both the literature (Davis, 1958) and PSCC's 24-hour load profile it became evident that

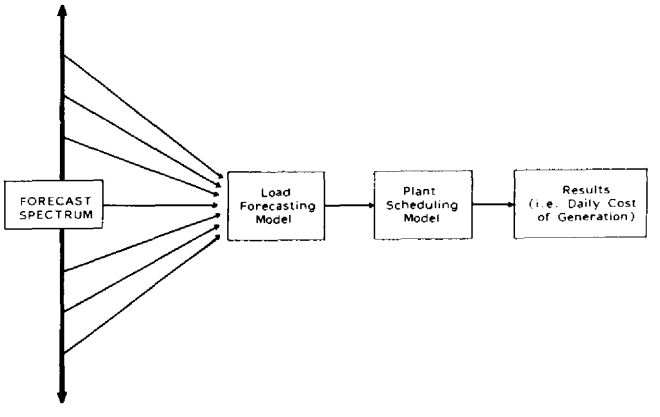

Fig. 15 Sequence of experiments performed to establish the potential economic value of improved weather forecasts to an electric generation utility.

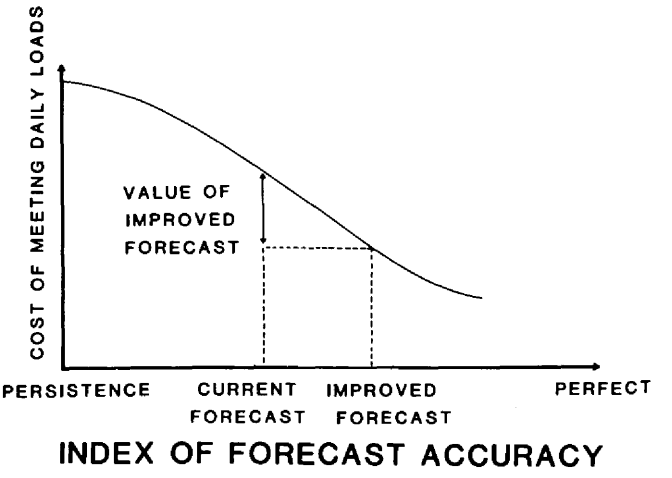

Fig. 16 Conceptual illustration of the relationship of reduced generation costs to improved weather forecast accuracy.

weather factors played an important role. Peak loads coincided with peak temperatures in the summer. Humidity, cloud cover, precipitation and wind speed also affect air conditioning requirements and hence shape demand. Important too is the fact that cloud cover and visibility influences the use of lighting. In addition, it was expected that thermal storage in Denver's large office buildings would necessitate the use of lagged temperature in the load equations.

Since all weather data utilized in the study were recorded at one location only (Denver's Stapleton Airport), one would anticipate that some demand would go unexplained. Weather fluctuations and consumption patterns peculiar to the PSCC's non-Denver customers would be the most likely cause for such unexplained variation.

(a) Procedure.

PSCC's system load was disaggregated into its principal components. The fixed portion, or base load, reflects the "normal" pattern of commercial and residential usage. It is shaped by day of week, time of day, and season. The remaining variation stems from the influence of weather and the "capricious" factors illustrated above.

Separate equations were obtained for each hour in the day, for weekends, weekdays, and each month during the summer (June, July and August). These equations were modified slightly to account for the use of weather forecasts be it a true forecast or simply persistence. Three different sets of equations (one set for each month) form the foundation upon which the entire study was based. Each set contains 48 hourly equations; 24 for both weekends and weekdays. These sets are distinguished only by the weather component and the inclusion of lagged generation.

The daily model (Eq. 1) utilizes a single forecast and the previous day's observed weather.

$$Y_t = f(D, W, W_{-1}) \qquad (1)$$

where $t = 1, 2, \ldots, 24$; Y_t is the load demand each hour; D is the day of week; W is a set of forecast

meteorological variables for the day in question; W_{-1} is the previous day's weather. However, in the absence of the current day's weather forecast, only past occurrences (W_{-1}) would be available and the resultant load forecast error would be larger.

One could also conceive of a set of equations whereby information about recent loads in addition to a sequence of weather forecasts would improve the model (Eq. 2).

$$Y_t = f(D, Y_{t-a}, W_t, W_{t-a+1}) \qquad (2)$$

where Y_{t-a} is the demand for hour (t-a), W_t is a set of meteorological measurements (forecasts) for hour t, W_{t-a+1} is the meteorological set for period (t-a+1). In this model temperature, wind velocity, etc. must be projected for a number of hours into the future. The chief difference between this approach and the previous model is the sequence of meteorological readings and the inclusion of lagged generation, Y_{t-a}. The latter is available to the utility and may well capture enough of the weather's influence to enable the scheduler to utilize lagged generation alone. This possibility spurred the development of a third equation set.

$$Y_{t+1} = f(D, Y_t, Y_{t-1}, \ldots, Y_{t-a}) \qquad (3)$$

where all variables have been defined in Eqs. (1) and (2). Y_{t+1} is used to compute Y_{t+2}, and Y_{t+2}, Y_{t+3} and so on. A load profile could be derived by simply knowing the pattern of generation prior to the current time period. The profile could then be revised in light of actual occurrences and a new profile systematically made available to the plant scheduler.

Before proceeding to estimate the three models just discussed, several preliminary steps were taken to determine the appropriateness of the regression technique. First, the distribution of electric demand for selected hours was tested for normality; the hypothesis that the distribution was normal was not rejected. Second, a plot of temperature vs. demand shown in Figs. A1 and A2 (Appendix A) strongly suggest a linear relationship despite a substantial temperature range.

The specific expression estimated for Eq. (1) above is given in Eq. (4).

$$\hat{Y}_t = \hat{b}_{0t} + \hat{b}_{1t}M + \hat{b}_{2t}F + \hat{b}_{3t}H + \hat{b}_{4t}HxH(-1) + \hat{b}_{5t}H(-1) + \hat{b}_{6t}L \qquad (4)$$

$$t = 1, 2, \ldots, 24$$

where: $\hat{b}_{0t}, \hat{b}_{1t}, \ldots, \hat{b}_{6t}$ are estimated coefficients,

$$M = \begin{cases} 1 \text{ if Monday} \\ 0 \text{ otherwise,} \end{cases}$$

$$F = \begin{cases} 1 \text{ if Friday} \\ 0 \text{ otherwise,} \end{cases}$$

H = the high temperature of the day,

H(-1) = the high temperature of the previous day,

L is the low temperature of the day.

Tuesdays, Wednesdays and Thursdays were treated as one category. The effect of weather variables on the day's demand can be derived as

$$\frac{\partial Y_t}{\partial H} = b_{3t} + b_{4t}H(-1) \quad t = 1, 2, \ldots, 24 \qquad (5)$$

for the high temperature and

$$\frac{\partial Y_t}{\partial L} = b_{6t} \quad t = 1, 2, \ldots, 24 \qquad (6)$$

for the low temperature. Equation (5) shows that the effect of the day's high temperature on demand at hour t increases by b_{4t} MW per 1°F increase above the previous day's high temperature. Equation (6) shows that if the low temperature increases by 1°F, demand increases by b_{6t} MW. The results for weekdays and weekends are displayed in Tables B1 through B3 (Appendix B).

The model for weekend days, Eq. (7), can be interpreted in the same way.

$$\hat{Y}_t = \hat{b}_{0t} + \hat{b}_{1t}X_1 + \hat{b}_{2t}X_2 + \hat{b}_{3t}S + \hat{b}_{4t}HDY + \hat{b}_{5t}H + \hat{b}_{6t}HxH(-1) + \hat{b}_{7t}H(-1)\,\hat{b}_{8t}L \qquad t = 1, 2, \ldots, 24 \qquad (7)$$

where:

$$X_1 = \begin{cases} 1 \text{ if July} \\ 0 \text{ otherwise,} \end{cases}$$

$$X_2 = \begin{cases} 1 \text{ if August} \\ 0 \text{ otherwise,} \end{cases}$$

$$S = \begin{cases} 1 \text{ if Saturday} \\ 0 \text{ otherwise,} \end{cases}$$

$$HDY = \begin{cases} 1 \text{ if holiday} \\ 0 \text{ otherwise.} \end{cases}$$

The results for the weekend model are displayed in Table B7 (Appendix B).

The specific form for the second equation set is given in Eq. (8).

$$\hat{Y}_t = \hat{b}_{0t} + \hat{b}_{1t}M_t + \hat{b}_{2t}F + \hat{b}_{3t}Y_{t-a} + \sum_{i=t-a+1}^{t} \hat{C}_{jt}T_i \qquad (8)$$

$$t = 1, 2, \ldots, 24$$

$$i = 1, 2, \ldots, a$$

where: Y_{t-a} = demand at hour (t-a),

T_i = temperature at hour i (= t-a+1).

The other variables are defined as before. The term $\hat{b}_{3t}Y_{t-a}$ captures the effect of hour (t-a) on the demand at t. The term $\sum_{i=t-a+1}^{t} \hat{C}_{it}T_i$ exhibits the combined effect of temperatures from hour (t-a+1) through hour t. Note that weather factors other than temperature have been omitted. Their exclusion

reflects the fact that they did not contribute any significant explanatory power to the model. The estimated coefficients and resultant statistics are displayed in Tables B4 through B6 in Appendix B[1].

Lastly, the omission of weather factors yields the following model:

$$\hat{Y}_t = \hat{b}_{ot} + \sum_{i=t-a}^{t-1} \hat{b}_{it} Y_i \qquad (9)$$

All variables have been defined elsewhere except the right-hand term which is similar to that in Eq. (7). It captures the combined effects of the previous hours generation on the current generating requirements. The results are provided in Tables B8 through B10 in Appendix B.

A review of PSCC's generation statistics revealed that the system's peaks occurred between the summer hours of 2 to 3 p.m. Table 5 illustrates the extent to which temperature influences demand. For example, during the month of August a one-degree error in both forecast high and low temperature results in a respective 14.8 MW and 10.6 MW difference in demand. The combined effect of a 10-degree (F) error is 254 MW, enough of a variation to cause a significant impact on scheduling costs.

4.1.3 Predicting the Weather and Forecasting Loads.

The value of predicting the weather is linked to how the prediction translates into an improved load forecast. Moreover, load forecast must induce a change in the way plants are scheduled. If neither of these transpire then knowing the weather in advance will be of little or no value to the generating company. Several criteria for evaluating load forecasts may be drawn from these considerations.

1. The first and probably the most important criterion is the maximum error. The utility company is committed to supply the total amount of electricity demanded by customers. If the accuracy of load forecasting is low, it is necessary to carry substantial amounts of capacity over the actual demand to prevent the system from power failure.

2. An error late at night may be less critical then during peak hours. Late night loads are normally only a fraction of the peak, and the utility company usually carries capacity well above nightly demands. This is because large generating units are designed for continuous operation. Hence, minor fluctuations experienced during these off-peak hours can easily be accommodated by adjusting the output of these base units.

3. Galiana (1976) suggests statistical criteria for evaluating error. A 24-hour peak load prediction for a system with a peak load of 5000 MW will fall into one of the following classes:

   - A "good" performance means less than 2 percent error
   - A "fair to poor" performance means 2-5 percent error.
   - A "gross" error means more than 5 percent error.

Table 5 Effects of temperatures on the electric demand at 2-3 p.m. in June, July and August.

	High (MW/°F)	Low (MW/°F)	Combined High and Low
June	9.9	19.0	28.9
July	15.4	5.2	20.6
August	14.8	10.6	25.4
Weekend	10.3	6.9	17.2

It is difficult to reduce the results of our three models so as to evaluate them according to Galiana's criteria. Root mean square errors computed for each model are shown in Table 6. Based on these results it appears that we have been able to reduce error to 2.5 to 4 percent of the average load of 2500 MW. Figures 17 to 19 demonstrate the day-to-day fluctuation in the performance of each model. The plots show the difference between forecast and actual load. As expected, the better the weather forecast, the narrower the band of error.

(a) Electric Generation Model.

The purpose of this section is to develop an electric generating model which can be used to evaluate different kinds of load forecasting systems. Operating and maintenance costs as well as fuel costs are calculated hourly. Although output data are generated hourly, the information is summarized daily to facilitate comparison for alternate load forecasting systems. The results include generating costs, start-up costs and penalty if the load cannot be met.

The schematic diagram in Fig. 20 builds on the introductory model sketched in Fig. 14. (The weather data and load models were discussed previously.) The resultant demand projections form a vital cog in the generation program. These demands, merged with system operating data and policy, formed the framework from which the value of improved forecasts are derived. The operations data provide the raw ingredients for costing the various units which could potentially be called upon to meet demand. System operating policy and information about the operation of hydro- and nuclear units frame the constraints to which eventual operating plans must conform.

Plant maintenance is scheduled so as to insure that system reserves are not compromised. This problem is accommodated within the generation model by allowing the user to decommission one or more units for a specified period of time. By doing so these

[1]The weekend model was not estimated for this equation set since a single high/low forecast replicates the load profile actually observed. Hence, any improvement in the structure of forecast, i.e. a sequence instead of a single 24-hour prediction, cannot improve the model's predictive abilities.

Table 6 Maximum positive difference and mean square error of demand estimates for three weather dependent demand models.

	Model 1						Model 2[1]		Model 3[2]	
	Actual High and Low		Forecast High and Low		Previous Day (Lagged) High and Low		Short-Term With Weather Factors		Short-Term Without Weather Factors	
	a[3]	b[4]	a	b	a	b	a	b	a	b
June	-1.9	48	-18.9	71	4.8	91	-2.1	34	-0.4	53
July	-1.2	63	3.0	85	0.9	104	1.8	51	-3.5	64
August	-2.0	62	-17.0	84	5.3	108	-9.1	53	-3.4	64
Average of 3 Months	-1.7	58	-11.0	80	3.7	101	-3.1	46	-2.4	60

(1) Forecasts were made twice a day; once at hour 9 and once again at hour 15.

(2) Same as footnote (1).

(3) a is the mean deviation (MW) completed as follows: Σ (estimated value - actual value)/number of observations.

(4) b is the mean square error (MW) given by: Σ (estimated value - actual value)^2/number of observations.

plants are made unavailable to meet the day's projected loads. Hydro, pumped hydro, and nuclear units are treated in a similar fashion.

Conventional hydroplants are scheduled each day by specifying the period over which generation (MW) is to occur. This problem is treated in the model as a simple downward shift in the load which must be met via the thermal units (see Fig. 21). Pumped hydro-units consist of a turbo-alternator located between two reservoirs, one higher than the other. As illustrated in Fig. 22, storage can be used to supply power during peak load periods. This ability to store energy results in a flatter generation curve. As a result, the thermal capacity needed during the peak hours is reduced and the demand is transferred to the off-peak base units which are more fuel efficient. This means that water is pumped from lower reservoirs to higher reservoirs at night, and is used to generate hydropower in the afternoon.

Since the PSCC's nuclear units have proved to be an unreliable source of power, the model was designed to treat these units in a fashion similar to that described for scheduled maintenance. The PSCC's Fort St. Vrain plant can be taken off-line for a specified period during which the generation model will only select thermal plants to meet the hydro-adjusted loads.

Firm purchase/sales commitments are the last exogenous constraint built into the model. Due to a lack of capacity, PSCC is not currently obligated to sell electricity to other companies. In fact, often throughout the summer the company must purchase power. The contract to buy electricity specifies the cost and the upper limit which may be purchased for each day and over the course of the month. In order to simplify the problem, the scheduling model restricts the amount that may be purchased, i.e. one-thirtieth of the monthly contract. The purchased power is then treated much like another thermal plant. Its marginal cost is ranked with the other plants and power is utilized up to the daily limit.

(b) Unit Commitment.

Start-up and synchronization can require from seven to nine hours for the large coal fire base units, one to seven hours for the intermediate plants and about twenty minutes for combustion turbines and hydrofacilities. Because of some of these fairly lengthy lead times, the PSCC must determine early in the day which generating units will be committed and available for scheduling as demand dictates. It is assumed that commitment proceeds with an eye toward minimizing costs subject to the maintenance of a safety margine, i.e. spinning reserve[2].

More specifically, unit commitment is a product of the following interwoven factors:

1. Short-term load forecast - The day's load profile provides the basis for initial commitment.

2. System reserve requirements - PSCC maintains excess capacity because of unanticipated load fluctuations. If perfect hourly forecasts could be obtained from the demand model then such a reserve would be unnecessary. The user may specify any reserve requirement thought to be prudent, given current forecasting accuracy.

[2]Spinning reserve is a safety cushion of reserve power which could be utilized to meet unanticipated load fluctuations. It is defined as the generating capacity that is on-line in excess of system load.

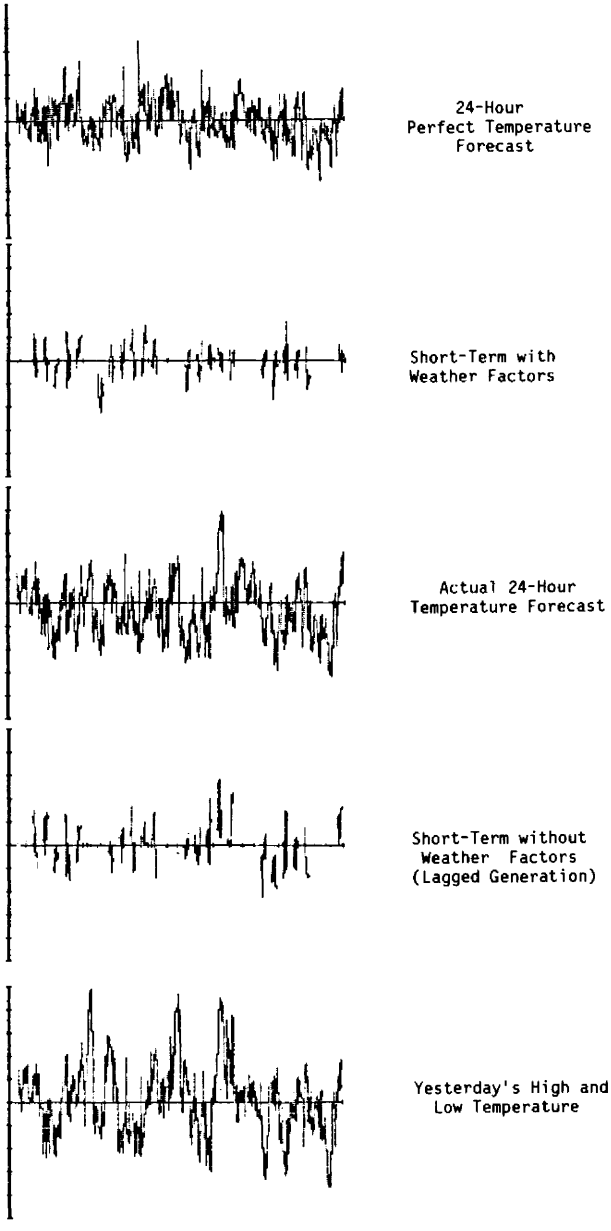

Fig. 17 Comparative errors (40 MW/unit) for typical daily demand forecasts by each of the demand models summarized in Table 6, for June.

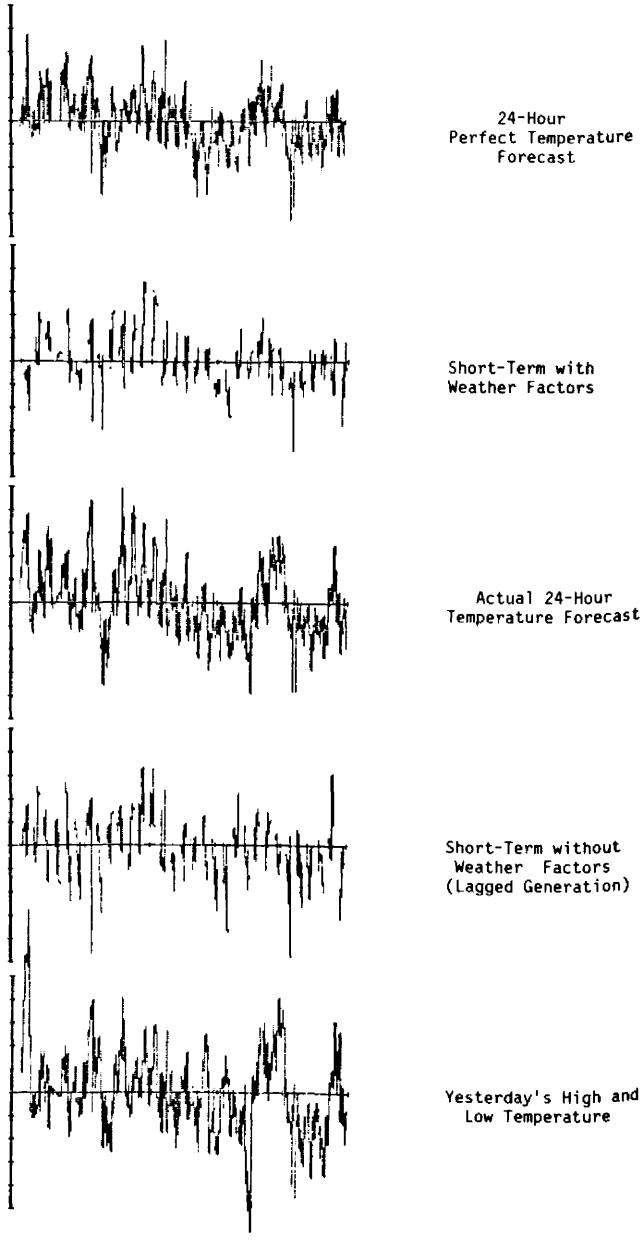

Fig. 18 Similar to Fig. 17, except for July.

3. System security - PSCC must also maintain a reserve in the event of unexpected unit or transmission line failure. This reserve, too, is a variable which the model allows the user to specify. The spinning reserve maintained for both system reserve and security is designed to protect the company's generation system from the hazards of blackouts (brownouts). It does this by enabling the company to supply enough temporary generating capacity until additional units may be activated or emergency purchases are secured. There are several rules of thumb which apply to spinning reserve: a) 25-20 percent of the expected load, b) maximum generation of the largest unit in operation; and c) the margin of error in the load forecast (percent) plus the capacity lost if the system's largest unit were to fail. For the purposes of this assessment plant failure was ignored and a spinning reserve of 100 MW was assumed to cover security requirements.

4. Start-up and shutdown cost - Start-up costs are unique for each of the PSCC's plants, being positively related to generating capacity. For example, PSCC's Commanche 1

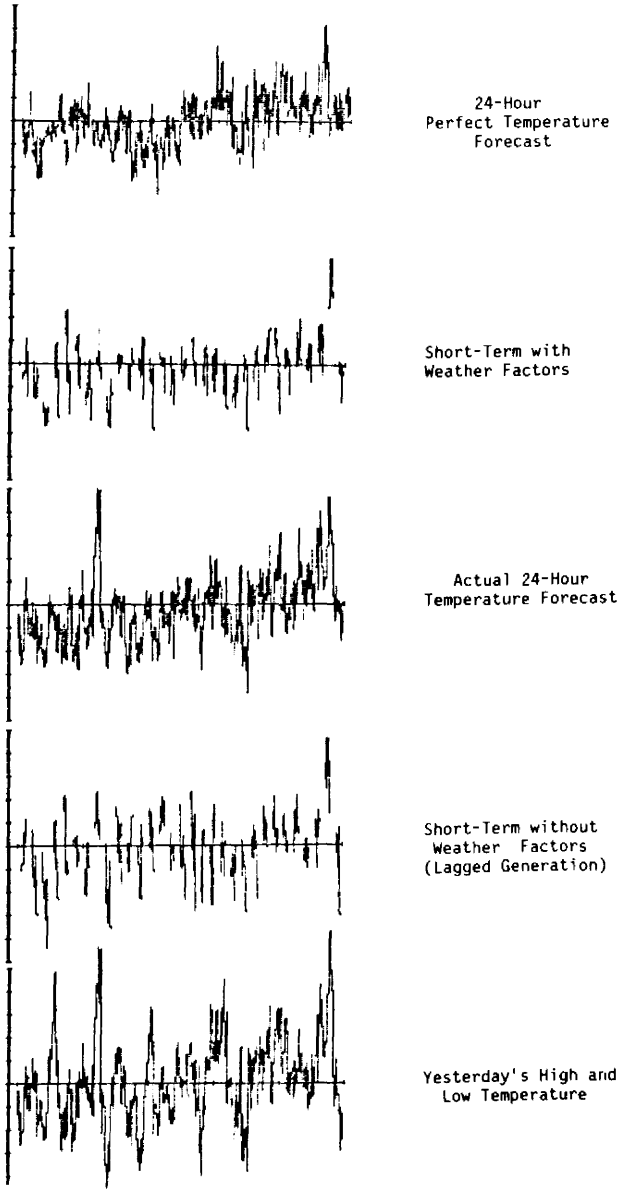

Fig. 19 Similar to Fig. 17, except for August.

(300 MW maximum power) costs $6633 to activate, where Arapahoe 2 (48 MW) only costs $355. Shutdown costs were considered negligible enough to be omitted from the analysis.

5. Minimum level of fuel costs - Once activated a plant will sustain fuel costs reflecting a minimum power setting.

6. Incremental (marginal) fuel costs - The relationship between fuel used and power generated was established for each of PSCC's units. The resultant linear regression equations explain 99 percent of the operating costs. Because of this relation it was possible to utilize a constant marginal cost

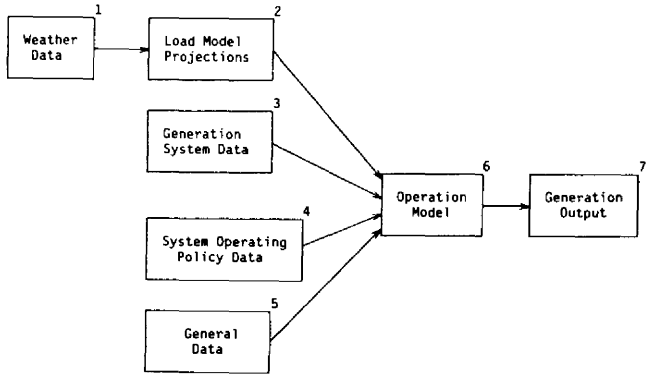

1) Weather Data:
These are supplied outside generation schedule. The specific meteorlogic factors were discussed in Section 4.1.2.

2) Load Data:
The hourly load forecast is produced with or without using weather data. See Section 4.1.2 for the models utilized.

3) Generation System Data:
a) Individual Unit Characteristics:
Maximum Output (MW)
Minimum Output (MW)
Fuel Cost ($/Btu)
b) Hydrounits
c) Pumped Hydrounits
d) Nuclear Units

4) System Operating Policy Data:
a) Spinning Resume Rules
b) Securing Requirement
c) Unit Maintenance Scheduling
d) Commitment/Dispatch Criteria

5) General Data:
a) Study Time Period
b) Firm Purchase and Sale

6) Operating Model is Described in Text

7) Generation Output:
a) Generating Cost
b) Start-up Cost
c) Purchase Cost
d) Penalty

Fig. 20 Basic elements of the demand scheduling model. Note that blocks 1 and 2 also implicitly include the nonmeteorological factors illustrated in Fig. 14.

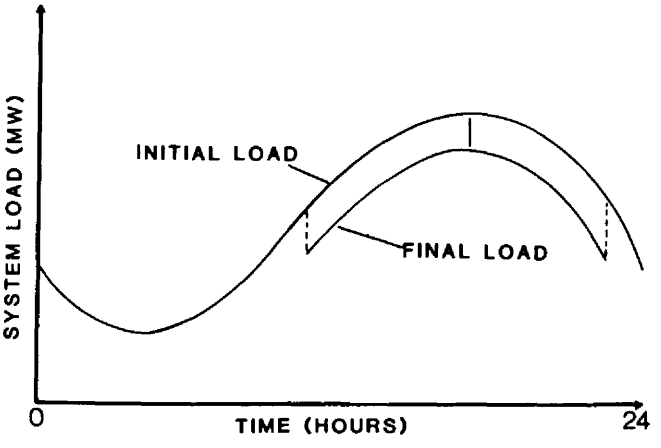

Fig. 21 Illustration of the reduction of peak thermal system loading achieved by hydroscheduling.

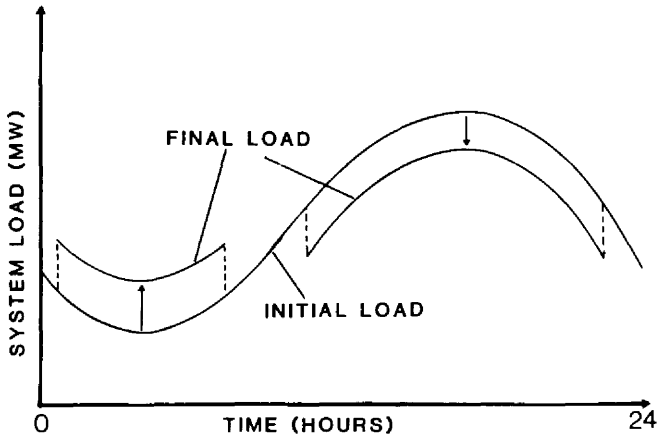

Fig. 22 Flattening of the diurnal load curve by pumped hydroscheduling. Pumping occurs during off-peak hours and hydrogeneration during peak hours.

relationship for all units. This finding proved fortuitous in that it simplified the mechanics of obtaining minimum cost solutions, a point discussed in greater detail below.

7. Minimum and maximum level of generation - These technical constraints are specified for each unit.

8. Maintenance and operating costs - Normal maintenance and operation costs were not included in the incremental fuel equations. These costs were obtained instead by dividing total operations and maintenance expenses by the megawatts generated. The resultant outlay per megawatt by plant was utilized to factor the daily cost of meeting loads.

9. Cost of purchasing interchange power - This cost is specified by contract.

10. Cost due to transmission losses - Transmission losses are negligible for the intrafirm transfer of electricity, but they must be accounted for whenever interchange power is purchased. An X percent loss was factored into the contract purchase price as follows:

$$\text{Adjusted Marginal Cost} = \text{Original Marginal Cost} \cdot \left(\frac{1}{1-\frac{X}{100}}\right)$$

$$\text{Adjusted Hourly Cost} = \text{Origional Hourly Cost} \cdot \left(1-\frac{X}{100}\right)$$

Based upon the above information the commitment problem can be formalized so as to determine the unique plant schedule which minimizes total operating cost while obeying each of the system's constraints. The cost function for both thermal generating units and purchased power can be represented by,

$$c_i = a_i + b_i G_i \qquad i = 1, \ldots, m, m+1 \ldots M(k)$$

where $c_i \equiv$ cost of generating power from unit i,

$a_i \equiv$ start-up cost of generator i,

$G_i \equiv$ power generated from i,

$m \equiv$ number of thermal units,

$M-m \equiv$ number of purchase possibilities,

$b_i \equiv$ marginal cost of unit i.

Note that the cost is represented by the sum of start-up plus the marginal cost times generated power. That is, each megawatt of power generated requires approximately the same amount of fuel, regardless of generation level. Hence, operation costs are simply this constant increment times the power generated.

The object of commitment is to minimize the total daily cost of meeting anticipated loads. Hence, Eq. (10) must be expanded to include the entire 24-hour period. Several additional constraints must be appended to the problem. First, purchased power is restricted to daily limit, referred to below as "P". Second, an individual thermal unit operates within a restricted range, i.e. G_i has a lower and upper bound. Third, the maximum output from the thermal units must meet or exceed the hourly demand plus spinning reserve. Both the objective function and the associated constraints are given in Eqs. (11) through (15).

$$\text{Daily Cost} = \sum_{t=1}^{24} \sum_{j=1}^{M} (\gamma_{it} a_t + b_i G_{it}) \tag{10}$$

subject to:

$$\gamma_{it} = q_{it} - q_{it-1}, \text{ where } q_{it} = \begin{cases} 1 \text{ if } G_{it} \neq 0 \\ 0 \text{ if } G_{it} = 0 \end{cases} \tag{11}$$

$$\gamma_{it} \geq 0 \tag{12}$$

$$\sum_{i=1}^{M} \bar{G}_{it} \geq D_t + S_t \tag{13}$$

$$\underline{G}_i \leq G_{it} \leq \bar{G}_i \tag{14}$$

$$\sum_{t=1}^{24} G_{it} \leq P \tag{15}$$

The gamma term in Eq. (11) simply reflects the need to activate a unit any hour during the day. This will only occur if the $G_{it} \neq 0$ and $G_{it-1} = 0$. Equation (13) reflects the load plus spinning reserve constraint (S_t). Equation (14) represents the power band for each of the units. Equation (15) constrains the amount of electricity purchased.

Equations (11) through (15) are the foundation for simulating the process whereby units are committed to meet the anticipated profile of daily loads. The hourly demand for electricity is developed from the statistical models discussed earlier. The simulation procedure is based on the principle that minimum cost can be achieved by loading units according to their marginal costs, where the lowest cost plants are loaded first. Loading proceeds until constraint (13) is obeyed; that is, the hourly demand and spinning reserve are met. Loading begins at the peak hour and plants are either powered down or deactivated altogether. Which option the routine selects depends upon the relative cost of shutdown vs. the cost of maintaining excess capacity during the off-peak hours. Once a cost minimizing commitment schedule is obtained

power is dispatched according to the actual loads experienced throughout the day.

(c) Hourly Thermal Unit Dispatch.

Unit dispatch is the process of determining the amount of electricity to be generated by each plant committed. This problem is almost identical to that discussed in the preceding section. Here too the costs of generating and purchasing are minimized subject to the constraints of demand (net of power produced through hydro, pumped hydro, nuclear). Stated formally the problem is one of minimizing the cost expression shown in Eq. (16).

$$F_t = \sum_{i=1}^{R_s} b_{it} G_{it} \qquad (16)$$

subject to

$$\sum_{i=1}^{R_s} G_{it} = D_t \qquad (17)$$

where R_s is the mix of thermal units committed plus anticipated outside purchases. Equation (16) represents the total cost of meeting actual loads in the period t, given that a set of R_s options are available to the dispatcher. Equation (17) insures that what is generated, G_{it}, is demanded, D_t. Once again the optimum mix of plants at any hour, t, is determined by loading the R_s units available in ascending order of their marginal costs. The solution to the dispatch problem yields a solution which is then fed into Eq. (11). The result is the cost of meeting the demands of the day.

The scheduling procedure described by Eqs. (10) through (15) can be summarized in two steps. First, power is scheduled from the committed units according to their marginal cost of operation. Beginning with the day's peak hour, power is dispatched as shown in Fig. 23. Units 1 through 7 are required to make up the difference between the forecast load and the minimum load which each plant must produce after commitment. Units 8 and 9 are needed to meet the spinning reserve requirements. A similar approach is taken to schedule units during the off-peak hours. Given the relatively large swings in the daily summer demand, these off-peak periods are likely to exhibit demands which can be met by shutting down one or more plants. Whether such a strategy is economically efficient hinges on the relative costs of maintaining the unit on-line at minimum power, or shutting it down and then reactivating it the next day. The computations are, of course, complicated by the fact that the outside purchases are limited by contract and do not contribute to spinning reserve requirements. Appendix C illustrates the entire process from commitment to a 24-hour scheduling, utilizing a simple numerical example.

(d) Rationale for Separating Commitment and Dispatch.

Ideally both the start-up and shutdown costs should be addressed in conjunction with the unit's marginal cost. Under certain circumstances failute to do so would lead to suboptimal solutions. However, a simultaneous analysis of these costs would require an immense amount of computational time, especially if

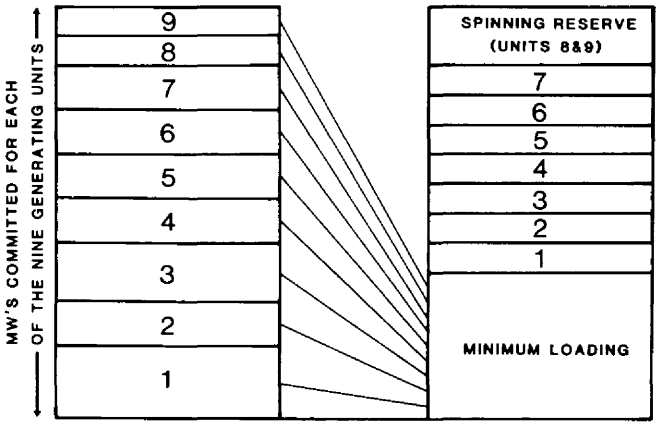

Fig. 23 Illustration of the generation scheduling procedure. The left-hand side shows the total megawatt capacity committed to both the reserve capacity of committed units plus the required spinning (emergency) reserve.

they proved to be quadratic. Given that the relationship between fuel and production turned out to be linear, the marginal cost of each unit is unique, regardless of production level. Hence, the priority list of costs is absolute. One final reason for believing that unit commitment and dispatch can be safely separated lies in the relative cost of start-up. It normally comprises less than 0.5 percent of the daily total. Hence, even if there is a slight discrepancy in the results it is not likely to affect significantly the conclusions. Therefore, the simpler procedure of first committing plants according to their marginal cost and then dispatching power with an eye toward the cost of shutting down units appears to be justified.

4.1.4 Results.

The scheduling model was exercised for a three-month period: June, July and August of 1980. Actual hourly weather information was utilized to forecast demand and schedule units. The resultant daily cost of meeting loads, given different types of forecasts, is displayed in Tables 7 through 9. These results were developed utilizing the assumption that generating deficiencies would result in a penalty payment. That is, if an insufficient number of units had been scheduled and the daily purchase limit was exceeded, then a penalty cost was assigned to each megawatt of deficiency. A penalty payment is not the only means for dealing with the problem of power shortages. As will be explained below the demand forecast could also be adjusted to account for error in the load equations. However, the results displayed in Tables 7 through 9 were developed utilizing the former procedure. The numbers in parentheses to the right of both daily costs and summary totals represent these penalties.

The summary statistics developed in Tables 7, 8 and 9 illustrate the potential savings that could result through improved load forecasts. As expected, the lowest cost forecast is provided by perfect loads. That is, if PSCC knew precisely what its load pattern would be 12 hours in advance, then the total cost of meeting the demands over the entire 90-day period is $47.561 million. This sets the lower bound on cost;

Table 7 Daily cost of meeting electric demand by forecast type: month of June.

Date		Perfect Load	Perfect H & L	Forecast H & L	Yesterday's H & L	Perfect 6-Hour Temperature Forecast
6-1	S	382.1	382.1	382.8	382.8	382.8
2	M	463.0	462.9	463.3	463.2	463.3
3	T	477.5	477.0	477.0	477.0	477.0
4	W	502.0	503.7	502.5	502.5	502.2
5	T	503.9	503.6	502.4	503.8	502.4
6	F	505.3	504.5	505.0	505.4	504.6
7	S	399.8	399.8	401.9	404.0	401.9
8	S	351.8	347.8	347.8	347.8	347.8
9	M	475.3	478.0	478.0	479.6	478.2
10	T	489.8	489.8	489.8	490.0	490.0
11	W	524.2	524.5	524.2	523.4	524.2
12	T	545.0	546.0	545.0	546.6	545.0
13	F	540.5	540.4	540.5	541.5	540.5
14	S	446.7	446.7	446.8	446.7	446.8
15	S	377.3	379.9	380.1	381.7	380.1
16	M	506.9	504.6	507.3	506.0	504.9
17	T	506.9	505.4	505.9	505.7	505.7
18	W	531.6	532.5	532.7	535.7	532.7
19	T	492.2	492.0	493.2	494.7	492.8
20	F	496.9	495.5	496.1	496.1	495.5
21	S	425.8	425.8	425.8	425.8	425.8
22	S	404.6	405.0	405.2	405.0	405.2
23	M	568.3	568.2	569.1	572.3	570.0
24	T	576.9	577.2	579.5	579.1	577.2
25	W	597.2	598.8	598.9	601.7	600.4
26	T	595.1	594.9	595.3	595.7	594.8
27	F	591.0	591.0	591.7	593.0	590.4
28	S	474.8	474.8	474.8	474.8	474.8
29	S	458.0	458.0	458.9	459.0	458.9
30	M	623.5	624.9	625.6	624.9	625.5
Total Cost ($1,000)		14,833.9	14,835.3	14,847.1	14,865.5	14,841.3

Table 8 Daily cost of meeting electric demand by forecast type: month of July.

Date		Perfect Load	Perfect H & L	Forecast H & L	Yesterday's H & L	Perfect 6-Hour Temperature Forecast
7-1	T	538.5	538.5	542.9	562.5	539.2
2	W	515.2	514.8	514.9	514.8	514.9
3	T	509.0	509.3	510.1	509.0	508.9
4	F	405.6	405.6	405.6	404.7	405.6
5	S	446.8	446.9	446.9	446.9	446.9
6	S	449.7	449.7	449.7	449.8	449.7
7	M	601.1	610.0	622.4	619.2	607.1
8	T	597.6	599.6	597.7	604.7	598.4
9	W	632.3	632.4	632.5	632.7	637.1
10	T	585.4	585.2	597.2	595.1	589.4
11	F	563.9	565.2	569.2	563.7	563.6
12	S	446.8	446.8	446.8	446.8	446.8
13	S	419.2	419.2	419.2	419.2	419.2
14	M	577.1	579.4	579.4	579.0	578.5
15	T	602.9	605.1	602.9	604.4	604.4
16	W	616.9	617.2	618.5	617.2	620.0
17	T	645.8	644.8(25MW)	644.5(25MW)	644.5(25MW)	652.9(25MW)
18	F	591.5	593.4	591.6	600.8	591.7
19	S	483.2	483.2	483.2	483.2	483.2
20	S	434.1	434.3	434.6	434.2	434.6
21	M	556.8	559.1	558.6	559.1	556.6
22	T	606.4	606.5	604.6	611.9(8MW)	608.0
23	W	603.2	605.4	605.6	609.2	604.4
24	T	583.8	585.0	585.6	587.6	584.8
25	F	533.4	533.3	535.0	540.6	533.9
26	S	447.6	447.5	447.7	447.5	447.7
27	S	430.3	430.3	430.3	430.7	430.3
28	M	628.9	630.0	630.1	630.6	630.6
29	T	684.8	677.0(130MW)	672.9(225MW)	672.9(225MW)	685.2(15MW)
30	W	646.1	645.0(15MW)	652.5	654.5	645.0(15MW)
31	T	634.2	634.9	634.2	634.8	634.2
Total Cost ($1,000)		17,018.1	17,034.6	17,066.4	17,110.8	17,046.9
(Insufficiency)			(170MW)	(250MW)	(258MW)	(55MW)

any of the other forecasting methods will involve errors and consequently a larger expense. For example, if the PSC only utilized yesterday's high and low temperatures in committing units to meet the subsequent day's demands, the total cost of generation is estimated to be 0.335 million higher. The added expense reflects additional penalty charges (283 MW @ $500 per MW) and the cost of maintaining excess capacity when demands failed to materialize. This latter cost amounted to nearly $0.198 million of the total.

Of course, this comparison is somewhat unrealistic but it does serve to illustrate the widest possible difference in cost and, hence, the greatest potential savings. The load forecasts embody both modelling and weather forecast errors. Given the current state of the art, i.e. the demand equations shown in Appendix B and the current skill of the weather forecasts, the 90-day costs jump to $47.846 million. This represents a slight improvement ($44 thousand) over a persistence forecast.

The extent to which these savings are tied to forecast skill can be obtained by observing the total costs assuming that PSC knew the day's high and low temperature 12 hours in advance. A perfect meteorological forecast results in a much lower cost, i.e. $47.651 million. This means that the value of improving temperature forecasts of this nature is at most $0.195 million over the 90-day period.

The extent to which such savings could be achieved hinges on the degree of forecasting improvement that can be anticipated. Obviously a perfect temperature forecast is out of the question. However, a dramatic improvement in short-term forecasting could be achieved yielding substantial rewards. Note in Table 10 that a perfect four-hour forecast would reduce the PSC's cost to $47.716 million, implying a savings of nearly $0.174 million.

The savings and costs cited above were derived for the peak period of June, July and August. One can only guess how these results might be altered for the other seasons of the year. It may not be unreasonable to anticipate winter savings to be one-half and fall and spring to be one-third of those realized in summer. If so, the present worth of annual savings are computed to be $5.17 million for a perfect high-low temperature forecast and $3.77 million for a perfect short-term (4-hour) temperature forecast[3].

Aside from the value estimates just provided, the models provided some useful insights into several related areas. First, it was discovered that temperature forecasts did not alter scheduling over weekends.

[3]These estimates were obtained by discounting the annual savings in perpetuity (10 percent).

Table 9 Daily cost of meeting electric demand by forecast type: month of August.

Date		Perfect Load	Perfect H & L	Forecast H & L	Yesterday's H & L	Perfect 6-Hour Temperature Forecast
8-1	F	635.5	635.5	635.6	636.4	635.6
2	S	510.8	511.0	511.0	511.1	511.0
3	S	470.7	470.7	470.7	470.7	470.7
4	M	556.5	556.4	556.4	569.3	556.4
5	T	578.0	578.9	581.3	581.3	582.6
6	W	635.3	638.8	637.3	637.3	643.0
7	T	671.3	669.9(25MW)	664.99(145MW)	671.0(25MW)	664.9(145MW)
8	F	570.9	572.4	583.4	589.4	570.9
9	S	479.4	479.4	479.4	479.4	479.4
10	S	433.9	434.0	434.0	434.0	434.0
11	M	581.2	583.5	586.4	583.4	583.5
12	T	609.7	610.8	611.3	611.3	612.3
13	W	575.3	576.9	575.4	581.9	576.7
14	T	541.6	542.0	542.0	542.0	541.8
15	F	528.3	528.3	528.0	527.9	528.0
16	S	423.8	423.8	423.8	423.8	423.8
17	S	393.3	393.1	393.1	393.1	393.1
18	M	552.6	552.8	554.6	554.8	553.3
19	T	547.0	485.4	547.3	550.9	547.4
20	W	519.3	546.0	519.7	522.8	519.8
21	T	535.0	534.1	535.5	534.1	535.5
22	F	556.0	555.9	556.1	558.1	556.0
23	S	457.9	458.0	457.9	458.0	457.9
24	S	409.4	410.3	410.3	410.7	410.3
25	M	505.9	507.3	507.2	507.8	507.4
26	T	505.6	504.8	504.2	505.1	504.2
27	W	507.2	506.5	507.3	506.1	507.2
28	T	523.7	522.8	523.1	522.8	522.8
29	F	504.6	504.7	504.4	504.4	504.5
30	S	389.9	389.9	394.0	394.2	394.0
Total Cost ($1,000) (insufficiency)		15709.6	15,683.9 (25MW)	15,735.6 (145MW)	15,773.1 (25MW)	15,728.0 (145MW)

Table 10 Summary results for the three-month period.

Forecast Type	Three-Month Cost to Meet Demand (Assuming $500/MW Penalty)
Perfect Load	$47,561,000
Perfect High & Low Temperature Forecast	$47,651,600
Forecast High & Low	$47,846,600
Perfect Four-Hour Forecast	$47,716,200

The load profile proves to be much flatter than that of the weekday. As a result, the demands can be met with the base units and weather forecasts play no role; power purchases and commitment of peaking power are of little or no concern over weekends. Hence, weather data which are tied to both decisions are not essential.

It is also interesting to note that the simple load demand models shown in Appendix B are capable of explaining 92 to 95 percent of the variation in demand throughout the peak period. Despite the fact that the model's explanatory power drops during the off-peak period, the cost of meeting demands is not appreciably affected by the model's error. Apparently it is accurate for the periods of the day when scheduling is most critical. The value of improving the model can be gleaned from the results displayed in Table 10. The cost of generation given a perfect load profile is $47.561 million; the equivalent cost given a perfect high-low temperature forecast is $47.651, only $90,000 higher. It appears that the major contributing factor to the cost of generating power is not error in the demand model but error in the temperature forecast.

The use of penalty costs may be subject to criticism in that a meaningful cost of a shortage may be difficult to establish. The power may be available from outside sources; however, utilities normally would like to avoid such occurrences. One way of determining a penalty cost is to force the scheduling model to commit enough units to cover the unanticipated demands. This can be done by utilizing the standard error derived from the load forecasting model. By adding a margin of three standard errors to the demand projection, shortages can be avoided. An experiment was performed utilizing this approach. The results show that the cost of generation increased by the equivalent of $500 for each megawatt the company is short.

It is difficult to generalize from these findings. The PSCC service area is dispersed geographically, yet Denver's demand looms large relative to the rest of the state. Consequently, climate and weather information is easily incorporated into the problem. Forecasting temperatures for Denver alone is sufficient to determine the PSCC's daily load profile. In other regions of the country where the geographical dispersion is matched by regional variability in loads, the value of more sophisticated demand models may be enhanced. It should also be noted that the results are limited to the daily scheduling of units which is just one area of PSCC's concern. Weather forecasting may prove most valuable in scheduling the maintenance of plants, line repair and/or cash flow projections (based upon anticipated electric usage). However, these issues were not addressed in this brief report.

4.2 COST EFFECTIVENESS OF AIR CONDITIONING SYSTEM RETROFITS.

4.2.1 Introduction.

In this section we describe an attempt to measure the cost effectiveness of retrofits to air conditioning systems in several commercial buildings. Eight buildings in the northern Colorado and southern Wyoming area were chosen for analysis. Three of these buildings were deleted from the study as the project progressed due to unavailability of complete data. The five remaining buildings included three in Fort Collins, Colorado, one in Laramie, Wyoming, and one in Greeley, Colorado.

In all but one of these buildings (Laramie, Wyoming) the space conditioning systems were predominantly electrical with natural gas used only for heating. In the Laramie building the retrofit under consideration converted the air conditioning system from a gas-fueled absorption cooler to an electrical chiller unit. In this case both natural gas and electricity consumption analyzed and the pay back analysis was based on a comparison of these quantities. In the remaining buildings the analysis was based on KWH of electricity.

Consumption data were obtained from the respective utility companies on a monthly basis for one full year before and after completion of each retrofit.

Additional information regarding the motivation for each retrofit decision and the physical characteristics and use patterns for each building were obtained through interviews with the building managers.

Regression analysis was used to determine the effects of the retrofit on energy consumption for each building. Cooling degree days were included in the regression models as the normalizing independent variable.

Using the results of the regression analysis, monetary values and pay back periods were calculated for the reduced energy consumption attributable to each retrofit. To determine the economic effectiveness of each retrofit, the payback was then compared to the return expected on a comparable investment in an interest-bearing asset at a contemporary interest rate.

4.2.2 Method of Analysis.

In order to "capture" the effect of the retrofit on energy consumption, a dummy variable was included in each regression model indicating "prior to" and "after" completion of the retrofit. The coefficient associated with this variable indicates the magnitude and direction of change in consumption resulting from completion of the retrofit. To isolate the effects of variable external temperatures, cooling degree days were included as an additional regression variable. The coefficient associated with the cooling degree day variable will provide an indication of the magnitude and direction of change in consumption due only to temperature variation. Using the retrofit and the cooling degree day variables as predictors one can then estimate consumption as a combined function of these two variables. The pay back period is calculated by application of a general equation for determining the net present value of an investment in an energy conserving retrofit over time. This equation is:

$$NPV = \int_0^T S \cdot [P_o e^{rt}/e^{it}]\, dt - C_o \qquad (18)$$

where NPV is the net present value,

S is the annual reduction in the rate of use,

P_o is the current price of electricity,

e^{rt} is the growth factor for electricity price,

e^{it} is the discount factor,

C_o is the cost of the retrofit,

T is the pay back period.

The right-hand side of the above equation may also be considered an annuity, the value of which can be obtained from Eq. (19).

$$C = S\left[\frac{1-e^{-i'T}}{i'}\right] \qquad (19)$$

where $i' = r-i$,

r = real growth rate of price,

i = real interest rate.

By substituting various values for T (e.g. T=1,2,3,...) the pay back period can be determined. The value of T indicating the exact pay back period is then the value closest to the ratio, C/S. Additional details of this method of analysis are provided (for residential buildings) by Reiter et al., 1980.

4.2.3 Building No. 1.

This building is a 38,600 ft^2, four-story commercial bank building in Fort Collins, Colorado. It was built in 1967 and is constructed primarily of concrete and glass. According to the building manager, the decision to retrofit was motivated by the energy conservation requirements of the federal government [Energy Building Temperature Regulation, (EBTR)]. The cost of the retrofit was $7,800.

The regression model of best fit for this building was a simple linear model as follows:

$$Y = 78400 - 28232\, X_1 + 69.2\, X_2$$

where

Y = KWH of electricity consumed per month

X_1 = the retrofit dummy variable

X_2 = cooling degree days per month

R^2 (adjusted for 22 degrees of freedom) = 66.8%

T - ratio for X_1 = -6.85

T - ratio for X_2 = 2.53.

For a base period electricity price[4] of $0.045/KWH, the monthly reduction in the cost of electricity resulting from the retrofit is given by multiplying the coefficient of X_1 times the price (-28232 KWH X $0.045/KWH = $1270.44). The annual savings is then 12 times this amount or $15,245.28.

It is immediately apparent that this retrofit will pay back in less than one year irrespective of the electricity growth factor and discount rate.

4.2.4 Building No. 2.

This building is a 57,400 ft^2, two-story complex housing the city government, police department, fire department, city library, and museum for the city of Greeley, Colorado. The building was completed in 1967 and is constructed of concrete and glass. The reported motivation for the retrofit to this building's space conditioning system was to meet the federal government's (EBTR) mandated temperature requirements. The cost of the retrofit was $10,000.00.

The regression model of best fit was:

$$Y = 94265 - 14363\, X_1 + 121\, X_2$$

where

Y = KWH of electricity consumed per month

X_1 = the retrofit dummy variable

X_2 = cooling degree days per month

[4] Calculated from the rate schedules provided by Fort Collins Light and Power.

R^2 (adjusted for 22 degrees of freedom) = 45.2%

T - ratio for X_1 = -2.63

T - ratio for X_2 = 4.28.

Using the electricity price and the method of calculation of savings and pay back period outlined above, the annual savings for this building resulting from the retrofit is:

14363 KWH x $.045/KWH x 12 mo = $7,756.02

With this savings the retrofit would pay back within less than two years (at T=2, pay back or return would be $15,327.45).

4.2.5 Building No. 3.

This building is a 150,000 ft^2, three-story hospital in Laramie, Wyoming. The specific retrofit analyzed in this building was one phase of a multi-phase retrofit program undertaken for general cost reduction through energy conservation. This retrofit is peculiar in that it replaced a gas fueled absorption cooling unit with an electric chiller. One would thus expect gas consumption to decrease and electricity consumption to increase after the retrofit.

In order to accommodate the dual nature of this retrofit, natural gas and electricity consumption were analyzed separately. The total change in combined consumption was then used to estimate the net change and, hence, net savings. The cost of this retrofit was $63,875.00.

The regression model of best fit for gas consumption was as follows:

$$Y = 3080 - 18.8\ X_1 + 12.0\ X_2$$

where

Y = gas consumption in MCF per month

X_1 = the retrofit dummy variable

X_2 = cooling degree days per month

R^2 (adjusted for 22 degrees of freedom) = 50.5%

T - ratio for X_1 = -4.86

T - ratio for X_2 = 4.28.

In this model X_2 is a "slope shifting" dummy variable. Consequently, the coefficient associated with X_1 represents the number of MCF per cooling degree day change in consumption associated with the retrofit. To estimate the annual change in gas consumption this figure must be multiplied by the number of cooling degree days (CDD) per year. The average value for the years 1973 through 1981 (510 CDD/yr) was used for this purpose.

The reduction in gas consumption associated with the retrofit is given by:

-18,8 MCF/CDD x 510 CDD/yr = -9588 MCF/yr

At a price of $2.056/MCF[5] this gives an annual savings of

9588 MCF x $2.056/MCF = $19,712.93.

The model of best fit for electricity consumption was:

$$Y = 158000 + 212\ X_1 + 108\ X_2$$

where

Y = electricity consumption in KWH per month

X_1 = the retrofit dummy variable

X_2 = cooling degree days per month

R^2 (adjusted for 22 degrees of freedom) = 51.8%

T - ratio for X_1 = 2.76

T - ratio for X_2 = 1.94.

Immediately we see that, as expected, electricity consumption increased after the retrofit was completed.

Again we have used a "slope shifting" dummy variable giving the KWH/CDD change in consumption. Thus, we have an annual change of consumption of

212 KWH/CDD x 510 CDD = 108,120 KWH/yr.

Using a price of $0.045/KWH we thus obtain:

108120 KWH x 0.045/KWH = $4,865.40.

This increase in cost for electricity must be subtracted from the savings derived from gas to determine total annual savings. Hence,

$19,712.93	(gas savings)
4,865.53	(increased electricity cost)
$14,847.53	Total annual savings.

From the pay back equation it can be determined that pay back will occur at about 4.3 years.

4.2.6 Buildings No. 4 and No. 5.

The remaining two buildings analyzed included a restaurant and a newspaper complex in Fort Collins, Colorado. Both of these retrofits were undertaken in order to reduce energy costs.

The regression analysis for these two buildings did not explain a sufficiently large percentage of the variation of electricity consumption to allow a cost-benefit or pay back analysis. However, for the sake of completeness, the regression models are included although the very low T-ratios and R^2 values obtained for these two buildings indicate insufficient relationship to attempt any conclusions regarding the effects of the retrofits.

[5] The mean price per MCF over the two-year period of the analysis.

Building No. 4:

$$Y = 35739 - 2052\ X_1 + 40.3\ X_2$$

where

Y = KWH electricity consumed

X_1 = the retrofit dummy variable

X_2 = cooling degree days

R^2 (adjusted for 22 degrees of freedom) = 8.9%

T - ratio for X_1 = -0.62

T - ratio for X_2 = 1.97

Building No. 5:

$$Y = 73791 - 997\ X_1 + 40.4\ X_2$$

where

Y = KWH electricity consumed

X_1 = the retrofit dummy variable

X_2 = cooling degree days

R^2 (adjusted for 22 degrees of freedom) = -4.7%

T - ratio for X_1 = -0.16

T - ratio for X_2 = 0.96

4.2.7 Conclusion.

The relatively crude analyses performed for each of the five buildings do not address all of the factors which are likely to affect energy consumption at each site. However, for three of the buildings the magnitude of effects are such that they can be considered useful for the determination of pay back periods within an acceptable range of uncertainty.

Determination of the exact factors resulting in the failure of the analyses to explain the variation in consumption in Buildings No. 4 and No. 5 is beyond the scope of this preliminary study. It is apparent that additional factors affected consumption in these buildings, besides cooling degree days and the retrofits undertaken in each. It is significant, however, that the retrofit investment in the latter two cases was relatively small ($2,500 and $4,300) compared to the other three buildings. Also, in Buildings 1, 2 and 3 there were full-time building managers who had incorporated the desirability of conserving energy into building maintenance routines. Such personnel were absent from the other two buildings. Finally, the size of the ventilation and air conditioning systems and magnitudes of consumption for Buildings 1, 2, and 3 provided relatively greater potential and, hence, greater incentive for cost reduction through investment in conservation than was apparent in Buildings 4 and 5.

Another notable factor identified in this study is based on the fact that, in each case, the building owner or manager expressed a concern for saving energy and, hence, reducing costs. Also, in three of the five cases the reported motivation for the retrofit was in part to meet the Federal Energy Building Temperature Regulation requirements.

5.0 EXECUTIVE SUMMARY

5.1 RESEARCH TASKS.

The research efforts between 1 January 1981 and 31 December 1981 under the Department of Energy Contract DE-AS02-76EV01340 were concerned with:

(1) Large-scale feedback mechanisms within the ocean-atmosphere-continent system that control long-term atmospheric variability. Progress in this subject area has been published in several reports and scientific journal articles and is not repeated here.

(2) Data development for, and application of, weather dependent models of community energy demand on a regional scale.

(3) Development and testing of a "physical model" of energy requirements for air conditioning during the cooling season.

(4) Refinement of methods to simulate local variations of the weather parameters controlling energy demand for space conditioning in large urban areas.

(5) Analysis of the value of improved weather forecast information for energy and cost savings in the production of electric power.

(6) Analysis of the cost effectiveness of energy conservation through modifications and retrofits of air conditioning systems in large buildings.

5.2 REGIONAL SCALE MODELLING OF ENERGY DEMAND FOR SPACE HEATING.

Among the original objectives of our research studies was the development of reliable methods for the identification of potential future energy shortfalls over large areas in response to severe weather and/or supply interruptions. Focussing on energy demand for space conditioning, the projection of future energy needs on a national, regional, or even local basis is a complex task. In addition to non-uniform growth of demand due to new construction in each of the multiple climatic regimes, improved weatherization and replacement of inefficient heating and cooling systems have significantly modified energy requirements for new and established structures throughout the country. Moreover, local and regional differences in life styles and economic circumstances further complicate the overall problem.

In pursuit of the above-stated objective we previously developed and tested several successful models of community energy demand for space conditioning. These models include a "physical model" that utilizes the bulk structural details of all buildings in an area to compute total energy requirements to maintain internal comfort levels. We have also developed a statistical (regression) reference model that quickly determines a response function relating daily community energy demand to local weather observations. These models have been combined into a physical-reference model. This hybrid model applies a statistical response function as well as structural data for new or modified buildings to adjust current energy requirements for both new growth and for the impact of conservation measures in older buildings. These models were previously used to estimate successfully total daily energy demand for several heating seasons in Greeley, Colorado, Cheyenne, Wyoming and Minneapolis, Minnesota.

We are now developing efficient methods for applying these models to much larger (regional) domains. The principal difficulties in this phase of our work are inherent in the development of rather massive quantities of input data. If satisfactory data acquisition and management procedures are obtained, the models will be of significant value to individual utilities for securing adequate (but not excessive) future supply commitments and to the nation itself.

Preliminary statistical reference modelling has been performed for a large region served by a utility company that distributes natural gas to most of the state of Colorado. Results of these studies are presented in Section 2.0. The region has been divided into ten smaller "service areas". These diverse areas include clusters of small farming communities in the eastern plains of Colorado, the Denver metropolitan area, mountain resort communities, and mineral development "boom-towns" in western Colorado. Diverse topography and elevation within the State of Colorado creates distinctly different climatological factors for each of these areas.

As expected, strong differences were found in the per-customer rates of energy demand. After adjusting the data base for industrial gas consumption and heating degree days, mean per-customer demand differed by as much as a factor of two between some areas. Initial inquiries pointed to structural (building census characteristics) and life-style differences as major contributing factors to these diverse demand rates.

The modelling results obtained so far are based on crude, but readily accessible, meteorological data and only a short record of daily energy demand values (59 days). Nevertheless, the accuracy of the demand predictions are fairly good. The mean absolute daily error of predictions for the ten service areas ranged from 12.2 percent for the eastern "high plains" service area to 2.9 percent for the Rifle area in western Colorado. In general, temperature-related variables were found to be the dominant factors controlling demand predictions but specific secondary variables (combinations of wind and insolation) varied considerably from area to area.

A major effort to develop more detailed input data for each service area has been undertaken. Bihourly-averaged values of temperature, wind speed and insolation have now been obtained for each area. Acquisition of building census data for all areas is a more difficult problem because computerized (digital tapes) data are not available for most cities in the region. Consequently, we are relying on the previously developed statistical representation of structures in Greeley, Colorado, adjusted for local differences in growth rates, to apply in most small- and medium-sized towns. A copy of the Denver assessor's tape, containing detailed information for nearly 300,000 buildings, has also been obtained. This tape will provide basic structural data for the only large metropolitan center within the region.

5.3 PHYSICAL MODEL OF ENERGY DEMAND FOR AIR CONDITIONING.

In addition to the regional study of energy demand for space heating we have also continued our investigation of the weather dependent aspects of energy use for air conditioning (cooling). We previously developed statistical-reference models for a number of individual buildings and demonstrated that considerable differences existed in the efficiency and sensitivity of each to weather. Our objective is to develop a physical-reference model of energy demand for air conditioning. This model will be used to assess the potential impact on peak power (electric) demand of broad-based system retrofits and various peak shaving strategies.

We have now constructed a simple physical model for air conditioning of large buildings and attempted to use the Group Method of Data Handling (GMDH) to optimize the coefficients of the terms in the standard heat flow equations. This GMDH procedure was previously very useful for constructing simple physical models of space heating energy requirements for more than 50 distinct building types. However, the air conditioning problem has proven to be much more difficult. Using structural, energy demand and meteorological data for the most weather sensitive building studied with our statistical reference model of air conditioning, the GMDH has repeatedly failed to provide stable, physically realistic coefficients for the physical model. The reasons for this failure are not completely resolved, but inadequate parameterizations of complex inflitration factors and, possibly, indirect radiation and shading of the structure appear to be involved.

Although energy consumption for air conditioning in individual buildings appears to vary in diverse and complex ways, we hope that a composite model for the total demand of a group of buildings can be made to yield more favorable results. Proceeding in this direction, we have compiled an extended and detailed energy demand and meteorological data set for 15 large commercial office buildings in Denver, Colorado.

5.4 URBAN CLIMATE MODELLING.

Energy demand for space conditioning tends to be heavily concentrated in urban areas. Because this energy demand is quite sensitive to weather variables and because cities act to modify climate locally (i.e. the urban heat island), it is necessary to account for the urban climate effects in modelling community energy demand. We have previously relied on local mesoscale networks of meteorological instruments to obtain details of urban wind and temperature fields. The installation and operation of such networks is rather costly. Now we have devised and tested an urban climate modelling procedure to supply these data by adjusting values obtained from a single set of local observations. Allowing for the small impact of solar radiation on the heating needs of most existing buildings, only variations of wind and temperature are considered. Wind speed is adjusted for local surface roughness by an empirical power law. Temperature, the dominant demand related variable, is adjusted for urban effects using a simple model of cumulative advective warming as rural air passes through a city.

An analysis of wintertime heat island data (collected in Minneapolis, Minnesota) suggests that the key assumption of the temperature model is valid; that is, a surface-based, neutrally buoyant layer of air appears to form in stable rural air as it passes over the city. Supporting results for case studies under diverse meteorological conditions are presented.

Urban surface heat budgets are determined from detailed parameterizations of heat released from space heating, traffic and electric power consumption. The depth and intensity of surface-based rural temperature inversions, an important model parameter, are estimated from rural cooling rates and empirical estimates of the depth of forced turbulent mixing. The inversion profile estimator is shown to provide lapse rate

values that are highly correlated with values required by the advective model to reproduce observed heat island intensities. The model itself is modified to consider local "canopy" effects by allowing for vertical and horizontal variations of wind speed.

This urban climate model will be used in the regional energy demand study to adjust single observations of local temperatures and wind speed to urban values. These adjusted data will, in turn, yield mean, energy demand weighted values for more accurate statistical reference modelling of multiple urban areas. Later, these same methods will be used for physical-reference modelling of projected growth and development in each city.

5.5 THE IMPACT OF WEATHER FORECASTS ON THE COST OF GENERATING ELECTRICITY.

It is well known that demand for electric power is strongly correlated to weather factors, especially during the summer cooling season. Consequently, accurate load projections based on improved weather forecasts could enable utility companies to utilize more efficient schemes for scheduling generating plants and thereby reduce fuel and operating costs. A three-part study was undertaken to assess the potential value of improved weather forecasts to the generation and transmission utilities. These three parts included the estimation of the effects of weather variables on electricity demand, the construction of a model to schedule generating plants in light of load forecasts, and the estimation of the actual economic value of improved weather forecasts by determining how they alter load forecasts and subsequent generation schedules.

The study centers on the area supplied by the Public Service Company of Colorado (PSCC), the regional energy utility serving most of the State of Colorado. Seventy percent of PSCC's power customers are located in the Denver metropolitan area; hence it was presumed that most of the company's load variability was closely linked to conditions in this one relatively concentrated geographical location.

The demand forecasting model reflects this assumption. The weather-related load was predicted using temperature, wind speed and humidity data. The proportion of the load which is sensitive to the patterns of industry and commerce was related to the time of day, day of the week, month and to lagged values of demand. Weekends were treated differently than weekdays, and Mondays and Fridays were distinguished within the work week. A set of 24-regression equations was utilized to capture the hour-by-hour variation in load stemming from the normal behavioral patterns anticipated throughout the day. The end product is a model which forecasts the PSCC 24-hour load profile. These forecasts can be made sensitive to either anticipated temperature variations or they can be obtained by assuming some form of persistence in the weather or load pattern.

A direct relationship between weather and load forecast accuracy can be demonstrated. However, the worth of improving PSCC's ability to predict the hourly profile hinges on the cost of generating electricity to meet the anticipated demand. Such costs, in turn, are shaped by the marginal expense of individual generating units, start-up and shutdown costs, spinning reserve requirements, and the amount paid to other producers for supplemental power. The benefits of improving the PSCC's ability to predict its load profile are derived from: 1) a reduction in the number of instances when excess capacity is unnecessarily maintained, 2) a reduction in the number of times when expensive power is unnecessarily purchased from outside sources, and 3) an improvement in overall scheduling efficiency.

A variety of weather forecasts were fed to the load forecasting model. The resultant hourly demands were used to drive an economic model which was designed to minimize the daily cost of meeting these loads. The resultant costs were then compared to determine the value of refining weather forecasts. The conclusions were sharpened through a series of experiments performed to determine both the accuracy and timing needed before a utility, such as PSCC, would routinely utilize weather forecast data in its day-to-day scheduling operations.

The notable conclusion from this exercise is that, given the modular nature of system scheduling, the accuracy of weather forecast information rather than the accuracy of weather driven demand models limited the usefulness of system scheduling procedures. The implication here is that the excess reserve of the last generating unit brought on-line to meet anticipated loads is generally more than adequate to accommodate the errors in rather crude weather driven demand models. However, load forecast errors associated with the accuracy of typical weather forecasts are much larger. Consequently, it appears as though the power generation industry may benefit more directly from improved weather forecasts than from improved demand models.

5.6 COST EFFECTIVENESS OF AIR CONDITIONING SYSTEM RETROFITS.

In a prior study of natural gas consumption in Greeley, Colorado, we were able to demonstrate a 20 percent drop in the demand (adjusted for weather) by established buildings between 1975 and 1980. Part of this decrease may be attributed to broad acceptance of energy-consciousness life styles by the building occupants. Lower thermostat settings is a typical illustration of this factor. However, some portion of the demand decrease is also attributable to improved weatherization and more efficient heating systems in the existing older buildings. Increased energy costs have made such retrofits and modifications more attractive to building owners.

A preliminary study has been initiated to assess more precisely the cost effectiveness and hence the potential demand impact of broad-based upgrading of air conditioning systems in large buildings. Of the buildings for which complete data could be obtained, the pay back realized through reduced energy costs was sufficient to recover costs of the retrofits within one to four years. The costs of these retrofits ranged from $2,500 to $64,000. Other findings indicated that daily attention to conservation by resident building managers was very useful in reducing energy costs and that concern over the now expired Federal Energy Building Temperature Regulations was at least partial motivation for most of the retrofits undertaken.

APPENDIX A

This appendix contains plots illustrating the relationship of observed temperature (°F) to total PSCC generation system demand for electricity in megawatts. The first set of figures (Fig. A1a, b and c) show this relationship for early morning, midafternoon and early evening hours for typical weekdays during the summertime. The second set of figures (Fig. A2a, b and c) show comparable plots for the same time of day but for weekends.

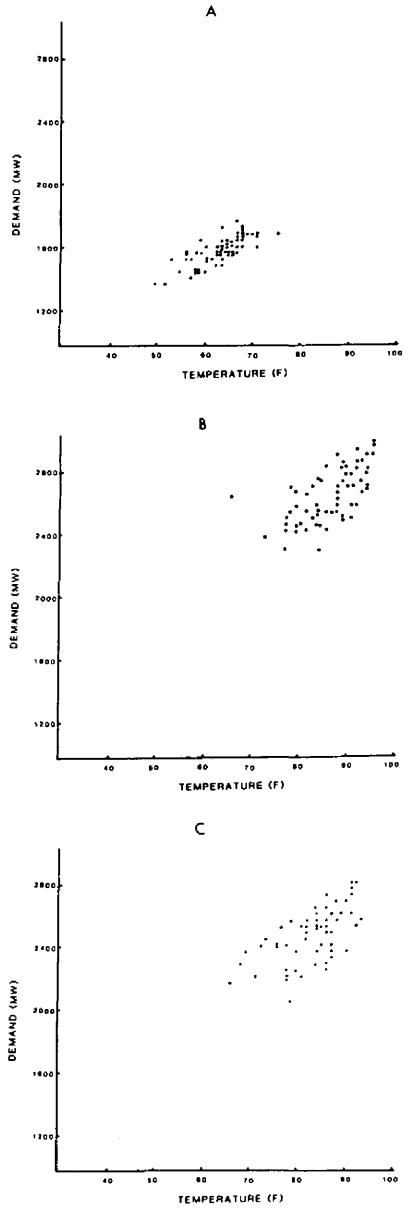

Fig. A1 Relationship of electric demand and hourly temperature: summer, weekday.

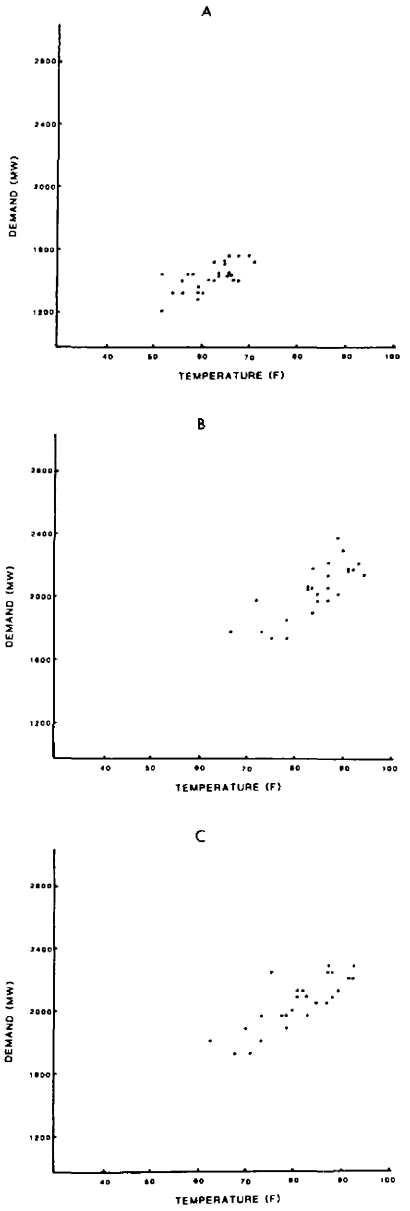

Fig. A2 Relationship of electric demand and hourly temperature: summer, weekend.

APPENDIX B

This appendix lists sets of regression coefficients and results of statistical tests for the three power demand forecasting models, Eqs. 1, 2, and 3 in Section 4.0. In addition to all hourly coefficients for each model, the coefficients of determination, standard deviations of hourly forecast errors, F test and Durbin-Watson test statistics are presented. Results for Eqs. 1 and 2 for weekdays are given in Table B1 through B6. Table B7 gives weekend data for Eq. 1 only. Tables B8, 9 and 10 give results for Eq. 3 for weekdays only.

Table B1 Regression results for Eq. (1) for June (weekdays).

Hour	Constant	Monday	Friday	High	HT-LHT	LHT	Low	R^2	SD	F	DW
0-1	4920	-85	23	-50.311	.58326	-43.699	8.339	87	51	15.7	2.42
	(2684)	(34)	(30)	(30.991)	(.34991)	(30.934)	(4.033)				
1-2	2897	-72	19	-27.768	.32401	-21.848	9.480	93	35	31.1	2.36
	(1846)	(24)	(20)	(21.315)	(.24066)	(21.276)	(2.774)				
2-3	3849	-83	-3	-36.979	.44361	-35.844	11.224	84	49	12.5	2.05
	(2577)	(33)	(28)	(29.752)	(.33592)	(29.697)	(3.871)				
3-4	3254	-56	-3	-31.318	.36976	-28.808	11.468	85	42	15.6	2.30
	(2221)	(28)	(24)	(25.649)	(.28959)	(25.649)	(3.338)				
4-5	2717	-50	-6	-25.493	.28058	-21.996	13.353	83	45	11.3	1.81
	(2383)	(30)	(26)	(27.561)	(.31067)	(27.465)	(3.581)				
5-6	697	-8	23	-3.88	.00945	1.773	11.124	74	54	6.7	2.04
	(2848)	(36)	(31)	(32.889)	(.37133)	(32.828)	(4.280)				
6-7	5045	-22	8	-47.267	.50324	-39.756	7.906	63	54	4.0	1.29
	(2853)	(36)	(31)	(32.948)	(.37200)	(32.887)	(4.287)				
7-8	4013	1	-16	-32.071	.39017	-33.366	11.793	75	49	7.2	1.53
	(2561)	(33)	(28)	(29.574)	(.33390)	(29.519)	(3.848)				
8-9	-150	132	51	10.504	-.08949	10.961	20.201	82	73	11.0	1.77
	(3818)	(49)	(42)	(44.090)	(.49780)	(44.009)	(5.737)				
9-10	3535	82	57	-30.286	.36729	-31.003	23.153	89	55	18.3	2.04
	(2876)	(37)	(32)	(33.213)	(.37499)	(33.151)	(4.322)				
10-11	6008	34	22	-56.928	.68978	-58.613	21.350	88	57	17.3	2.52
	(2997)	(38)	(33)	(34.605)	(.39071)	(34.541)	(4.503)				
11-12	5910	50	38	-55.854	.68545	-58.863	23.252	90	55	21.1	2.52
	(2882)	(37)	(32)	(33.278)	(.37573)	(33.217)	(4.330)				
12-13	5596	58	52	-51.852	.65451	-56.134	22.821	88	63	17.4	2.45
	(3303)	(42)	(36)	(38.139)	(.43061)	(38.069)	(4.963)				
13-14	6210	66	20	-58.294	.75653	-64.784	22.040	95	43	42.9	1.49
	(2251)	(29)	(25)	(25.991)	(.29345)	(25.943)	(3.382)				
14-15	6823	58	26	-63.737	.81779	-69.852	19.218	94	44	35.9	1.62
	(2295)	(29)	(25)	(26.502)	(.29923)	(26.454)	(3.449)				
15-16	5754	48	18	-49.932	.68349	-59.957	19.656	93	46	31.9	1.67
	(2438)	(31)	(27)	(28.153)	(.31759)	(28.101)	(3.663)				
16-17	5805	34	22	-49.498	.68185	-59.585	17.387	86	67	14.2	1.69
	(3497)	(45)	(39)	(40.383)	(.45595)	(40.309)	(5.253)				
17-18	5649	40	-27	-47.122	.66648	-58.045	15.218	86	64	14.9	1.61
	(3345)	(42)	(37)	(38.626)	(.43611)	(38.555)	(5.026)				
18-19	5278	24	-35	-45.108	.64838	-53.717	13.075	88	65	17.0	2.29
	(3397)	(43)	(37)	(39.220)	(.44282)	(39.148)	(5.104)				
19-20	10864	-19	-30	-109.331	1.36523	-115.527	10.512	89	58	19.5	2.42
	(3026)	(39)	(33)	(34.938)	(.39447)	(34.874)	(4.546)				
20-21	9116	13	-55	-90.550	1.11754	-92.029	9.440	87	59	16.0	2.65
	(3091)	(39)	(34)	(35.697)	(.40303)	(35.631)	(4.645)				
21-22	7036	2	-87	-66.813	.88297	-71.934	5.329	86	62	14.1	2.28
	(3283)	(42)	(36)	(37.912)	(.42805)	(37.842)	(4.933)				
22-23	8918	10	-72	-88.068	1.10884	-90.512	4.946	82	72	10.5	1.81
	(3764)	(48)	(41)	(43.456)	(.49064)	(43.376)	(5.655)				
23-24	6727	24	10	-60.935	.77404	-65.792	4.097	51	91	2.4	1.79
	(4768)	(61)	(53)	(55.058)	(.62614)	(54.957)	(7.164)				

LHT is yesterday's high temperature.
HT is today's high.
No. of Cases = 21

Table B2 Regression results for Eq. (1) for July (weekdays.)

Hour	Constant	Monday	Friday	High	HT·LHT	LHT	Low	R^2	SD	F	DW
0-1	-2438	-92	17	32.525	-.28483	37.953	2.880	67	70	5.06	1.14
	(7280)	(44)	(49)	(81.191)	(.90682)	(80.232)	(7.059)				
1-2	-304	-93	59	8.785	-.02916	9.876	8.635	63	65	4.33	.85
	(6750)	(38)	(46)	(75.280)	(.84080)	(74.391)	(6.545)				
2-3	-2811	-75	58	34.402	-.34926	37.260	12.847	55	69	3.05	.94
	(7276)	(40)	(50)	(80.882)	(.70414)	(79.967)	(7.051)				
3-4	-2089	-62	27	27.287	-.27926	32.606	8.781	59	57	3.59	1.05
	(5863)	(33)	(40)	(65.387)	(.73031)	(64.615)	(5.685)				
4-5	-1552	-61	32	20.054	-.20396	26.997	8.875	75	42	7.31	.87
	(4299)	(24)	(29)	(47.945)	(.53550)	(47.945)	(4.169)				
5-6	-2061	-62	52	27.760	-.25472	30.677	7.900	77	41	8.54	2.18
	(4292)	(24)	(29)	(47.391)	(.52931)	(46.831)	(4.121)				
6-7	2875	-32	24	-34.289	.38861	-22.765	14.377	66	62	4.85	1.74
	(6455)	(36)	(44)	(71.987)	(.80402)	(71.137)	(6.259)				
7-8	1711	-53	34	-8.051	.15213	-4.923	4.549	69	48	5.51	1.76
	(5008)	(28)	(34)	(55.850)	(.62379)	(55.190)	(4.856)				
8-9	9974	16	55	-104.291	1.21190	-95.292	8.016	75	51	7.53	1.04
	(5281)	(29)	(36)	(58.902)	(.65788)	(58.207)	(5.121)				
9-10	-1141	43	55	22.451	-.11760	21.237	9.915	83	50	11.80	1.51
	(5219)	(29)	(35)	(58.202)	(.65006)	(57.515)	(5.061)				
10-11	-2553	10	46	42.867	-.28827	35.765	6.199	84	54	12.71	1.49
	(5563)	(31)	(38)	(62.039)	(.69292)	(61.307)	(5.394)				
11-12	3112	11	63	-18.071	.43351	-30.040	5.609	86	53	15.54	1.14
	(5482)	(31)	(37)	(61.140)	(.68287)	(60.418)	(5.316)				
12-13	-1921	27	51	37.779	-.18801	25.375	7.058	82	63	11.65	1.60
	(6508)	(36)	(44)	(72.585)	(.81070)	(71.728)	(6.311)				
13-14	1958	18	-25	-4.551	.26801	-13.801	3.846	90	47	21.53	1.29
	(4851)	(27)	(33)	(54.102)	(.60427)	(54.102)	(4.704)				
14-15	381	-27	-16	14.771	.07070	1.489	5.165	81	67	10.82	.98
	(6929)	(39)	(47)	(77.272)	(.86306)	(76.360)	(6.719)				
15-16	2900	-19	5	-12.566	.35738	-26.643	7.144	78	67	8.75	1.13
	(6937)	(39)	(47)	(77.368)	(.86413)	(76.455)	(6.727)				
16-17	-1215	-25	-62	45.187	-.22596	21.881	-4.277	74	81	6.95	1.18
	(8352)	(47)	(57)	(93.142)	(1.04031)	(92.043)	(8.099)				
17-18	4573	43	-2	-18.275	.55592	-47.718	-7.626	80	78	9.99	1.09
	(8022)	(45)	(54)	(89.469)	(.99929)	(89.469)	(7.779)				
18-19	-6938	77	-8	108.606	-.89592	85.928	-11.826	68	98	5.03	1.14
	(11933)	(56)	(81)	(132.272)	(1.50521)	(134.862)	(9.887)				
19-20	-11997	30	-55	163.875	-1.56252	144.222	-9.107	67	93	4.74	1.54
	(11319)	(54)	(77)	(125.462)	(1.42772)	(127.919)	(9.378)				
20-21	-12644	42	-42	171.532	-1.58207	143.322	-6.683	70	100	5.49	1.22
	(12138)	(58)	(82)	(134.550)	(1.53113)	(137.185)	(10.057)				
21-22	-2348	147	4	40.469	-.15163	27.756	-3.735	72	111	6.02	1.83
	(13464)	(64)	(91)	(149.240)	(1.69830)	(152.162)	(11.155)				
22-23	-12504	33	-66	156.973	-1.56331	142.870	5.538	55	107	3.00	1.56
	(11028)	(61)	(75)	(122.992)	(1.37371)	(121.540)	(10.694)				
23-24	-10576	45	-27	144.558	-1.39752	126.198	-8.072	43	112	1.92	1.26
	(11571)	(64)	(79)	(129.043)	(1.44129)	(129.043)	(11.220)				

LHT is yesterday's high temperature.
HT is today's high.
No. of Cases = 22

Table B3 Regression results for Eq. (1) for August (weekdays).

Hour	Constant	Monday	Friday	High	HT-LHT	LHT	Low	R^2	SD	F	DW
0-1	-1773	-119	-24	26.524	-.27840	34.662	4.656	.71	71	5.83	.77
	(3354)	(43)	(47)	(38.042)	(.42231)	(36.091)	(4.031)				
1-2	-1610	-116	12	25.198	-.27071	34.186	2.007	.82	49	10.89	1.08
	(2343)	(30)	(33)	(26.575)	(.29501)	(25.212)	(2.816)				
2-3	-3401	-114	-25	43.687	-.47367	52.115	4.001	.89	40	18.02	.96
	(1886)	(24)	(26)	(21.383)	(.23738)	(20.287)	(2.266)				
3-4	-1973	-101	-29	28.701	-.31015	36.663	3.301	.86	38	14.54	.87
	(1818)	(24)	(25)	(20.624)	(.22895)	(19.566)	(2.185)				
4-5	-302	-96	-3	12.640	-.13174	18.430	1.493	.81	37	10.22	.93
	(1765)	(26)	(25)	(20.020)	(.22224)	(18.993)	(2.121)				
5-6	-1417	-31	-23	23.929	-.27274	30.057	6.774	.79	38	8.56	2.09
	(1785)	(23)	(25)	(20.247)	(.22476)	(19.208)	(2.145)				
6-7	2558	-25	13	-18.485	.21474	-9.948	1.298	.57	66	3.04	1.82
	(3159)	(41)	(44)	(35.825)	(.39769)	(33.987)	(3.796)				
7-8	-464	-47	-38	17.374	-.19873	24.120	6.572	.61	59	3.71	1.47
	(2827)	(37)	(39)	(32.055)	(.35584)	(30.410)	(3.396)				
8-9	929	-38	-60	3.383	-.01272	9.262	5.735	.65	67	4.42	1.31
	(3183)	(41)	(44)	(36.097)	(.40071)	(34.246)	(3.825)				
9-10	1	7	-37	12.840	-.09000	16.452	8.606	.61	96	3.59	.89
	(4567)	(59)	(63)	(51.795)	(.57497)	(49.138)	(5.488)				
10-11	2052	9	-5	-9.949	.19724	-6.529	5.627	.69	95	5.11	1.01
	(4504)	(58)	(63)	(51.073)	(.56696)	(48.453)	(5.411)				
11-12	4589	-30	-32	-36.578	.48823	-33.892	6.224	.60	107	3.53	1.23
	(5103)	(66)	(71)	(57.867)	(.64237)	(54.898)	(6.131)				
12-13	4979	-10	-30	-40.362	.55256	-40.318	6.829	.69	115	3.63	.88
	(5450)	(71)	(76)	(61.805)	(.68610)	(58.635)	(6.548)				
13-14	3885	-24	-52	-26.853	.43648	-31.323	7.931	.67	112	4.77	.84
	(5361)	(69)	(75)	(60.793)	(.67486)	(57.674)	(6.441)				
14-15	227	-47	-66	15.017	-.02580	7.848	10.570	.80	82	9.23	1.06
	(3901)	(51)	(54)	(44.242)	(.49113)	(41.973)	(4.688)				
15-16	913	-42	-59	9.174	.04052	1.591	8.136	.77	84	7.69	.85
	(3995)	(52)	(56)	(45.305)	(.50293)	(42.981)	(4.800)				
16-17	2895	10	-22	-11.520	.30218	-20.187	2.772	.80	80	9.43	1.25
	(3803)	(49)	(53)	(43.131)	(.4788)	(40.919)	(4.570)				
17-18	3712	27	-19	-19.080	.39486	-27.837	-1.618	.79	80	9.18	1.08
	(3795)	(49)	(53)	(43.037)	(.47775)	(40.829)	(4.560)				
18-19	4463	29	13	-25.542	.44896	-32.870	-5.793	.66	98	4.78	1.14
	(4670)	(61)	(65)	(52.956)	(.58786)	(50.239)	(5.611)				
19-20	4819	18	-3	-32.631	.50860	-37.836	-2.919	.73	79	6.27	2.20
	(3763)	(49)	(52)	(42.678)	(.47377)	(40.489)	(4.522)				
20-21	2126	12	-42	.346	.13032	-6.847	-2.301	.76	65	7.23	1.00
	(3097)	(40)	(43)	(35.115)	(.38981)	(33.314)	(3.721)				
21-22	3928	59	-18	-21.293	.38963	-28.174	-4.664	.68	91	4.86	1.09
	(4313)	(56)	(60)	(48.909)	(.54293)	(46.400)	(5.182)				
22-23	3299	-8	12	-15.077	.35114	-26.344	-4.190	.66	102	4.61	.86
	(4854)	(63)	(67)	(55.041)	(.61101)	(52.218)	(5.832)				
23-24	4147	-3	84	-26.284	.39470	-30.202	-5.923	.36	117	1.33	1.05
	(5546)	(72)	(77)	(62.890)	(.69814)	(59.664)	(6.663)				

LHT is yesterday's high temperature.
HT is today's high.
No. of Cases = 21

Table B4 Regression results for Eq. (2) for June (weekdays).

Hour	Constant	Monday	Friday	GER(9-10)	GER(15-16)	Current Temp.	Lagged Temperature Temp(-1)	Temp(-2)	Temp(-3)	Temp(-4)	Temp(-5)	R^2	SD	F
10-11	140	-31	-32	.9610		.6585						.91	46	41.40
	(180)	(27)	(27)	(.1168)		(2.448)								
11-12	239	2	9	.8907		22.582	-21.388					.95	37	58.30
	(167)	(24)	(25)	(.1064)		(9.922)	(10.143)							
12-13	-22	5	7	1.0085		30.014	-28.159	-.8311				.95	42	41.00
	(208)	(27)	(29)	(.1305)		(12.424)	(23.459)	(13.864)						
13-14	-179	19	-30	1.0051		15.615	16.462	-31.018	2.119			.94	50	27.22
	(319)	(34)	(35)	(.1873)		(22.666)	(45.501)	(37.680)	(17.298)					
14-15	-283	49	-7	.8929		39.637	-41.510	62.641	-50.602	4.840		.94	45	24.98
	(317)	(33)	(32)	(.1726)		(16.311)	(38.551)	(52.984)	(40.894)	(17.389)				
15-16	34	10	-7	.7923		18.387	3.841	-41.220	77.679	-53.024	.427	.95	41	28.18
	(314)	(38)	(29)	(.1564)		(11.126)	(27.656)	(38.993)	(49.412)	(39.552)	(18.048)			
16-17	97	-8	5		.9200	.986						.93	45	50.27
	(172)	(24)	(26)		(.0987)	(1.974)								
17-18	-245	11	-53		1.0288	19.457	-18.153					.96	32	81.49
	(156)	(11)	(18)		(.0915)	(5.564)	(6.274)							
18-19	-407	-15	-54		1.0050	8.465	7.062	-12.457				.94	45	37.26
	(202)	(25)	(28)		(.1422)	(9.901)	(17.199)	(11.011)						
19-20	-417	-23	-64		.9020	25.942	-19.229	21.729	-22.374			.95	42	33.94
	(245)	(23)	(31)		(.1391)	(10.539)	(21.911)	(25.738)	(14.657)					
20-21	90	-20	-75		.6883	-4.643	30.604	-12.394	-4.879	-2.665		.94	43	23.76
	(259)	(31)	(39)		(.1450)	(10.450)	(25.582)	(34.075)	(34.102)	(17.723)				
21-22	-183	-24	-123		.7633	-1.228	-5.132	30.098	-17.743	26.654	-25.812	.95	41	24.35
	(244)	(29)	(37)		(.1371)	(12.696)	(17.718)	(25.164)	(32.567)	(32.119)	(16.686)			

GRE (9-10) and GRE (15-15) are the electric demand at hours (9-10) and (15-16), respectively.
No. of Cases = 21

Table B5 Regression results for Eq. (2) for July (weekdays).

Hour	Constant	Monday	Friday	GER(9-10)	GER(15-16)	Current Temp.	Lagged Temperature Temp(-1)	Temp(-2)	Temp(-3)	Temp(-4)	Temp(-5)	R^2	SD	F
10-11	210	-38	-12	.7922		5.286						.82	52	19.76
	(283)	(30)	(34)	(.1527)		(3.013)								
11-12	191	-28	-3	.7004		21.637	-13.200					.86	51	19.92
	(280)	(30)	(34)	(.1566)		(16.288)	(16.232)							
12-13	100	-21	-8	.8815		-23.418	69.361	-41.976				.91	45	24.64
	(248)	(26)	(30)	(.1508)		(12.291)	(24.439)	(17.204)						
13-14	337	-20	-80	.6818		2.409	2.347	16.808	-13.671			.88	53	14.03
	(315)	(31)	(44)	(.1795)		(17.347)	(25.698)	(29.490)	(20.165)					
14-15	208	-63	-92	.7681		10.254	-23.510	31.123	16.473	-27.896		.89	55	13.44
	(350)	(33)	(46)	(.1845)		(12.316)	(21.074)	(26.368)	(30.296)	(20.738)				
15-16	585	-47	-75	.6396		.395	6.279	-21.952	23.044	28.097	-30.135	.81	70	5.51
	(454)	(42)	(59)	(.2382)		(18.156)	(38.219)	(48.680)	(49.545)	(41.421)	(26.764)			
16-17	180	-34	-73		.7549	5.562						.91	44	42.52
	(235)	(26)	(30)		(.1138)	(2.142)								
17-18	-119	78	-43		.6625	-.607	11.854					.93	44	43.64
	(235)	(26)	(31)		(.1140)	(5.759)	(7.089)							
18-19	-202	37	20		.7238	14.209	-7.882	3.156				.86	66	15.11
	(379)	(40)	(46)		(.1896)	(16.929)	(30.607)	(19.716)						
19-20	-123	5	6		.5660	11.253	1.148	.126	.507			.94	42	32.93
	(271)	(30)	(30)		(.1218)	(6.810)	(12.590)	(20.127)	(13.710)					
20-21	-523	31	-10		.8902	4.969	3.701	-1.932	5.084	-4.212		.89	64	13.60
	(416)	(45)	(46)		(.2048)	(10.002)	(20.868)	(30.854)	(39.232)	(24.269)				
21-22	14	50	-27		.7432	-28.24	59.688	-80.476	47.889	13.353	-9.504	.75	115	4.07
	(748)	(81)	(90)		(.3690)	(38.897)	(61.856)	(60.041)	(70.1)	(80.455)	(49.481)			

GRE (9-10) and GRE (15-15) are the electric demand at hours (9-10) and (15-16), respectively.
No. of Cases = 22

Table B6 Regression results for Eq. (2) for August (weekdays).

Hour	Constant	Monday	Friday	GER(9-10)	GER(15-16)	Current Temp.	Lagged Temperature Temp(-1)	Temp(-2)	Temp(-3)	Temp(-4)	Temp(-5)	R^2	SD	F
10-11	-93	-5	12	.9658		3.366						.91	46	42.34
	(198)	(27)	(25)	(.0919)		(1.826)								
11-12	82	-48	-20	.8956		-.492	4.859					.84	65	15.93
	(286)	(40)	(35)	(.1298)		(13.925)	(15.255)							
12-13	-37	-43	-13	.9449		7.544	3.578	-7.142				.86	68	14.41
	(303)	(45)	(38)	(.1489)		(20.653)	(39.152)	(24.203)						
13-14	-383	-42	-44	.9745		25.926	-35.946	24.521	-6.421			.88	71	13.39
	(349)	(47)	(41)	(.1752)		(23.913)	(55.676)	(59.071)	(29.949)					
14-15	-104	-54	-29	.8223		-1.441	44.454	-74.056	68.002	-27.954		.91	60	14.63
	(295)	(40)	(34)	(.1481)		(8.263)	(25.143)	(47.942)	(50.028)	(25.307)				
15-16	201	-68	-34	.7297		-5.427	12.922	23.777	-52.722	64.914	-36.012	.88	67	9.37
	(328)	(45)	(43)	(.1643)		(23.556)	(47.633)	(40.917)	(54.661)	(55.921)	(28.084)			
16-17	17	29	-1		.8466	4.149						.96	34	95.81
	(139)	(20)	(18)		(.0722)	(1.322)								
17-18	77	32	-29		.7225	8.226	-1.461					.95	39	54.40
	(164)	(23)	(21)		(.0840)	(5.791)	(5.574)							
18-19	310	30	-14		.6233	-3.318	20.368	-10.878				.81	72	10.21
	(320)	(48)	(42)		(.1554)	(16.778)	(27.870)	(14.807)						
19-20	202	5	-17		.6457	8.150	-7.543	14.966	-9.258			.86	59	11.55
	(295)	(40)	(35)		(.1278)	(10.174)	(19.711)	(26.069)	(14.149)					
20-21	532	3	-38		.4965	-4.206	20.710	-22.373	22.481	-9.172		.90	44	13.88
	(265)	(30)	(28)		(.1313)	(10.966)	(23.379)	(22.688)	(22.946)	(12.745)				
21-22	95	27	-90		.4764	28.528	-31.236	23.340	6.003	-29.983	15.875	.85	69	7.09
	(411)	(49)	(46)		(.2078)	(17.357)	(27.518)	(37.974)	(35.755)	(35.634)	(20.082)			

GER (9-10) and GER (15-16) are the electric demand at hours (9-10) and (15-16), respectively.
No. of Cases = 21

Table B7 Regression results for Eq. (1) for weekends.

Hour	Constant	July	Aug.	Sat.	HDY.	HIGH	HT-LHT	LHT	Low	Cases	R^2	SD	F	DW
0-1	-242	40	70	60	-15	15.141	-.13681	13.514	6.405	28	58	85	3.3	1.41
	(3071)	(45)	(42)	(35)	(94)	(36.751)	(.43292)	(35.100)	(5.814)					
1-2	1484	39	68	64	16	-6.454	.11631	-6.918	5.268	28	67	68	4.8	1.23
	(2447)	(36)	(33)	(28)	(75)	(29.282)	(.34494)	(27.967)	(4.632)					
2-3	1176	46	60	77	4	-4.519	.10127	-5.180	5.809	28	73	67	6.4	1.32
	(2409)	(36)	(33)	(28)	(74)	(28.829)	(.33960)	(27.534)	(4.560)					
3-4	-1423	104	87	37	-60	32.016	-.30517	26.313	1.214	28	56	85	3.1	1.49
	(3055)	(45)	(43)	(35)	(93)	(36.568)	(.43077)	(34.926)	(5.785)					
4-5	86	61	66	56	23	10.650	-.08541	8.038	5.361	28	76	51	7.6	1.18
	(1830)	(27)	(25)	(21)	(56)	(21.898)	(.28796)	(20.914)	(3.494)					
5-6	-522	44	51	58	1	14.467	-.16903	16.454	8.335	28	79	46	8.9	1.52
	(1648)	(24)	(23)	(19)	(50)	(19.721)	(.23731)	(18.834)	(3.120)					
6-7	1009	13	61	134	-29	-3.682	.06466	-1.181	4.754	28	81	57	10.0	1.22
	(2051)	(30)	(28)	(24)	(63)	(24.551)	(.28921)	(23.448)	(3.884)					
7-8	-1346	-5	32	181	-83	25.472	-.28517	29.890	2.641	28	86	59	14.2	1.41
	(407)	(31)	(29)	(24)	(64)	(25.212)	(.29700)	(24.079)	(3.988)					
8-9	1543	41	44	228	101	-8.351	.13103	-4.491	1.599	28	95	38	45.7	1.79
	(1352)	(20)	(18)	(16)	(41)	(16.186)	(.19067)	(15.459)	(2.560)					
9-10	3898	32	36	262	53	-36.694	.47377	-32.113	3.206	28	93	52	31.1	1.20
	(1875)	(28)	(26)	(21)	(57)	(22.444)	(.26438)	(21.435)	(3.550)					
10-11	2660	51	35	254	33	-20.309	.30389	-18.339	3.393	28	92	59	26.4	1.04
	(2103)	(31)	(29)	(24)	(64)	(25.172)	(.29653)	(24.041)	(3.983)					
11-12	2179	34	35	247	-11	-14.773	.25364	15.087	6.354	28	92	59	29.0	1.29
	(2111)	(31)	(29)	(24)	(66)	(25.271)	(.29769)	(24.135)	(3.997)					
12-13	758	54	55	194	-34	3.883	.06905	-.856	6.569	28	89	69	19.5	1.38
	(2497)	(37)	(34)	(29)	(76)	(29.883)	(.35202)	(28.541)	(4.727)					

LHT is yesterday's high temperature.
HT is today's high.

Table B7 (Continued)

Hour	Constant	July	Aug.	Sat.	HDY.	HIGH	HT·LHT	LHT	Low	Cases	R^2	SD	F	DW
13-14	1051	46	22	141	-91	2.578	.10607	-4.776	5.364	28	86	73	14.7	1.04
	(2631)	(39)	(36)	(30)	(80)	(31.487)	(.37092)	(30.073)	(4.981)					
14-15	556	24	4	151	-87	8.999	.04679	-1.339	6.945	28	86	79	14.2	1.25
	(2857)	(42)	(39)	(33)	(87)	(34.190)	(.40275)	(32.654)	(5.408)					
15-16	240	24	24	143	-26	10.709	.03637	1.214	7.191	28	89	70	19.0	1.22
	(1533)	(37)	(35)	(29)	(77)	(30.318)	(.35714)	(28.956)	(4.796)					
16-17	-391	21	36	99	-46	19.342	-.05224	9.020	5.600	28	86	78	14.5	1.24
	(2804)	(41)	(38)	(32)	(86)	(33.550)	(.39531)	(32.051)	(5.308)					
17-18	-805	5	15	78	-23	26.683	-.14279	14.824	5.656	28	78	92	8.5	1.05
	(3323)	(49)	(45)	(38)	(102)	(39.769)	(.46848)	(37.983)	(6.291)					
18-19	-1010	-9	-1	78	-82	29.077	-.15171	17.084	3.071	28	80	90	9.5	1.09
	(3236)	(48)	(44)	(37)	(99)	(38.733)	(.45628)	(36.993)	(6.127)					
19-20	-2163	-29	2	52	-75	42.859	-.31671	30.932	2.760	28	82	79	10.9	1.12
	(2827)	(42)	(39)	(32)	(86)	(33.835)	(.39857)	(32.315)	(5.352)					
20-21	-973	37	50	23	-129	30.422	-.22145	22.159	1.631	28	63	102	4.0	1.20
	(3662)	(54)	(50)	(42)	(112)	(43.831)	(.51633)	(41.862)	(6.934)					
21-22	-458	-44	-36	-30	-141	23.608	-.12001	13.536	4.080	28	76	81	7.7	.99
	(2922)	(43)	(40)	(34)	(89)	(34.976)	(.41202)	(33.405)	(5.533)					
22-23	-2236	-6	-18	-41	-160	40.154	-.34751	34.191	6.287	27	81	73	9.4	1.39
	(2752)	(40)	(37)	(32)	(81)	(32.699)	(.38738)	(31.653)	(5.033)					
23-24	-3857	47	8	-27	-67	59.178	-.56383	50.754	5.368	28	82	69	10.5	1.34
	(2292)	(37)	(34)	(28)	(75)	(27.523)	(.32043)	(26.199)	(4.425)					

Table B8 Regression results for Eq. (3) for June (weekdays).

Hour	Constant	Monday	Friday	GER(-1)	GER(-2)	R^2	SD	F	DW
10-11	139	-34	-32	.9572	.0277	.91	46	41.2	1.96
	(180)	(25)	(27)	(.2114)	(.1985)				
11-12	-56	0	5	.7464	.3106	.98	25	171.9	1.63
	(98)	(14)	(15)	(.1335)	(.1378)				
12-13	-102	6	18	.7216	.3325	.98	22	238.4	2.29
	(88)	(12)	(13)	(.1946)	(.2043)				
13-14	55	6	-28	.8668	.1260	.90	56	35.2	2.39
	(220)	(30)	(34)	(.5943)	(.6204)				
14-15	199	2	9	.9572	-.0350	.98	25	175.0	2.21
	(92)	(13)	(15)	(.1095)	(.1140)				
15-16	137	-15	-2	.3183	.6288	.96	33	98.7	2.12
	(134)	(18)	(19)	(.3310)	(.3096)				
16-17	113	-6	8	1.2141	-.2671	.93	44	52.0	2.55
	(171)	(24)	(26)	(.3005)	(.3029)				
17-18	28	2	-46	.6112	.3531	.95	36	78.9	2.24
	(137)	(19)	(21)	(.1962)	(.1950)				
18-19	-186	-26	-12	.9301	.1122	.94	42	65.4	2.01
	(160)	(22)	(27)	(.2677)	(.2629)				
19-20	27	-13	2	.4348	.5001	.89	54	33.0	1.40
	(48)	(30)	(31)	(.3220)	(.3455)				
20-21	199	20	-28	.8822	.0233	.94	36	68.2	2.26
	(128)	(19)	(21)	(.1576)	(.1492)				
21-22	239	-4	-59	.0297	.8566	.92	44	46.5	2.11
	(164)	(24)	(27)	(.3003)	(.2798)				

GER (-1) and GER (-2) are lagged generation one hour and two hours ago.
No. of Cases = 21

Table B9 Regression results for Eq. (3) for July (weekdays).

Hour	Constant	Monday	Friday	GER(-1)	GER(-2)	R^2	SD	F	DW
10-11	317	-41	-22	1.1474	-.2418	.80	56	17.06	1.11
	(334)	(32)	(35)	(.2277)	(.2662)				
11-12	-55	-4	-11	.8451	.2135	.91	40	44.14	1.51
	(216)	(23)	(25)	(.1687)	(.1850)				
12-13	-16	14	-7	.8365	.1875	.92	40	48.63	1.13
	(205)	(22)	(26)	(.2349)	(.2516)				
13-14	278	-1	-81	.3011	.6179	.95	32	75.09	2.09
	(156)	(18)	(20)	(.1893)	(.1985)				
14-15	-97	-43	11	1.0511	-.0083	.95	33	75.74	1.22
	(180)	(19)	(27)	(.2050)	(.1867)				
15-16	208	10	13	.8679	.0480	.95	29	85.69	1.68
	(155)	(19)	(20)	(.2104)	(.2264)				
16-17	165	-9	-60	.4523	.4797	.88	50	32.17	2.00
	(267)	(29)	(34)	(.4201)	(.3933)				
17-18	-367	72	44	1.1390	-.0257	.95	37	77.61	1.33
	(196)	(21)	(27)	(.1713)	(.1777)				
18-19	-417	50	65	.7600	.3470	.92	46	46.11	2.28
	(266)	(34)	(36)	(.3358)	(.3694)				
19-20	517	-49	-63	1.2617	-.4708	.92	43	46.12	2.07
	(221)	(25)	(33)	(.2263)	(.2534)				
20-21	-142	-14	-26	.4681	.5572	.91	52	39.92	1.51
	(231)	(31)	(36)	(.2731)	(.2498)				
21-22	149	101	-2	.5264	.3655	.61	123	6.16	2.15
	(555)	(70)	(85)	(.2504)	(.5845)				

GER (-1) and GER (-2) are lagged generation one hour and two hours ago.
No. of Cases = 22

Table B10 Regression results for Eq. (3) for August (weekdays).

Hour	Constant	Monday	Friday	GER(-1)	GER(-2)	R^2	SD	F	DW
10-11	-118	-7	15	.9413	.1487	.90	51	34.64	1.86
	(306)	(33)	(30)	(.2606)	(.3530)				
11-12	193	-48	-30	.8536	.1047	.89	54	31.37	2.17
	(224)	(31)	(29)	(.2614)	(.2886)				
12-13	-120	-1	-10	.6332	.4390	.95	37	79.95	2.14
	(151)	(23)	(21)	(.1741)	(.1746)				
13-14	-145	-6	-15	.8275	.2504	.96	34	114.67	1.89
	(137)	(20)	(18)	(.1912)	(.2067)				
14-15	422	-9	13	1.2170	-.3715	.90	53	36.63	1.87
	(204)	(31)	(29)	(.3798)	(.4068)				
15-16	170	-4	-6	.7841	.1519	.98	25	163.66	2.16
	(99)	(15)	(13)	(.1143)	(.1059)				
16-17	-36	36	0	.8890	.1107	.94	43	58.10	1.82
	(178)	(25)	(23)	(.3990)	(.3799)				
17-18	66	5	-24	1.0313	-.0774	.96	35	86.34	1.71
	(143)	(22)	(19)	(.2040)	(.2117)				
18-19	234	-8	18	1.4820	-.5931	.90	49	37.19	1.14
	(192)	(28)	(27)	(.3490)	(.3426)				
19-20	177	-9	-2	.5974	.2913	.97	24	140.01	2.20
	(95)	(14)	(13)	(.1112)	(.1054)				
20-21	495	2	-34	.5443	.2550	.94	30	63.38	2.11
	(131)	(17)	(16)	(.2609)	(.2361)				
21-22	-194	38	-6	.5593	.4848	.86	54	25.41	1.52
	(310)	(32)	(33)	(.4413)	(.3747)				

GER (-1) and GER (-2) are lagged generation one hour and two hours ago.
No. of Cases = 21

APPENDIX C

NUMERICAL EXAMPLE

The purpose of this Appendix is to demonstrate how the electric generation model operates by utilizing a simple numerical illustration. In this example we assume that there are only five power generating units and no hydro, pumped hydro or nuclear sources. Table C1 describes the characteristics of each hypothetical plant.

In order to simplify the demonstration, electric load forecasts are made for a five-hour day and the forecasts are assumed to be given prior to scheduling. Once the preliminary generation schedule is developed, revisions may be made up to 30 minutes prior to the occurrence of the actual loads.

Scheduling of the committed plants proceeds as follows. The peak load is assumed to occur at hour four. Units A, B and C must be committed to meet the anticipated load while still meeting the spinning reserve. The minimum power that A, B and C can produce is 240 MW at an hourly cost of $2,200. In order to meet the electric demand during hour 4 (Table C2) all three sources must be tapped. However, since unit B is the power purchased from outside sources it cannot be counted as part of spinning reserve. Therefore, the 550 MW demand (plus a 50 MW reserve requirement met) will be met by producing maximum power from A, 100 MW from C and 85 MW from B. The fact that 85 MW are required in hour 4 means that only 75 MW's are available for all other hours during the day[1]. If spinning reserve is not a constraint then the optimal schedule would still result in maximum output from A, but C would also be called upon to produce its maximum (150 MW). Outside purchases would make up the remainder of the load. This schedule results in zero reserve capacity. In order to maintain the required 50 MW reserve, unit C had to be reduced by 50 MW and outside purchase increased to make up the difference. The total cost of meeting the optimal schedule is:

Total Cost=$2,200+$9(165)+$10(60)+$15(85)=$5,560
(hour 4)

The electric loads assumed for this example are displayed in Table C2.

[1]These values were computed given that the daily purchase was limited to 160 MW.

Table C2 Electric loads.

Hour	1	2	3	4	5
Forecast Load	400	300	500	550	450
Actual Load	450	280	520	580	450

The 50 MW spinning reserve requirement pertains to all of the day's five hours. As specified in the report, the optimal strategy for committing units is based on their respective marginal costs. Hence, units should be utilized in order of their incremental fuel costs as (displayed in column 4, Table C1). Based on this policy a commitment priority list is given by Table C3.

Table C3 Commitment priority list.

Rank No.	Unit	Incremental Fuel Cost ($/MWH)
1	A	9
2	C	10
3	B	15
4	E	20
5	D	39

Hour 3 is scheduled in a similar fashion except the daily limit for outside purchases is now 85 MW. The 500 MW demand and 50 MW reserve are best met by generating 365 MW from A, 100 MW from C and purchasing 35 MW. As in hour 4, the 50 MW reserve is met by turning unit C down. The total cost for scheduled units according to the forecast for hour 3 is

Total Cost=$2,200+$9(165)+$10(60)+$15(35)=$4,810
(hour 3)

The schedules for the remaining three hours are computed in the same fashion. The results for these computations are shown in Table C4.

Table C4 reveals that unit C is turned on to meet the anticipated demands of hour 1. It is then turned off during hour 2 and back on again for hours 3, 4 and 5. Given the fact that C's shutdown and start-up cost is $100 one could question the wisdom of such a strategy. It is advantageous to at least compare the costs of maintaining C at minimum power for one hour versus

Table C1 Performance data for hypothetical power generating units.

Unit	Maximum Power (MW)	Minimum Power (MW)	Incremental Fuel Cost ($/MWH)	Minimum Load Production Cost	Full Load Production Cost	Start-up Time (Hours)	Start-up Cost	Day Unit
A	365	200	9	1800	3240	10	150	None
B	100	0	15	0	1500	.5	0	160
C	150	40	10	400	1500	5	100	None
D	30	30	39	1170	1170	.3	30	None
E	25	25	20	500	500	1.7	40	None
Penalty	∞	0	M					

Table C4 Generation schedule.

Unit	Hour 1	2	3	4	5
A	360	300	365	365	365
C	40	0	100	100	85
B	0	0	35	85	0
E	0	0	0	0	0
D	0	0	0	0	0
Total Generation (MW)	400	300	500	550	450
Spinning Reserve (MW)	115	65	50	50	65
Total Cost ($)	3640	2700	4810	5560	4135

shutting down altogether. If allowed to remain on-line, the cost of generation for unit C would be $2,740 ($2,200 cost of production at minimum power plus 60 MW at $9/MW). If C is shut down for hour 2, the cost would be $2,700 plus the additional $100 start-up or $2,800.

Since the latter option is more expensive than the former, the optimal schedule will result in C being left on. See Table C5.

Table C5 Final schedule.

Unit	Hour 1	2	3	4	5
A	360	260	365	365	365
C	40	40	100	100	85
B	0	0	35	85	0
E	0	0	0	0	0
D	0	0	0	0	0
Total Generation (MW)	400	300	500	550	450
Spinning Reserve (MW)	115	215	50	50	65
Total Cost ($)	3640	2740	4810	5560	4135

The schedule shown in Table C5 is based on forecast loads. Actual loads were assumed to be known with a 30-minute warning. New units must be scheduled whenever the spinning reserve falls below 50 MW. Hence, only units which exhibit start-up times less than 30 minutes can be activated. Of course, if the actual load turns out to be less than that forecast, no one action is taken.

The forecast load for hour 1 proved to be 50 MW short of what actually occurred (see Table C2). The spinning reserve during this period was 115. Therefore, the utility company need not adjust its mix of plants because after subtracting the unanticipated demand it is left with sufficient reserves (65 MW) to meet its obligations. The results are not as straightforward for hour 2. Here actual loads exceed the forecast ones by 20 MW. Spinning reserve is only 50 MW, therefore an additional quick-start unit must be activated, or power has to be purchased. Units B and D (purchase) meet the 30-minute start-up requirement. Given the relative price of the two, the least-cost alternative is to purchase an additional 20 MW of power. Unit C is then throttled back to meet the 50 MW requirement.

REFERENCES

Benkley, C.W. and L.L. Schulman, 1979: Estimated hourly mixing depth from historical meteorological data. J. Appl. Meteor. (18), 772-780.

Blakadar, A.K., 1976: Modelling the nocturnal boundary layer. Preprints, Third Symp. on Atmospheric Turbulence, Diffusion and Air Quality, Raleigh, Amer. Meteor. Soc., 46-49.

Bowling, S.A. and C.S. Benson, 1978: Study of the subarctic heat island at Fairbanks, Alaska. EPA-600/4-78-027, Environmental Monitoring Series. Environmental Sciences Research Laboratory, Office of Research and Development, U.S. Environmental Protection Agency, Research Triangle Park, North Carolina.

Davis, H., 1958: The relationship between weather and electricity demand. Proc. IEEE, Oct. pp. 27-37.

Deardorff, J.W., 1972: Parameterization of the planetary boundary layer for use in general circulation models. Mon. Wea. Rev., (100), 93-106.

Delage, Y., 1974: A numerical study of the nocturnal atmospheric boundary layer. Quart. J. Roy. Meteor. Soc., (96), 91-114.

Galiana, F.D., 1976: Short-term load forecasting. Proc. on Forecasting Methodology for Time of Day and Season Electric Utility Loads, Special Report 31, Edited by J.W. Boyd, March, pp. 19-20.

Henderson-Sellers, A., 1980: A simple numerical simulation of urban mixing depths. J. Appl. Meteor., 19 (2), 215-218.

Leahey, D.M. and J.P. Friend, 1971: A model for predicting the depth of the mixing layer over an urban heat island with application to New York. J. Appl. Meteor., 10 (12), 1162-1173.

Oke, T.R., 1976: The distinction between canopy and boundary layer heat islands. Atmosphere, (14), 268-276.

Plate, E.J., 1971: Aerodynamic characteristics of atmospheric boundary layers. U.S. Atomic Energy Commission, Office of Information Services, 190 pp.

Reiter, E.R., G.R. Johnson, W.L. Somervell, Jr., E.W. Sparling, E. Dreiseitl, B.C. Macdonald, J.P. McGurik and A.M. Starr, 1976: The effects of atmospheric variability on energy utilization and conservation. Environmental Research Paper No. 5, Colorado State University, Ft. Collins, CO. 72 pp.

_____, E. Dreiseitl, G.R. Johnson, H.H. Leong, B.C. MacDonald, W.L. Somervell, Jr., A.M. Starr and K. Timbre, 1978: The effects of atmospheric variability on energy utilization and conservation. Environmental Research Paper 14, Coloardo State University, Ft. Collins, CO.

_____, C.C. Burns, E. Dreiseitl, G.R. Johnson, H.H. Leong, B.C. Macdonald, J.D. Sheaffer, and A.M. Starr, 1979: The effects of atmospheric variability on energy utilization and conservation. Environmental Research Paper 18, Colorado State University, Ft. Collins, CO.

_____, C.C. Burns, H. Cochrane, H.H. Leong, G.R. Johnson, J.R. McKean, J.D. Sheaffer, A.M. Starr and J. Webber, 1980: The effects of atmospheric variability on energy utilization and conservation. Environmental Research Paper 24, Colorado State University, Ft. Collins, CO.

_____ and D.R. Westhoff, 1981: A planetary-wave climatology. J. Atmos. Sci., 38 (4), 732-750.

_____, C.C. Burns, H. Cochrane, G.R. Johnson, H. Leong, and J.D. Sheaffer, 1981a: The effects of atmospheric variability on energy utilization and conservation. Progress Report submitted to the U.S. Department of Energy, Contract DE-AS02-76EV01340, July. 85 pp.

_____, C.C. Burns, H. Cochrane, G.R. Johnson, H. Leong, and J.D. Sheaffer, 1981b: The effects of atmospheric variability on energy untilization and conservation. Environmental Research Paper No. 31, Colorado State University, Ft. Collins, CO. 59 pp.

_____ and D.R. Westhoff, 1982: Linear trends in northern-hemisphere tropospheric geopotential height and temperature patterns. J. Atmos. Sci., 39 (3) (in press).

Spera, D.A. and T.R. Richards, 1978: A revised wind shear power law model. Wind Energy Project Office, Project Information Release No. 70, National Aeronautics and Space Administration.

Summers, P.W., 1965: An urban heat island model, its role in our pollution problems with application to Montreal. Paper presented at the First Canadian Conference on Micrometeorology. Toronto, 12-14 April.

Yu, T., 1978: Determining the height of the nocturnal boundary layer. J. Appl. Meteor., 17 (1), 28-33.

Author: Elmar R. Reiter et al. 551.588.7

THE EFFECTS OF ATMOSPHERIC VARIABILITY ON ENERGY UTILIZATION AND CONSERVATION

Subject Headings:

Energy Consumption
Energy Modelling
Urban Climate

Colorado State University
Department of Atmospheric Science

Environmental Research Paper No. 32
March 1982, 41 pp.

U.S. Department of Energy
Contract DE-AS02-76EV01340

Our statistical reference model of energy demand for space heating has been applied to estimate total daily demand for an entire region. Intraregional subareas exhibited considerable diversity in rates of demand, factors controlling demand and in overall accuracy of model predictions. Progress toward obtaining detailed building census and meteorological data for physical and physical-reference modelling of regional space heating energy requirements is also described.

A physical model of energy demand for air conditioning in large buildings has received preliminary testing. The Group Method of Data Handling (GMDH) algorithm failed in its first application to air conditioning data. The reasons for this failure are complex and not completely resolved. Presently however, this failure is viewed as an

Author: Elmar R. Reiter et al. 551.588.7

THE EFFECTS OF ATMOSPHERIC VARIABILITY ON ENERGY UTILIZATION AND CONSERVATION

Subject Headings:

Energy Consumption
Energy Modelling
Urban Climate

Colorado State University
Department of Atmospheric Science

Environmental Research Paper No. 32
March 1982, 41 pp.

U.S. Department of Energy
Contract DE-AS02-76EV01340

Our statistical reference model of energy demand for space heating has been applied to estimate total daily demand for an entire region. Intraregional subareas exhibited considerable diversity in rates of demand, factors controlling demand and in overall accuracy of model predictions. Progress toward obtaining detailed building census and meteorological data for physical and physical-reference modelling of regional space heating energy requirements is also described.

A physical model of energy demand for air conditioning in large buildings has received preliminary testing. The Group Method of Data Handling (GMDH) algorithm failed in its first application to air conditioning data. The reasons for this failure are complex and not completely resolved. Presently however, this failure is viewed as an

Author: Elmar R. Reiter et al. 551.588.7

THE EFFECTS OF ATMOSPHERIC VARIABILITY ON ENERGY UTILIZATION AND CONSERVATION

Subject Headings:

Energy Consumption
Energy Modelling
Urban Climate

Colorado State University
Department of Atmospheric Science

Environmental Research Paper No. 32
March 1982, 41 pp.

U.S. Department of Energy
Contract DE-AS02-76EV01340

Our statistical reference model of energy demand for space heating has been applied to estimate total daily demand for an entire region. Intraregional subareas exhibited considerable diversity in rates of demand, factors controlling demand and in overall accuracy of model predictions. Progress toward obtaining detailed building census and meteorological data for physical and physical-reference modelling of regional space heating energy requirements is also described.

A physical model of energy demand for air conditioning in large buildings has received preliminary testing. The Group Method of Data Handling (GMDH) algorithm failed in its first application to air conditioning data. The reasons for this failure are complex and not completely resolved. Presently however, this failure is viewed as an

Author: Elmar R. Reiter et al. 551.588.7

THE EFFECTS OF ATMOSPHERIC VARIABILITY ON ENERGY UTILIZATION AND CONSERVATION

Subject Headings:

Energy Consumption
Energy Modelling
Urban Climate

Colorado State University
Department of Atmospheric Science

Environmental Research Paper No. 32
March 1982, 41 pp.

U.S. Department of Energy
Contract DE-AS02-76EV01340

Our statistical reference model of energy demand for space heating has been applied to estimate total daily demand for an entire region. Intraregional subareas exhibited considerable diversity in rates of demand, factors controlling demand and in overall accuracy of model predictions. Progress toward obtaining detailed building census and meteorological data for physical and physical-reference modelling of regional space heating energy requirements is also described.

A physical model of energy demand for air conditioning in large buildings has received preliminary testing. The Group Method of Data Handling (GMDH) algorithm failed in its first application to air conditioning data. The reasons for this failure are complex and not completely resolved. Presently however, this failure is viewed as an

opportunity to obtain additional basic insight into weather-energy demand relationships.

A model of local climate variability that considers both topography and urban "heat island" effects has been refined to an advanced state of development. This climate modelling capability will allow regional scale physical and physical-reference modelling of energy demand to proceed by reducing the requirements for mesoscale observational networks to obtain energy demand-weighted meteorological data for each city.

The potential value of improved weather forecast information to a large electric generation and transmission utility company has been studied. A simple weather-driven demand model for electricity uses weather forecasts to predict hour-by-hour loads, one day in advance. These load forecasts are in turn used by a system scheduling model to determine the most economical generating configuration to meet forecast demands. The results demonstrate significant potential value for improved accuracy of weather forecast services.

Lastly, we have examined the actual cost effectiveness of structural modifications and system retrofits for reducing energy consumption for space conditioning in large buildings. Data obtained for five rather diverse alterations suggest that considerable broad-based conservation potential is available through applications of improved energy utilization technology.

opportunity to obtain additional basic insight into weather-energy demand relationships.

A model of local climate variability that considers both topography and urban "heat island" effects has been refined to an advanced state of development. This climate modelling capability will allow regional scale physical and physical-reference modelling of energy demand to proceed by reducing the requirements for mesoscale observational networks to obtain energy demand-weighted meteorological data for each city.

The potential value of improved weather forecast information to a large electric generation and transmission utility company has been studied. A simple weather-driven demand model for electricity uses weather forecasts to predict hour-by-hour loads, one day in advance. These load forecasts are in turn used by a system scheduling model to determine the most economical generating configuration to meet forecast demands. The results demonstrate significant potential value for improved accuracy of weather forecast services.

Lastly, we have examined the actual cost effectiveness of structural modifications and system retrofits for reducing energy consumption for space conditioning in large buildings. Data obtained for five rather diverse alterations suggest that considerable broad-based conservation potential is available through applications of improved energy utilization technology.

opportunity to obtain additional basic insight into weather-energy demand relationships.

A model of local climate variability that considers both topography and urban "heat island" effects has been refined to an advanced state of development. This climate modelling capability will allow regional scale physical and physical-reference modelling of energy demand to proceed by reducing the requirements for mesoscale observational networks to obtain energy demand-weighted meteorological data for each city.

The potential value of improved weather forecast information to a large electric generation and transmission utility company has been studied. A simple weather-driven demand model for electricity uses weather forecasts to predict hour-by-hour loads, one day in advance. These load forecasts are in turn used by a system scheduling model to determine the most economical generating configuration to meet forecast demands. The results demonstrate significant potential value for improved accuracy of weather forecast services.

Lastly, we have examined the actual cost effectiveness of structural modifications and system retrofits for reducing energy consumption for space conditioning in large buildings. Data obtained for five rather diverse alterations suggest that considerable broad-based conservation potential is available through applications of improved energy utilization technology.

opportunity to obtain additional basic insight into weather-energy demand relationships.

A model of local climate variability that considers both topography and urban "heat island" effects has been refined to an advanced state of development. This climate modelling capability will allow regional scale physical and physical-reference modelling of energy demand to proceed by reducing the requirements for mesoscale observational networks to obtain energy demand-weighted meteorological data for each city.

The potential value of improved weather forecast information to a large electric generation and transmission utility company has been studied. A simple weather-driven demand model for electricity uses weather forecasts to predict hour-by-hour loads, one day in advance. These load forecasts are in turn used by a system scheduling model to determine the most economical generating configuration to meet forecast demands. The results demonstrate significant potential value for improved accuracy of weather forecast services.

Lastly, we have examined the actual cost effectiveness of structural modifications and system retrofits for reducing energy consumption for space conditioning in large buildings. Data obtained for five rather diverse alterations suggest that considerable broad-based conservation potential is available through applications of improved energy utilization technology.